TSAC
TAHOE SCIENCE ADVISORY COUNCIL

Lake Tahoe Seasonal and Long-Term Clarity Trend Analysis

October 30, 2020

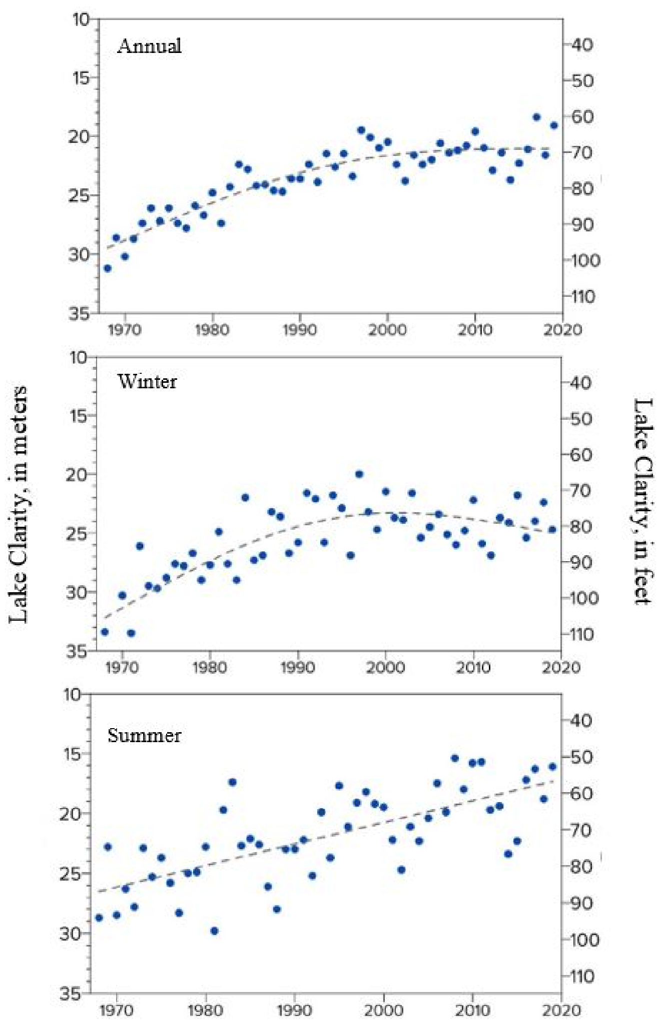

Acknowledgements

The authors wish to thank our colleagues on the Tahoe Science Advisory Council (TSAC) and from Tahoe Resource Agencies for their comments and suggestions on earlier drafts of this document. We also thank the TSAC Program Officer, Robert Larsen for his efforts in keeping the project on track. Funding support was provided by the Nevada Division of Environmental Protection. We recognize the contributions from Alicia Cortes (UC Davis), Shohei Watanabe (UC Davis), Lidia Tanaka (UC Davis) and Sebnem Elci (Izmir Institute of Technology).

This report is available at the Tahoe Science Advisory Council website:

https://www.tahoesciencecouncil.org/.

Preferred Citation:

Tahoe Science Advisory Council (TSAC) 2020, Lake Tahoe Seasonal and Long-Term Clarity Trend Analysis. TSAC Technical Report, October 2020. Incline Village, NV.

For more information contact:
Alison Toy
Tahoe Science Advisory Council
291 Country Club Dr., Suite 320
Incline Village, NV 89451
775-881-7566
natoy@ucdavis.edu

Outline

Executive Summary

The clarity of Lake Tahoe, observed using a Secchi disk, continues to be a sentinel metric. It is influenced by both physical and biological processes and has had a declining trend over decades of monitoring, with differences apparent between summer and winter patterns. This document summarizes key findings of an investigation on Lake Tahoe water clarity, its long-term variability, and the relative importance of several influencing variables and processes.

This investigation focused on factors relevant to the apparent divergence in clarity between summer and winter periods, on how in-lake physical and ecological drivers influenced both seasonal and historic clarity trends, and on evaluating five research hypotheses developed by Tahoe agencies.

The trend analyses confirm that clarity declines during the winter period (Dec-Mar) have plateaued (i.e. there is no longer a statistically significant trend up or down) over the last 20 years. The reasons for this are complex and not caused by a single factor but are the net result of multiple physical and biological processes. In evaluating clarity over monthly periods with the 50-year Secchi record, only two summer months, July and August, reveal statistically significant decreases in clarity for the 2000-2019 period.

What many of these processes appear to share are an association with changes in the climate at Lake Tahoe. Although the well documented warming air temperatures and the decreasing snow-to-rain ratio over the at lake Tahoe were not a focus of this study, the changes that they are producing were relevant. These changes include, but are not limited to, more extreme floods and droughts that increase and decrease external loads over multiple years, changes to the seasonality and duration of stratification, alterations to lake stratification and stream temperatures that impact the insertion depths of external loads, and the suppression of turbulence that changes the vertical location of algal blooms within the lake.

Analysis of streamflow records indicate that climate change plays a significant role on winter clarity. During the last 20 years, 50% of those years have been in drought, which has resulted in a disproportional effect on winter clarity. During drought years, winter clarity improves as lower contributions of fine sediments enter the lake. Conversely, above-average precipitation occurred in 20% of years over the last two decades, with significant contributions of fine sediments occurring recently during WY2017 and WY2019. During wet years, streamflow contributions of fine sediments are much greater and have an impact on summer clarity conditions from delayed hydrographs and higher discharge.

In-lake physical and ecological drivers also influenced seasonal and historic trends, with winter mixing having a significant impact on seasonal trends. Winter clarity improves during the winter months because deep winter mixing dilutes light attenuating particles and brings up clearer water from depth to the near surface. Months following deep mixing are influenced by the increase in nitrate that is brought to the surface and contributes to algal productivity during the spring and summer periods. Increases in lake temperatures due to climate change have resulted in the lake becoming stratified earlier and stratification lasting longer. The increase in temperatures at the near surface of the lake, combined with changing stream temperatures, affects the relative buoyancy of the lake and the insertion depths of incoming stream flows.

This analysis also provides insight on how the abundance of a small diatom, Cyclotella, influences fall and summer clarity. Counts of Cyclotella greater than 100 cells/mL have direct negative impact on clarity, whereas counts below this threshold do not show much impact. Finally, data collected at Emerald Bay suggest that Daphnia in the absence of the predator Mysis shrimp may contribute positively to both seasonal and annual clarity. The deliberate introduction of non-native Mysis shrimp over 50 years ago is having an impact on food webs. The subsequent disappearance of Daphnia (and other Cladocerans) has removed organisms that display the ability to remove both inorganic and organic fine particles.

This investigation evaluated Hypothesis 1 that stated clarity is controlled predominantly by the distribution and volumetric density of fine particles in suspension. This hypothesis was investigated using available in-lake fine particle data from the period 2008-2019, where fine particles include both inorganic particles from watershed loads and organic particles from small algal cells within the lake. The analysis results indicated that water clarity is negatively correlated with in-lake particle abundance. Clarity decline was also found to be more highly correlated with the abundance of particles in the 1.0-4.76 μm size range than the full 0.5-20 μm range of sizes, due to the optical properties of light scattering. Finally, the abundance of cells of the small diatom *Cyclotella* was also found to be negatively correlated with clarity.

Data limitations precluded a complete investigation of Hypothesis 2, which stated that the change in trend of winter clarity is a response to decreasing fine suspended sediment concentrations resulting from load reductions. Data describing fine sediment loading from urban areas to the lake are only available since 2014. A slight negative correlation, statistically significant, was found between urban fine particle loading and monthly lake clarity with a four-month lag. Another significant limitation is that particle abundance (number per unit volume) data from streams and urban inputs are only available 1-2 times per month, precluding computation of long-term continuous fine suspended sediment loading from streams. Findings from this analysis determined that time series of particle abundance in streams is highly correlated with simultaneous particle abundance in the lake.

The stability index and buoyancy frequency are two computed variables that indicate resistance to lake vertical mixing. Both were used to evaluate Hypothesis 3 which stated that changing hydrodynamic conditions within the lake are increasing thermal stability and resistance to mixing. Trend analyses performed on stability index and buoyancy frequency time series support the hypothesis that hydrodynamic conditions have evolved since 1969 to increase the lake's resistance to mixing. Time series analysis describing the date of maximum winter mixing depth indicated that deep mixing is occurring progressively earlier in the year. Lake stratification, as quantified by the stability index, is commencing earlier in the year, and extending a month longer. Early in the 50-year record it was uncommon for the greatest depth of mixing (frequently tied to the measurement of the year's highest lake clarity) to occur prior to April. In the two most recent decades, this condition has most frequently been observed prior to April 1, meaning that the peak mixing conditions are now included in any assessment of winter conditions (December – March).

Available data supports Hypothesis 4 which states that the trend in summer clarity is a result of earlier, prolonged and more intense stratification. Statistically significant correlations were found between summer clarity and 1) date of onset of stratification, 2) duration of stratification and, 3) buoyancy frequency. As stratification increases in intensity, summer clarity is reduced. Earlier stratification also reduces the summer clarity. Stronger, longer-duration stratification appears to influence suspended particle behavior and biological activity to collectively reduce summer clarity.

The data supporting hypothesis 5, that ecological (food web) interactions are causing changes in the trends of seasonal or annual clarity, was limited to examples from other systems and to intermittent monitoring within Lake Tahoe and Emerald Bay. This narrative assessment was motivated by a six-year study of *Mysis* disappearance and return in Emerald Bay. The available data and a large body of published literature are consistent with the inference that *Mysis* shrimp-induced food web changes are causing changes in the trends of seasonal or annual clarity. This food web investigation focused on the relationship between introduced *Mysis* shrimp, the native cladocerans (*Daphnia* and *Bosmina*) that were largely eliminated following *Mysis* introduction, and their impact on fine particles within the lake. The record of *Mysis* and other zooplankton data for Lake Tahoe is episodic and has large gaps. Consequently, statistical analyses as conducted with other variables were not possible. However, the long-term record indicates that the key impact was a change to the phytoplankton assemblage, where larger diatoms disappeared, likely due to *Mysis* grazing, only to be replaced by order-of-magnitude smaller *Cyclotella,* which has increased the abundance and volumetric density of total fine particles in suspension (biotic and abiotic).

Introduction

Lake Tahoe is designated an Outstanding National Resource Water and a “Waterbody of extraordinary ecological or aesthetic value” by the states of California and Nevada, respectively, for its remarkable clarity and striking blue color. Over the past half century, average annual clarity has diminished. The Lake Tahoe Total Maximum Daily Load (TMDL) Program was established to guide efforts and set targets to restore historic clarity conditions. The TMDL Program was predicated on the decline in water clarity being primarily the result of the inorganic fine sediment particle load entering the lake from watersheds. However, extremes in hydrological variables as well as in-lake processes may contribute to interannual variations in lake clarity.

Trends in clarity, as measured by Secchi depth, vary between summer and winter seasons. The long-term summer trend is consistently declining, with a noticeable cyclic pattern. Winter clarity is showing a different long-term trend. The ongoing summer clarity decline effectively offsets improvements in winter, confounding average annual clarity restoration efforts. The cause for the diverging seasonal clarity trends has not been well documented.

This work focused on key water quality management questions:

• What is driving the divergence in summer and winter clarity trends?

• How have in-lake physical and ecological drivers influenced seasonal and historic trends?

Quantitative observations of the clarity of Lake Tahoe date back to the late 19th century (LeConte, 1883). Goldman (1981) describes lake changes and the monitoring of them that began in the 1960s. This monitoring campaign has been augmented over the years and now includes many more parameters describing the physics, chemistry and biology of the lake and watershed (Schladow et al. 2019).

Clarity of the lake’s waters, as observed using a Secchi disk, continues to be a sentinel metric, potentially influenced by both physical and biological processes, and water clarity is also at least qualitatively obvious to laypersons. Clarity is measured on a nominally bimonthly basis and has had a declining trend over decades of monitoring, with differences apparent between summer and winter patterns (Figure 1.1). The trendlines (dashed lines) in Figure 1.1 are produced using a generalized additive model or GAM (Wood 2006), which allows for the incorporation of both non-linearity and smoothing.

The lake is over 500 m deep, with a surface area of 490 km^2, and the watershed – including the lake – is only 1300 km^2. The watershed has strong interannual variations in precipitation, steep topography, periodic forest fires, and environmental stresses associated with urbanization and high tourist visitation. These factors and several others have the potential to combine to negatively impact water clarity on both short- and long-term time scales.

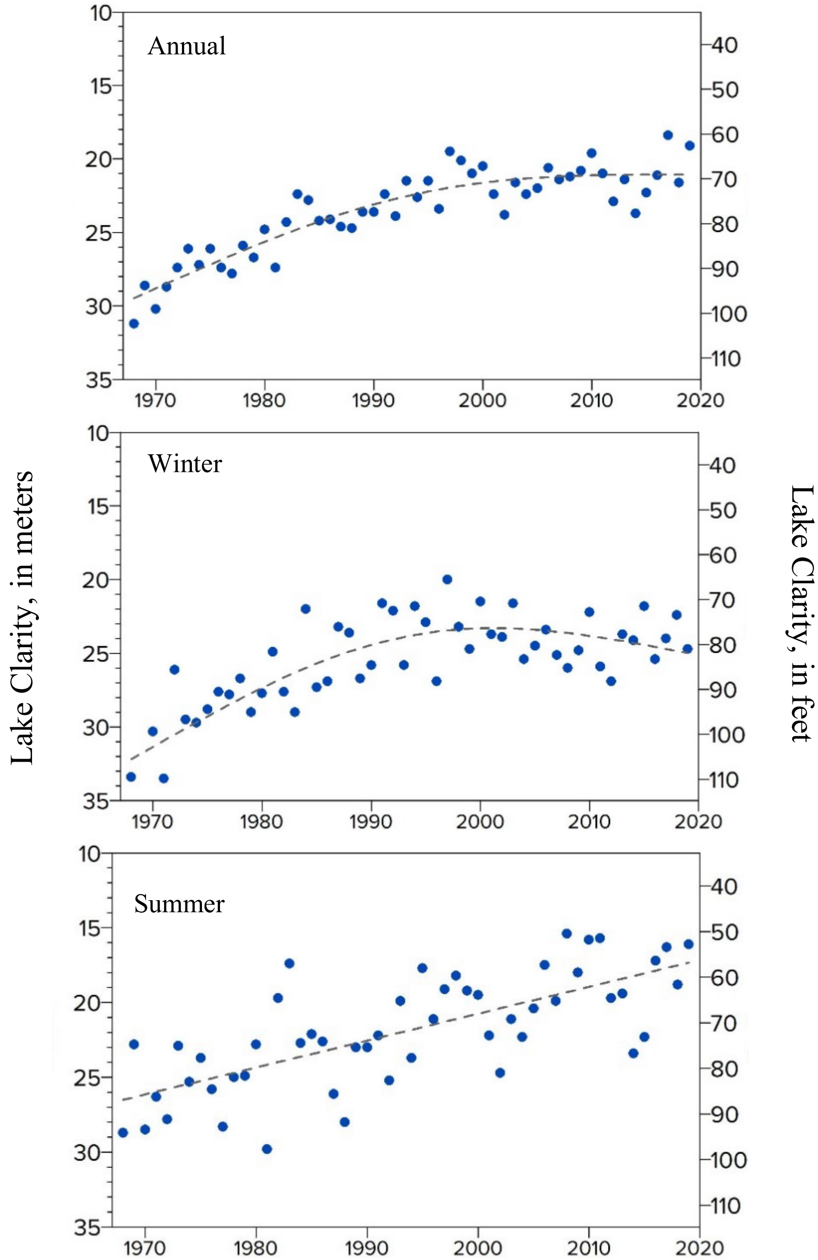

Figure 1.1. Lake clarity during annual (top), winter (middle) and summer (bottom) periods at station LTP (see Figure 1.2 for station locations). The dashed trend line is produced using a generalized additive model. Calendar year used to define annual values in this plot.

The objectives of this study were clearly defined to improve the understanding and linkages between long-term observations and drivers affecting lake clarity. Many of these variables have been influenced by climate change and the effects on water quality and lake ecosystem have been reported in the scientific literature. Climate change in the Tahoe basin has been reported to drive shifts in time-series trends of long-term weather and hydrological observations such as temperature, snow accumulation, snow to precipitation ratios, snow melt timing and stream runoff (Cayan et al., 2008; 2009; Coats, 2010; 2012; Dettinger and Cayan 1995; Hansen et al., 2006 Roberts et al., 2008). Future climate conditions have been used to investigate degradation of lake water quality caused by thermal stratification, nutrient and sediment influx (Sahoo et al, 2013; Riverson et al, 2012; Coats et al., 2013). Climate induced lake warming and strengthening of thermal stratification has also been shown to favor small-celled Cyclotella that have high surface to volume ratios (Winder et al., 2009). While climate change has resulted in Lake Tahoe temperature to become warmer and more stable (Stewart et al. 2005; Schneider et al. 2009; Sahoo et al. 2011) and length of stratification is expected to become longer and the lake as a whole to become more resistant to deep mixing (Sahoo et al, 2015). The body of scientific literature much of it reported more than a decade ago are consistent with the overall trends in observational data collected to date. The intent of this work is to address specific questions related to seasonal clarity based on observation data already influenced by climate change.

Purpose and Scope

The objective of this work is to investigate the role of clarity drivers and assess their relative influence on seasonal and long-term clarity conditions. Drivers currently suspected to influence clarity include, but are not limited to biological conditions, such as changing phytoplankton speciation and concentrations due to food web changes; thermal stratification; particle/nutrient insertion depths; and hydrological factors, such as the timing and delivery of external loads, and extreme climate conditions. The analysis included evaluating watershed and in-lake monitoring data to investigate the drivers of seasonal clarity conditions.

The work described in this report was performed to address several specific objectives:

1) Assimilate available data describing water clarity, stream inflows and sediment concentrations, urban runoff, meteorology, water chemistry, and biological parameters. Some of these data were already publicly available online but the other data have been compiled as a project deliverable for use by others.

2) Assess trends in water clarity within the lake, on different timescales, including differences between summer and winter trends.

3) Investigate five specific hypotheses:

Hypothesis 1 – Clarity is controlled predominantly by the distribution and density of fine particles in suspension.

Hypothesis 2 – The change in trend of winter clarity is a response to decreasing fine suspended sediment concentrations resulting from load reductions.

Hypothesis 3 – Changing hydrodynamic conditions within the lake are increasing thermal stability and resistance to mixing.

Hypothesis 4 – The trend in summer clarity is a result of earlier, prolonged, and more intense stratification.

Hypothesis 5 – Ecological (food web) interactions are causing changes in the trends of seasonal or annual clarity.

4) Answer the following water quality management questions:

• What is driving the divergence in summer and winter clarity trends?

• How have in-lake physical and ecological drivers influenced seasonal and historic trends?

No new data were collected to develop this report, and the effort did not include new numerical or analytical modeling. However, the data have been assimilated and investigated in new ways to evaluate potential trends in different parameters and processes that may be influencing water clarity on long-term time scales. This effort did not include efforts to predict future changes, but the findings may be useful for those who attempt to do so.

1.1 Available Data

The project included the compilation of existing datasets, some of them not readily or publicly available, for use within the project and by others. This section describes the scope of the effort to compile the data, how it is being provided, and how it is defined by metadata.

Most of the data utilized in this project came from one of the following sources:

- The long-term lake monitoring program led since the 1960s by the University of California-Davis (https://tahoe.ucdavis.edu/monitoring)
- U.S. Geological Survey National Water Information System (NWIS) monitoring stations (https://waterdata.usgs.gov/nwis)
- The Lake Tahoe Interagency Monitoring Program managed by the U.S. Geological Survey (LTIMP, Rowe 2000).
- The Tahoe Regional Stormwater Monitoring Program (RSWMP, Tahoe Resource Conservation District)

The data assimilated during this project are summarized in Table 1.1 below, with additional details on datasets provided in Appendices 1 and 2. Each time series is discussed briefly below. Many of the data collection sites are shown in Figure 1.2. Data that are readily, publicly available online, such as the U.S. Geological Survey data available via the NWIS site noted above, were not included in the dataset being provided as a deliverable of this project.

For the purposes of the analyses discussed in this report, “winter” is defined as January 1 through March 31 of a given year, combined with the preceding December. Summer is defined as June 1 through September 30. These definitions are consistent with the commonly used “water year” that extends from October 1 to September 30. October 1 of calendar year X is part of water year X+1. Monitoring data was organized by water year to be consistent with reported values of summer and winter clarity and to account for climatic and hydrological drivers. Differences may exist between reported calendar averages and water year annual average values reported herein.

Table 1.1. Summary of data assimilated in the project. LTP = Lake Tahoe Profile station, MLTP = Mid-Lake Tahoe Profile station, LTMP = Lake Tahoe (Interagency) Monitoring Program, SNOTEL = Snow Telemetry, TRCD = Tahoe Resource Conservation District.

Data Type	Parameter	Location	Collection Period
	Secchi depth	MLTP; LTP	1967-present
Lake Data	Temperature	MLTP; LTP	1969-present; 1967-1996
	Particle size distribution	MLTP; LTP	2008-present
	Nitrogen (NO3)	MLTP; LTP	1970-present; 1968-present
	Phosphorus (THP)	MLTP; LTP	1972-present; 1968-present
	Phosphorus (TP)	MLTP	1989 - 1992, 2000-present
	Chlorophyll a	LTP	1984-present
	Cyclotella	MLTP;LTP	MLTP (composite) 1992-2015; LTP: 1967-1988, 2001-present
	Mixing Depth	-	1974 to present
	Stratification Length (calculated)	-	1968 to present
	Peak Stratification (calculated)	-	1968 to present
	End of Stratification (calculated)	-	1968 to present
	Peak BuoyFreq (calculated)	-	1968 to present
	MaxBuoyFreq (calculated)	-	1968 to present
	Stability Index (calculated)	-	1968 to present
	Flow	LTMP	1986-present
Streams	Nutrients (N&P)	LTMP	1986-present
	SSC	LTMP	1986-present
	Particle size distribution	LTMP	2008-present
Atmospheric	Bulk (wet + dry) Total N		2003-present
	Bulk (wet + dry) Inorganic N		1998, 2000 to present
	Bulk (wet + dry) Total P		1998, 2000 to present
	Bulk (wet + dry) SRP		1998, 2000 to present
Meteorology	wind, air temp, solar radiation	6 buoys	2000-present
Climate	Precipitation	SNOTEL	1981 to present
	Snow Water Equivalent	SNOTEL	1981 to present
	Fine Sediment Particles	TRCD	2014 to present
Urban	Total Nitrogen	TRCD	2014 to present
	Total Phosphorus	TRCD	2014 to present
	Pollution Load Credits	-	2016 to present

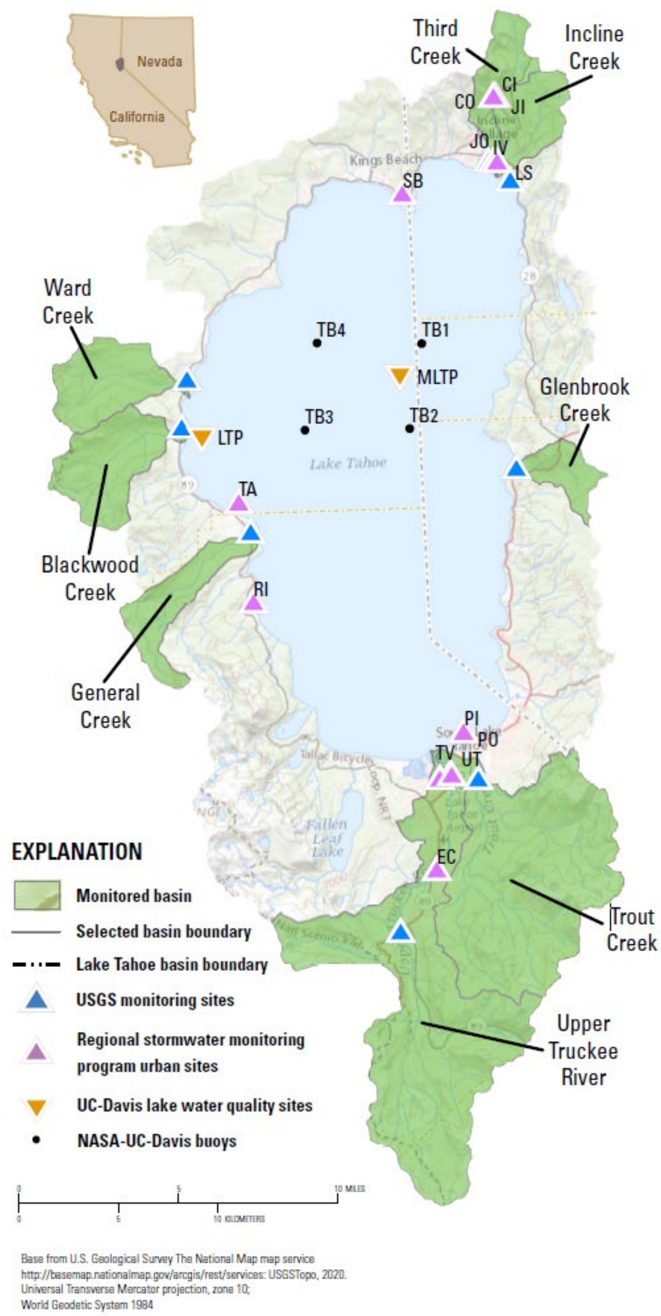

Figure 1.2. Data collection site locations. From 2019 State of the Lake report. TERC = Tahoe Environmental Research Center, LTIMP = Lake Tahoe Interagency Monitoring Program.

1.1.1 In-Lake Data

The data shown as “Lake Data” in Table 1.1 were collected as part of UC Davis’s long-term monitoring program at Lake Tahoe. Most of the datasets utilized within this report are collected at two sites, referred to as LTP and MLTP (Lake Tahoe Profiling and Mid-Lake Tahoe Profiling stations, Watanabe et al. 2015; Figure 1.2; Table 1.2).

Table 1.2. Locations of long-term monitoring stations in Lake Tahoe.

Site Name	Location (DDD MM SS)	Water Depth (m)
LTP	039 07 18 N 120 04 39 W	120
MLTP	039 07 52 N 120 00 10 W	460

Secchi disk (Transparency) data were used to define water clarity, in meters. Jassby et al. (1999) discuss the data collection methods and consistency. The methodology for the collection of Secchi disk data has remained constant throughout the measurement program, with data typically collected twice per month since 1967 at the LTP site and once per month since 1970 at the MLTP site.

Water temperature data collection methods at the long-term stations LTP and MLTP have changed since the onset of measurements in 1968. A bathythermograph was utilized at the onset of the monitoring program, through 1970, with data recorded at 3 m intervals. Beginning in 1970 a Martek instrument, with reduced vertical resolution, was utilized (see appendix 1 for details). From 1996-2006, an RBR-sourced sensor was used, and in 2006 the switch was made to the currently utilized Seabird instrumentation. Each sensor has different accuracy and resolution limitations, but for the purposes of this report the data were utilized as reported. Since 2000, water temperature data have been collected at six buoy locations around the lake.

Seabird instruments were incorporated into the program for water quality measurements in 2005. This has provided continuous (over the vertical) observations of water temperature, electrical conductivity, depth, dissolved oxygen, pH, turbidity, photosynthetically active radiation (PAR), and light transmission. PAR and ultraviolet (UV) light have been measured on the rooftop of the Tahoe Environmental Research Center building since 2007.

Particle size distribution data has been collected at the two long-term, in-lake sites since 1999 via laser diffraction using a bench-top instrument. The data since 2008 were utilized in this study because there are questions regarding the quality of some of the data prior to 2008. The post-2008 dataset includes, for multiple depths down to 50 m, the number of particles per mL within each of 14 different size classes, spanning a range of 0.5-20 μm.

The long-term, in-lake stations also feature the collection of chemical and biological time series datasets. Chemical parameters include nitrate as nitrogen, ammonium as nitrogen, total kjeldahl nitrogen, soluble reactive phosphorus, total hydrolyzable phosphorus, total phosphorus, particulate phosphorus, dissolved organic carbon, particulate organic carbon, dissolved inorganic carbon, and dissolved oxygen. Biological parameters include primary production, chlorophyll a, chlorophyll fluorescence and identification and enumeration of phytoplankton. Periods of record for these parameters vary, with many starting in the 1970s (see Appendix 1).

1.1.2 Stream Data

Nine stream gauging stations are routinely monitored by the U.S. Geological Survey for discharge; eight of these stations feature water quality observations including nitrate as nitrogen, ammonia as nitrogen, dissolved phosphorus, soluble reactive phosphorus, suspended sediment concentration (SSC; Table 1.3). Discharge is now reported every fifteen minutes, whereas many of the other parameters are observed approximately 25 times per year. Each value is intended to represent a cross-sectional average across a stream. The USGS data are publicly available at https://waterdata.usgs.gov/nwis.

Table 1.3. USGS stream monitoring on Lake Tahoe tributaries. All listed stations include measurement of discharge, abbreviated as Q. Water quality (WQ) parameters are abbreviated as T = temperature, SC = specific conductivity, Tu = turbidity, SSC = suspended sediment concentration (including sediment particles of all sizes). Stage is monitored at all sites and discharge is calculated from stage-discharge rating curves.

Station	USGS Station Number	Parameters currently available on daily basis	Period of Record (including intermittent field samples)
Blackwood Creek near Tahoe City, CA	10336660	Q, T, Tu	1960-present for Q 1973-present for WQ
General Creek near Meeks Bay, CA	10336645	Q, T, Tu	1980-present for Q 1980-present for WQ
Glenbrook Creek at Glenbrook, NV	10336730	Q, T	1971-present for Q 1971-2011 for WQ
Incline Creek near Crystal Bay, NV	10336700	Q, T, Tu	1969-present for Q 1969-present for WQ
Third Creek near Crystal Bay, NV	10336698	Q, T, Tu	1969-present for Q 1969-present for WQ
Trout Creek near Tahoe Valley, CA	10336780	Q, T, Tu	1973-present for Q 1973-present for WQ
Upper Truckee River at South Lake Tahoe, CA	10336610	Q, T, Tu	1970-present for Q 1970-present for WQ
Upper Truckee River at Highway 50 above Meyers, CA	103366092	Q	1990-present for Q 1989-2011 for WQ
Ward Creek at Highway 89 near Tahoe Pines, CA	10336676	Q, T, Tu	1972-present for Q 1972-present for WQ

The Nevada Division of Environmental Protection, and the California Lahontan Water Board provided estimates of annual loads of fine sediment particles, total phosphorus, and total nitrogen from urbanized regions to the lake in 2004 and estimates of reductions to these loads achieved in each of the years 2016-2019, based on Pollutant Load Reduction Model (PLRM) results. Beginning in 2014 field estimates of loading from urban monitoring sites are derived from the Tahoe Regional Stormwater Monitoring Program (RSWMP, see California Tahoe Resource Conservation District 2020). Measured estimates from urban sites represent a small fraction of the total watershed, however, which is about 0.26% of the terrestrial portion of the lake watershed and 1.3% of total urban drainages to the lake.

Atmospheric deposition data were obtained from UC Davis, in the form of annual loads since 2000 at one location, with additional records in 1994 and 1998. Data include annual deposition of dissolved inorganic nitrogen, total nitrogen, and soluble reactive phosphorus (SRP).

Wind data were obtained for the period 2000-present from a measurement station at Tahoe City. Wind speed and direction are reported at ten-minute intervals.

Phytoplankton and zooplankton data from long-term monitoring of Lake Tahoe by UC Davis (Tahoe Environmental Research Center; TERC) were used. These data derived from both routine monitoring and from individual research projects dating back to the 1960s. For the routine monitoring we chose to use phytoplankton data from 5 m depth, as it was considered to serve as a good proxy for the impact of phytoplankton on clarity impairment.

We have provided the data used to reach our conclusions via a Microsoft Excel spreadsheet with separate tabs for each variable, with accompanying tabs providing metadata. Some details are also available in the appendices to this report. The data will be made publicly available via the Tahoe Science Advisory Council website.

2.0 Trends in Lake Tahoe Water Clarity

2.1 Background

Since 2011 it has been reported that winter clarity trends have stabilized while summer clarity continues to decline (SOTL, 2011 through 2020). This assessment evaluates the change in clarity and conducts trend analysis on seasonal and monthly data to confirm the signa and significance of the trends. The nearly 50-year record can be evaluated over the full duration or during periods that are important to evaluating restoration activities. The annual and seasonal clarity can vary widely among different climate conditions and periodic updating of the trend analysis can inform whether clarity improvements or declines are statistically significant. Trend analysis on different time periods may yield slightly different results and avoiding bias when selecting which periods are evaluated is critically important. It is also important to recognize that trends in reported seasonal clarity may be dominated by only one or two months out of four. Therefore, investigating monthly clarity data provides more insight into seasonal trends and may shed light on the important processes and drivers.

2.2 Data Sets

Secchi disk data have been collected in Lake Tahoe about twice per month since 1967 at the LTP site, and since 1969 at the deeper MLTP site. Earlier analysis by Jassby et al. (1999) discuss the procedure and its repeatability and uncertainty. For the purposes of this report, water clarity will be taken to be expressed by Secchi depth.

2.3 Approach

Trends in water clarity were assessed in several different ways, considering both annual and seasonal variability, and focusing primarily on the LTP dataset. Clarity trends were first computed using the entire period of record using median monthly values with the Mann-Kendall test and nonparametric Sen’s slope method (Helsel and Hirsch 2002). In a previous evaluation of clarity trends, Jassby et al. (1999) noted variations at seasonal, interannual and decadal scales with statistically significant negative trends, except for the month of July. Here we apply a similar approach and use Sen's linear model to estimate the trend in annual and monthly clarity data. Using this approach, we separate the clarity data into three periods: 1968-79, 1980-1999 and 2000-2019 to evaluate linear trends in annual and monthly data. Separating the clarity data into these periods provide nearly 20-year periods to evaluate the statistical significance of long-term clarity trends. Because the p-values that reveal statistical significance are affected by sample size, consideration of shorter-term periods (5-10 year) for clarity trend analysis resulted in p-values that are greater than 0.05 and thus statistically insignificant. Trends are defined by the sign of the computed Z-value with negative and positive values representing negative and positive trends, respectively. If the value of the Z statistic is non-significant at a given alpha level (*p-value* = 0.05), one can infer that there is no trend in clarity, even if visual inspection suggests otherwise. At the 5% significance level (p=0.05), the null hypothesis of no trend is rejected if the absolute value of the Z-value is higher than 1.96.

2.4 Results

2.4.1 Annual, Winter and Summer Clarity Trends

Fitted linear trends through the annual, winter and summer clarity measurements over the three periods reveal a consistent decline in annual and summer clarity with the exception of a subtle change in the rate of decline during the 1980-2000 and 2000-2019 periods for winter (Figure 2.1). Considering the period between 1968 to 2019, there is a statistically significant negative trend in clarity for annual, winter and summer periods with a loss in clarity of -0.13 to -0.19 m/year ($p < 0.001$; Table 2.1). During the period 1968-1979, the clarity declines were significant at -0.36 to -0.62 m/year. From 1980-1999, the annual change in clarity remained negative but the rate of change decreased significantly from the previous analysis period to -0.19 to -0.22 m/year ($p < 0.05$) for both annual and winter periods, respectively. For the period 2000-2019, annual rates of clarity decline identified in this study are consistent with a previously estimated rate of -0.22 m/year by Sahoo et al. (2010) for the period 1996-2005; however, the trend was not statistically significant. For summer, the clarity trend was statistically significant only for the full period of record, from 1968-2019 ($p < 0.001$). For 2000-2019, the rate of decline in clarity appears to have decreased, but based on the significance level, no trend exists for annual, winter or summer clarity.

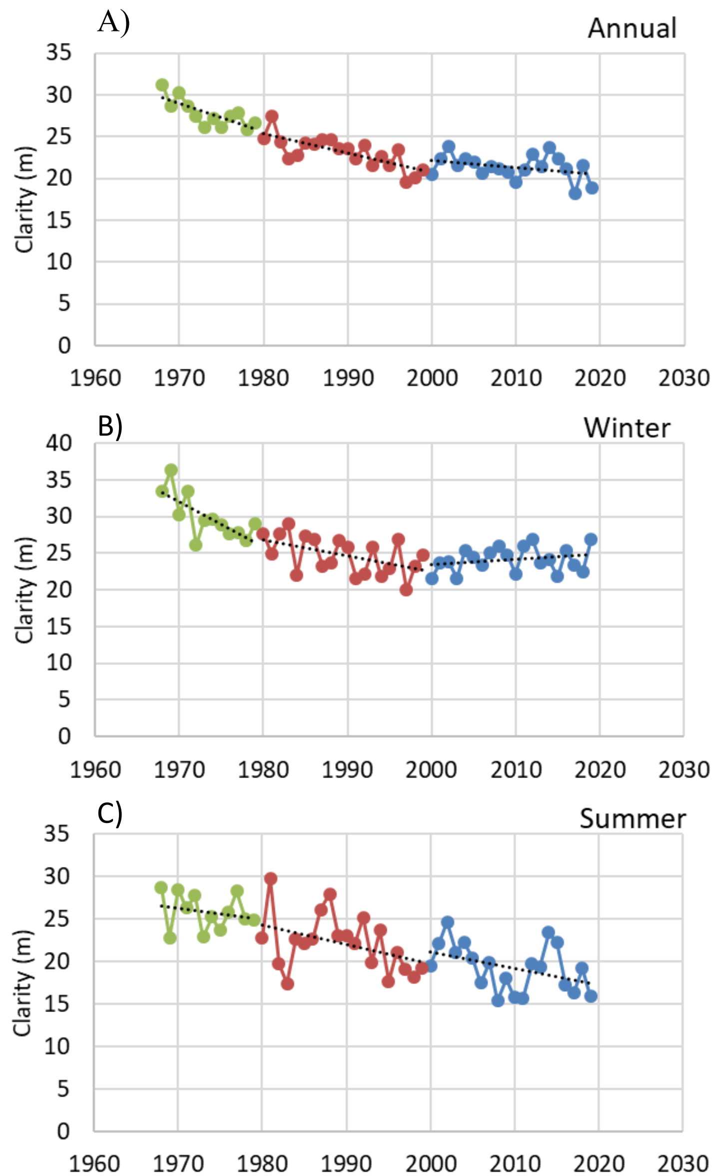

Figure 2.1. Lake clarity during annual (A), winter (B) and summer (C) periods at station LTP, for three periods: 1968-79, 1980-1999 and 2000-2019. Linear fit through observations are shown with black dash line.

Table 2.1. Results of trend analysis for annual, winter and summer seasons for 1968-2019, 1968-1979, 1980-1999 and 2000-2019 periods. Values of n represent the number of measurements, sign of test statistic Z indicates the sign of the trend (positive or negative), Sen's slope is the rate of change in clarity, in meters per year. Where p-values cell is blank, significance level is greater than 0.05.

	Annual	**Winter**	**Summer**
		1968-2019	
n	52	52	52
Test Z	-6.9	-4.4	-5.5
P-value	<0.05	<0.05	<0.05
Sen Slope	-0.17	-0.13	-0.19
		1968-1979	
N	12.0	12.0	12.0
Test Z	-2.4	-2.3	-0.9
P-value	<0.05	<0.05	
Sen Slope	-0.36	-0.62	-0.14
		1980-1999	
N	20	20	20
Test Z	-3.6	-2.3	-1.6
P-value	<0.05	<0.05	
Sen Slope	-0.22	-0.19	-0.24
		2000-2019	
N	20	20	20
Test Z	-1.1	1.0	-1.8
P-value			
Sen Slope	-0.08	0.08	-0.22

2.4.2 Monthly Clarity Trends

Monthly clarity data were evaluated during the same analysis periods as Annual, Winter and Summer data in section 2.1 (Figure 2.2). Evaluation of the clarity trends by month sheds light on Fall and Spring trends which are less evident in the annual reporting of clarity for Lake Tahoe. For example, trends in Fall (October and November) monthly clarity are similar to Winter (December to March; Table 2.2). This suggests that drivers of Winter clarity are influenced by processes that occur in Fall. Trend analysis reveals that November, December, and May clarity did not significantly decrease (no trend) during the period 2000-2019. Thus, evaluated seasonally and comparing the 1980-1999 and 2000-2019 analysis periods, changes from decreasing clarity to no trend were identified for Fall, Winter, Spring, and Summer months June and September. Several months were found to have statistically significant clarity declines in 1980-1999 that switched to no trend in 2000-2019: November (-0.37 m/yr), December (-0.33 m/yr), May (-0.19 m/yr) and August (-0.24 m/yr). During Summer, the greatest statistically significant ($p < 0.05$) declines were found in July (-0.33 m/yr) and August (-0.29 m/yr) over the 2000-2019 period. For these two months, the slope of clarity trend has changed little since 1967. During 2000-2019, the rate of decline slowed for June to -0.13 m/yr from -0.42 m/yr in 1980-1999. The rate of decline has also slowed for April (Spring) to -0.05 m/yr from -0.28 m/yr in 1980-1999.

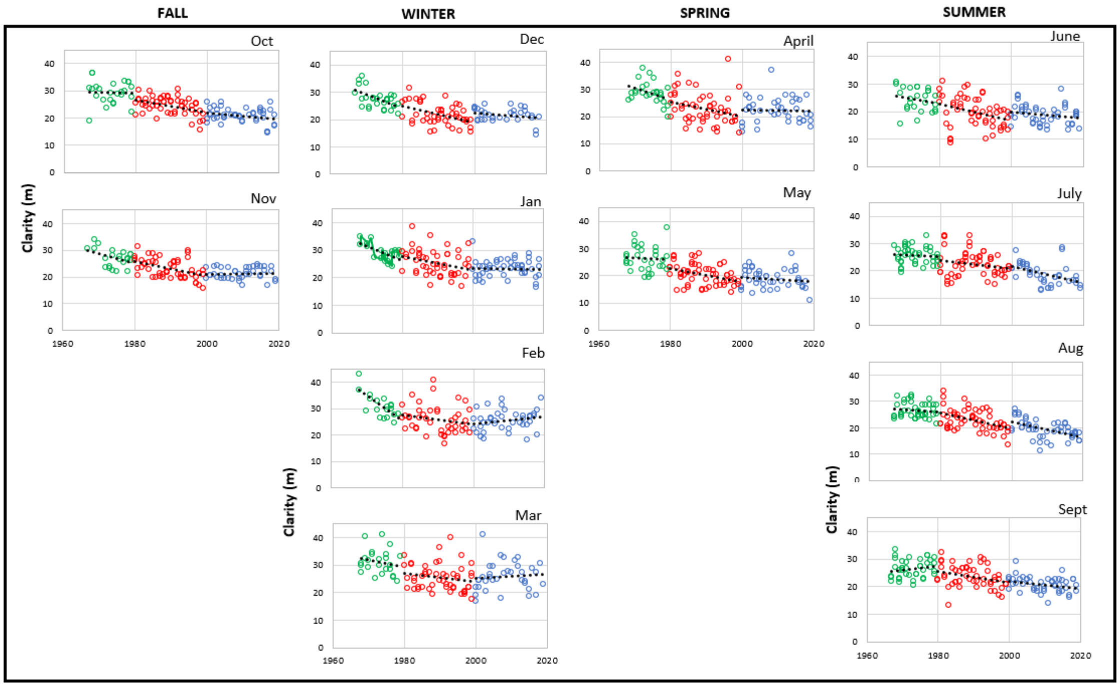

Figure 2.2. Observed Lake clarity in fall, winter, spring and summer periods during 1967-79 (green), 1980-1999 (red) and 2000-2019 (blue) periods. Linear fitted line through each group of observations is represented by black dotted line.

Seasonal variations in clarity are thought to be driven by seasonal drivers such as winter mixing, sediment inflows from streams and urban areas and by biogenic particles (Jassby et al., 1999; Sahoo et al., 2010). Throughout the extent of the clarity monitoring campaign, winter mixing, typically occurring in February or March, improves lake clarity by bringing up clear water from deep within the lake to the surface (Figure 2.3). However, during the 1980-1999 period, a reduction in the monthly median value of clarity occurred in all months, compared to the previous analysis period, despite continuation of the same temporal pattern. Since 2000, reductions in median clarity have occurred in Fall, Summer and May while median clarity values have not changed during the December through April months since 1980. The largest decline in median clarity (10 m) occurred during the month of October.

Table 2.2. Mann-Kendall analysis of clarity trends for individual months. Values of n represent the number of measurements, sign of test statistic Z indicates the sign of the trend, Sen's slope is the rate of change in clarity, in meters per year. Where p-value cells are blank, significance level is greater than 0.05. Results indicate statistically significant declines in clarity for the entire period of record. Trends analysis over 20-year periods with monthly data resulted in no apparent trends for 10 of 12 months.

	FALL		WINTER				SPRING		SUMMER			
	OCT	**NOV**	**DEC**	**JAN**	**FEB**	**MAR**	**APR**	**MAY**	**JUN**	**JUL**	**AUG**	**SEP**
1968-2019												
n	53	51	50	49	50	52	50	52	52	52	53	53
Test Z	-6.2	-5.0	-4.9	-4.1	-2.4	-2.1	-3.7	-4.8	-3.9	-5.0	-6.3	-4.8
P-value	<0.05	<0.05	<0.05	<0.05	<0.05	<0.05	<0.05	<0.05	<0.05	<0.05	<0.05	<0.05
Sen Slope	-0.20	-0.16	-0.17	-0.14	-0.09	-0.10	-0.17	-0.18	-0.16	-0.20	-0.21	-0.15
1968-1979												
n	13	11	13	10	10	12	12	12	12	13	13	13
Test Z	0.5	-0.6	-2.8	-1.3	-2.0	-0.5	-1.0	0.0	-1.0	-1.0	-0.2	1.0
P-value			<0.05		<0.05							
Sen Slope	0.28	-0.42	-0.55	-0.50	-0.80	-0.28	-0.41	0.00	-0.30	-0.34	-0.06	0.18
1980-1999												
n	20	20	20	19	20	20	20	20	20	20	20	20
Test Z	-1.6	-3.5	-2.4	-1.6	-0.7	-0.8	-1.9	-2.0	-1.9	-0.3	-2.3	-1.4
P-value		<0.05	<0.05					<0.05			<0.05	
Sen Slope	-0.19	-0.37	-0.33	-0.30	-0.15	-0.12	-0.28	-0.19	-0.42	-0.03	-0.24	-0.18
2000-2019												
n	20	20	17	20	20	20	18	20	20	19	20	20
Test Z	-0.7	0.6	-1.1	0.2	0.8	0.3	-0.5	-0.8	-1.5	-2.4	-2.1	-1.1
P-value										<0.05	<0.05	
Sen Slope	-0.07	0.04	-0.06	0.03	0.12	0.06	-0.05	-0.21	-0.19	-0.33	-0.29	-0.13

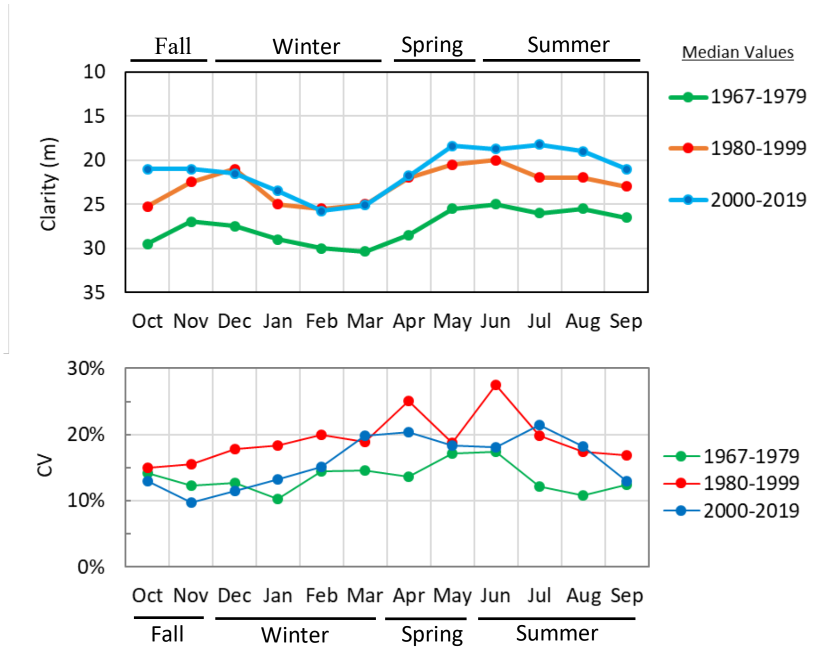

Figure 2.3. Seasonal changes in median (top panel) and coefficient of variation (lower panel; CV = 100 * (standard deviation/mean)) of monthly clarity values for periods 1967-1979, 1980-1999 and 2000-2019.

Variations in monthly clarity can reveal whether seasonal drivers are becoming influential. For example, for the period of record, variations in clarity have been lowest during the Fall and greatest in the Spring and Summer (Figure 2.3, lower panel). During the 1967 to 1979 period the coefficient of variation for clarity ranged from 10% to 17%. From 1980-1999, the corresponding range of variability was 15 to 27%. Values for the most recent period (2000-2019) are 10 to 21%. On average, the variation in clarity readings since 1967 during the Fall and Spring have been relatively stable with a 2% (13% to 11 %) and 3% (15% to 19%) difference since 1967. Since 2000, the variation in monthly clarity during January through September are greater than the variations measured during 1967-1979.

2.5 Summary of Findings for Assessment of Trends

Over the entire period of record (1968-2019), lake clarity has declined significantly, based on analysis considering each month, and for the annual data. However, the most profound findings of the trend analysis pertain to the data from the period 2000-2019. Since 2000, lake clarity values for 10 out of 12 months are not significantly decreasing. Over this period, the slope of the clarity trend cannot be differentiated statistically from zero, for ten months of the year. This is an improvement from the period 1980-1999, where one month in every season or 4 out of 12 months were significantly decreasing. July and August are the only months during the most recent period where statistically significant negative trends were identified. Further, the data shows more variability over Fall, Winter and Spring during the 1980-1999 period compared to other periods. The drivers of this previous variability should be investigated further because it may provide further insight to future clarity conditions during these seasons.

Investigation of Project Hypotheses

3.0 Hypothesis 1: Clarity is controlled predominantly by the distribution and (volumetric) density of *fine particles in suspension*.

3.1 Background

Early investigations of Lake Tahoe water clarity changes focused on phytoplankton productivity and the onset of cultural eutrophication (Goldman 1974, 1994). More recent work has concluded that inorganic particles play a larger role in controlling clarity (e.g. Swift et al. 2006). Jassby et al. (1999) concluded that particles less than 16 μm in diameter most significantly impacted clarity. Coker (2000) concluded that in-lake inorganic particles were dominated by the 1-10 μm size class. Subsequent investigations considered the spatial and temporal distribution of particles, their aggregation, abundance in streams, and impact on light attenuation (Sunman 2001, Terpstra 2005, Swift 2004, Swift et al. 2006). In this report a further refinement to investigate the impact of particles in the 1.0-4.76 μm size range was considered, based on previously published work on the impact of the size of suspended inorganic particles on light transmission. The impact of *Cyclotella* cells, which are organic in origin but contain a silica frustule, was also investigated.

3.2 Data Sets

The hypothesis was investigated by consideration of the fine particle data obtained by UC Davis at the two long-term, in-lake monitoring stations (MLTP, LPT). Characteristics of these datasets are provided in Table 3.1.The hypothesis is focused on the link between clarity and the abundance of particles per unit volume in the lake, regardless of their origin or type. Particle abundance is a more appropriate term than density, since the latter term typically refers to the mass per unit volume of individual particles.

Table 3.1. In-lake datasets used to investigate fine particle abundance and distribution within Lake Tahoe.

Site	LTP	MLTP
Start Date	7/2008	7/2008
End Date	11/2019	11/2009
Sampling Depths (m)	0,2,5,10,15,20,30,40,50	0,10,50
Size Classes (µm)	0.5-0.63, 0.63-0.79, 0.79-1, 1-1.41, 1.41-2, 2-2.83, 2.83-4, 4-4.76, 4.76-5.66, 5.66-6.73, 6.73-8, 8-11.31, 11.31-16, 16-20	0.5-0.63, 0.63-0.79, 0.79-1, 1-1.41, 1.41-2, 2-2.83, 2.83-4, 4-4.76, 4.76-5.66, 5.66-6.73, 6.73-8, 8-11.31, 11.31-16, 16-20

UC Davis uses a laser diffraction instrument (LiQuilaz, Particle Measuring Systems, Inc.) to measure particle abundance for each of 14 particle size classes, ranging from 0.5 to 20 micron (µm; Table 3.1), from discrete samples collected at each depth. Results are reported as particle counts per milliliter (mL). This measurement technique does not provide information on particle origin, shape, or material density.

Suspended particles absorb and attenuate a fraction of light impinging on them. The attenuation efficiency varies in a complex manner with particle size and composition. van de Hulst (1957) showed theoretically that the attenuation efficiency is a maximum at a particle diameter of 1.7 µm for inorganic particles such as quartz, and about 6.5 µm for organic particles, while Davies-Colley Smith (2001) reported corresponding values of 1.2 and 5 µm. At both smaller and larger particle sizes, the magnitude of light attenuation by suspended particles rapidly decreases. Diatoms, being both organic particles and possessing a silica frustule, may exhibit characteristics of both particle types, and given the size range of those commonly observed in Lake Tahoe, may be expected to scatter light at similar attenuation efficiencies. Swift et al. (2006) incorporated many of these concepts in the development of the Lake Tahoe clarity model, based on the data available at the time. Given the hypothesis proposed, the size resolution of the particle analyzer, and published information on light attenuation, particle analysis focused on both the total collection of particles (all sizes) and a subset representing finer inorganic particles in the 1.0-4.76 µm range. Abundance above 4.76 µm is very limited, so the chosen number for the upper bound of this range has little influence on light attenuation or particle size distributions.

3.3 Approach

Eleven years (2008-2019) of particle size data were investigated to determine trends in abundance over time, over depth, and in terms of grain size. *Cyclotella* cell abundance data, derived from labor-intensive microscopy, were available for a portion of the 11-year record.

Correlation analysis was performed to determine the influence of particle abundance on clarity. A separate correlation analysis revealed the impact of *Cyclotella* cell abundance on clarity. Both analyses considered data from the 5 m depth and deviation of clarity from the 20-year mean.

3.4 Results

The finest particles within the measured range of 0.5-20 µm consistently had the greatest abundance, and abundance had little depth-dependence within the range of depths considered. Figure 3.1 shows the abundance over time for the finest size class, observed at the shallower LTP site. This figure shows data from all available observations (typically twice per month) for the top 20 m of the water column (the depth range from 20-50 m shows similar temporal fluctuations in abundance). Other than an anomalous surface reading in 2011, thought to be erroneous, little depth dependence is observed. This is not surprising as particles in the sub-micron size range have Stokes' settling velocities (fall speeds) that are extremely small. A marked increase in particle abundance is evident in 2017, most likely due to the high inflows to the lake in that year following an extended drought. Some reduction is evident since that date, but the mean value for 2017-2019 is higher than over the previous decade.

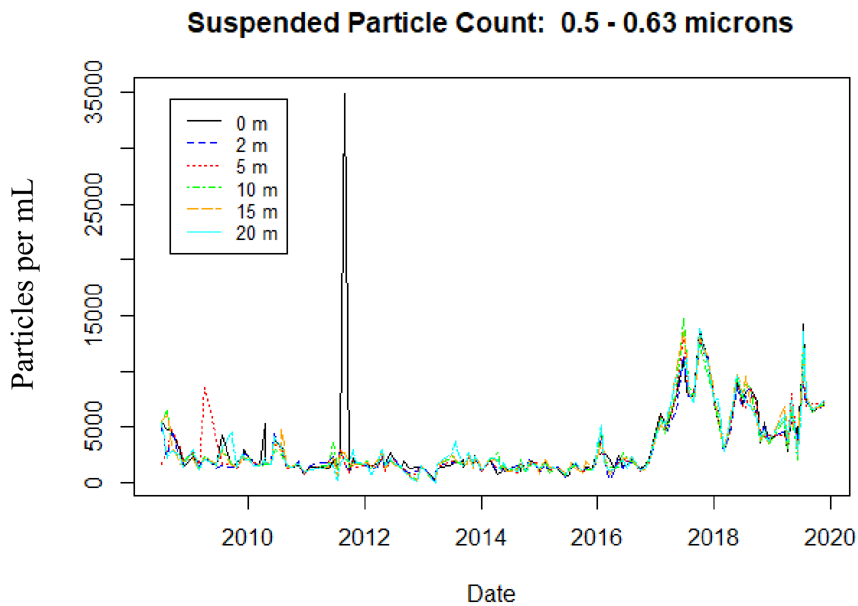

Figure 3.1. Particle count per mL for finest size class (0.5-0.63 µm) at LTP site. 2011 spike at 0 m depth is thought to be erroneous.

An annual periodicity is more evident in some of the time series for slightly larger size classes (Figure 3.2). The number of particles per unit volume decreases with increased particle size, as seen when comparing the scales on the y-axes in Figures 3.1 and Figure 3.2. The two smallest size classes (0.5-0.79 µm) typically represent 2/3 of the total number of particles in a sample. Above 4 µm, particle counts are in the range of tens to hundreds of particles per milliliter. The periodicity apparent in Figure 3.2 is less evident in the larger size classes, but all particle sizes reveal a large increase in abundance beginning in 2017. The annual periodicity may be partially attributable to seasonal abundance of cells, discussed further below.

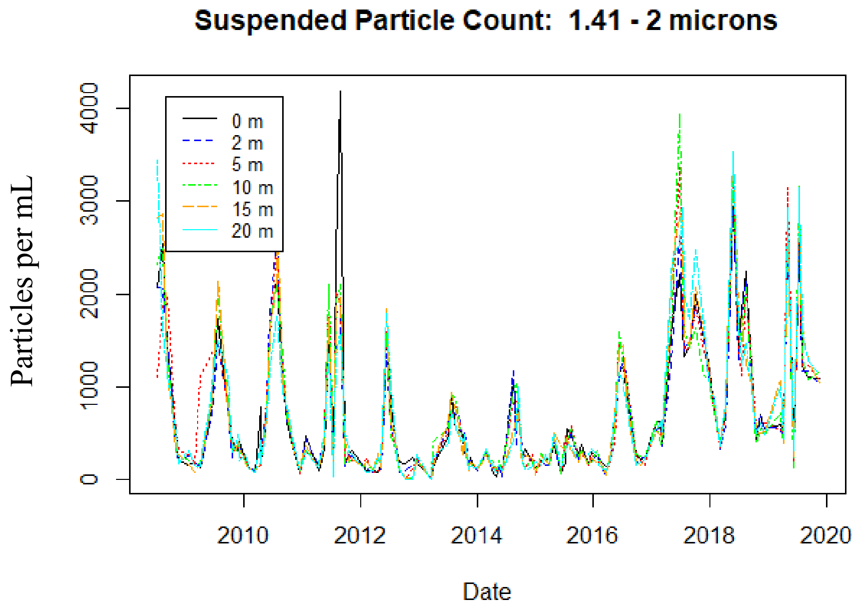

Figure 3.2. Particle count per mL for 1.41-2 µm size class at LTP site. 2011 spike at 0 m depth is thought to be erroneous.

Mean particle size was consistently between 0.8 and 1.2 microns, with little depth or time dependence. Analysis of the 2008-2019 time series data for each depth revealed that there are no statistically significant trends in the annual mean value of the mean grain diameter. However, the 11-year period analyzed is likely too short for interpretation of interannual trends.

Figure 3.3 shows particle abundance by season for 2008-2019, focusing on data from a depth of 5 m and particles in the optically significant 1.0-4.76 µm range. Each of the years 2016-2019 had a large increase in particle abundance, compared to previous years, but in different seasons. Significantly, though, rather than high concentrations of particles being present predominantly in the summer only (as was the case in 2009 to 2015, with the exception of spring 2009), the spring and even the fall had markedly high concentrations in 2017-2019. This extension of the “high particle concentration” time of year may influence the annual average clarity. The years 2012-2015 featured high clarity (mean Secchi depth 22.6 m). The years 2016-2019 featured lower clarity (mean Secchi depth of 22.0 m).

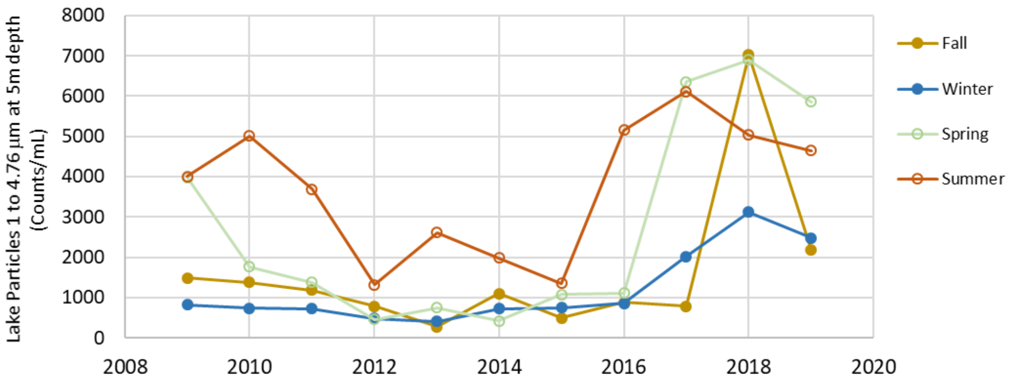

Figure 3.3. Interannual and seasonal variability in lake particle abundance for 1.0-4.76 µm size class, in particles per mL, observed at 5 m depth, 2009-2019. Each point represents a mean value for the season and year represented.

An example of seasonal dependence is evident in the time series showing the distribution of particles throughout the water column for 2018. Figure 3.4 reveals the influence of mixing events, occurring around March, that result in more particles appearing at greater depths and a dilution of particle abundance near the surface. During the rest of the year, most of the measured particles are above the 50 m depth, where most data are collected, and there is little depth-dependence in the particle abundance above this depth.

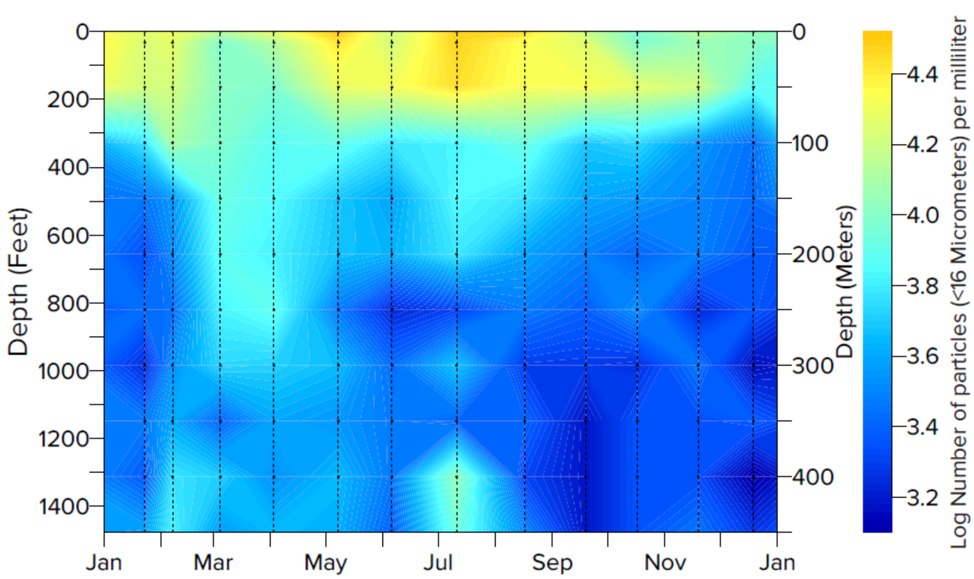

Figure 3.4. Time- and depth-dependence in number of particles in the lake per unit volume during calendar year 2018. Plot represents all measured particles with estimated sizes below 16 µm. From 2019 State of the Lake report (Schladow et al. 2019).

A similar analysis of particle abundance was conducted with the data from the MLTP site, where the depth resolution was limited to 0, 10, and 50 m. Results were similar to what was found at the LTP site, in that 70-80% of the suspended particles were less than or equal to one µm in size, little depth-dependence was evident down to 50 m, and there was a large increase in particle abundance in 2017 that likely resulted from high inflows of sediment from streams. No statistically significant trend was identified in the particle abundance versus time datasets for any depth. Correlation of particle abundance in the lake with that observed at streams will be discussed in the next section.

The mean value of water clarity for the 2008-2019 record was computed and subtracted from the clarity time series to yield a "clarity deviation" time series that is plotted as the gray line in the middle panel of Figure 3.5. The lower panel in this figure shows the correlation between clarity deviation and the log of the particle abundance for the 1.0-4.76 um range at 5 m depth. There is a weak negative correlation between clarity deviation and particle abundance at this depth (R^2 = 0.397). This correlation also indicates that during spring and summer periods, particle counts can exceed 1000 counts/mL and have a negative impact on lake clarity. Values less than 1000 do not appear to have a negative impact on lake clarity.

Figure 3.6 presents similar results based on estimated abundance of *Cyclotella* cells. *Cyclotella* are very small diatoms that were first reported in Lake Tahoe in 1975 (Richards et al. 1975) and more recently have been reported as displaying a decreasing size over time (Winder et al. 2008). A negative correlation between clarity deviation from the mean and *Cyclotella* is found (R^2 = 0.288). A negative impact to clarity is apparent when *Cyclotella* has exceeded 100 counts/mL which typically occurs in summer and fall. Counts of *Cyclotella* less than 100 do not appear to have a negative impact on lake clarity. Seasonal variation in *Cyclotella,* lake Particles and lake clarity are shown in Appendix A2.

Taken together, Figures 3.5 and 3.6 suggest that both the abundance of particles in the 1.0-4.76 µm range and the abundance of *Cyclotella* cells impact clarity, but do not fully explain observed trends. The quantitatively weak correlations indicate that other factors or processes are also influencing clarity.

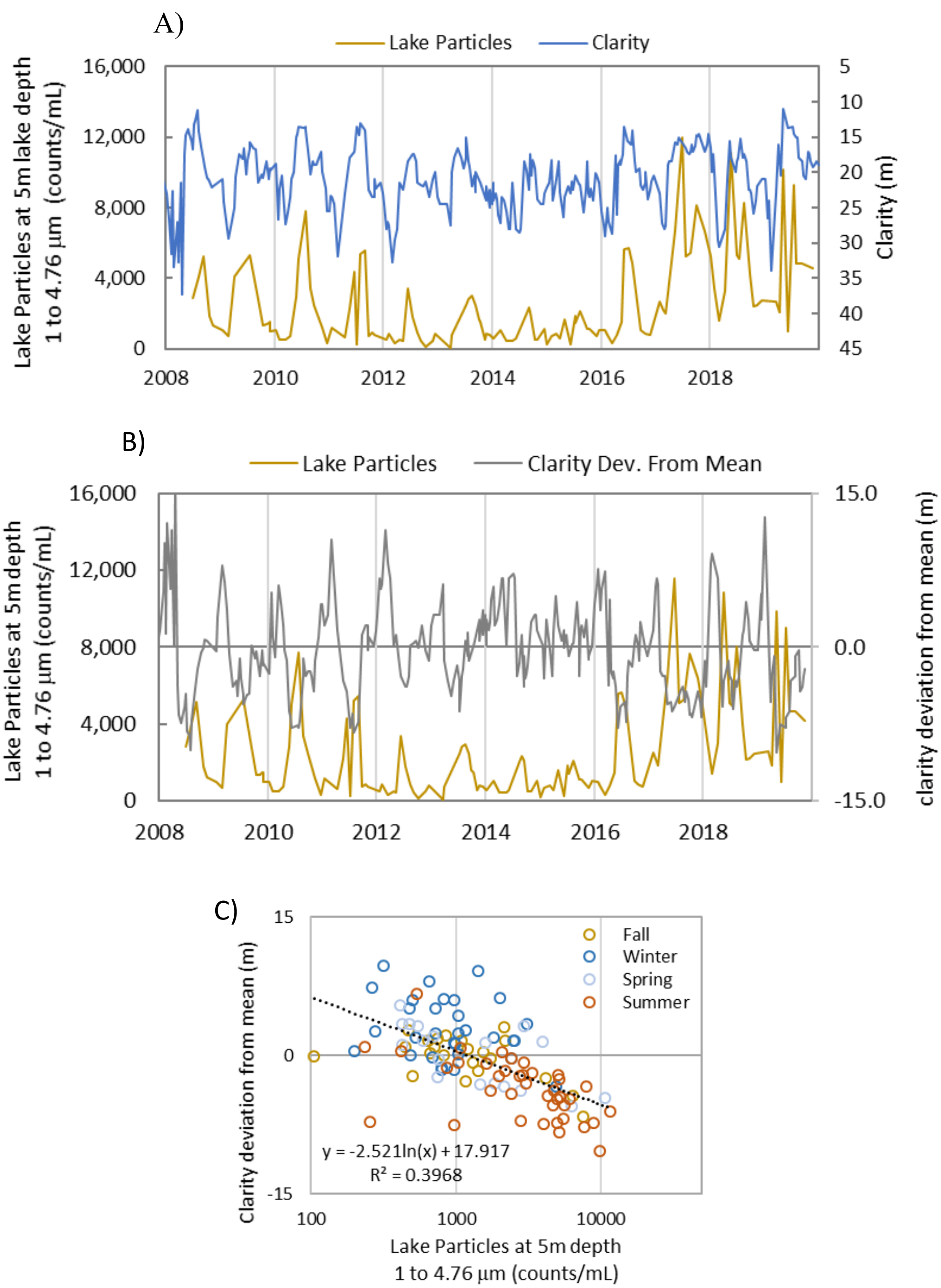

Figure 3.5. Time series of (A) clarity and particle abundance in the lake per mL within the 1 to 4.76 µm size range, (B) clarity deviation from mean and particle abundance and (C) clarity deviation from mean vs. Log of particle count per season with the best-fit line through all data (black dash).

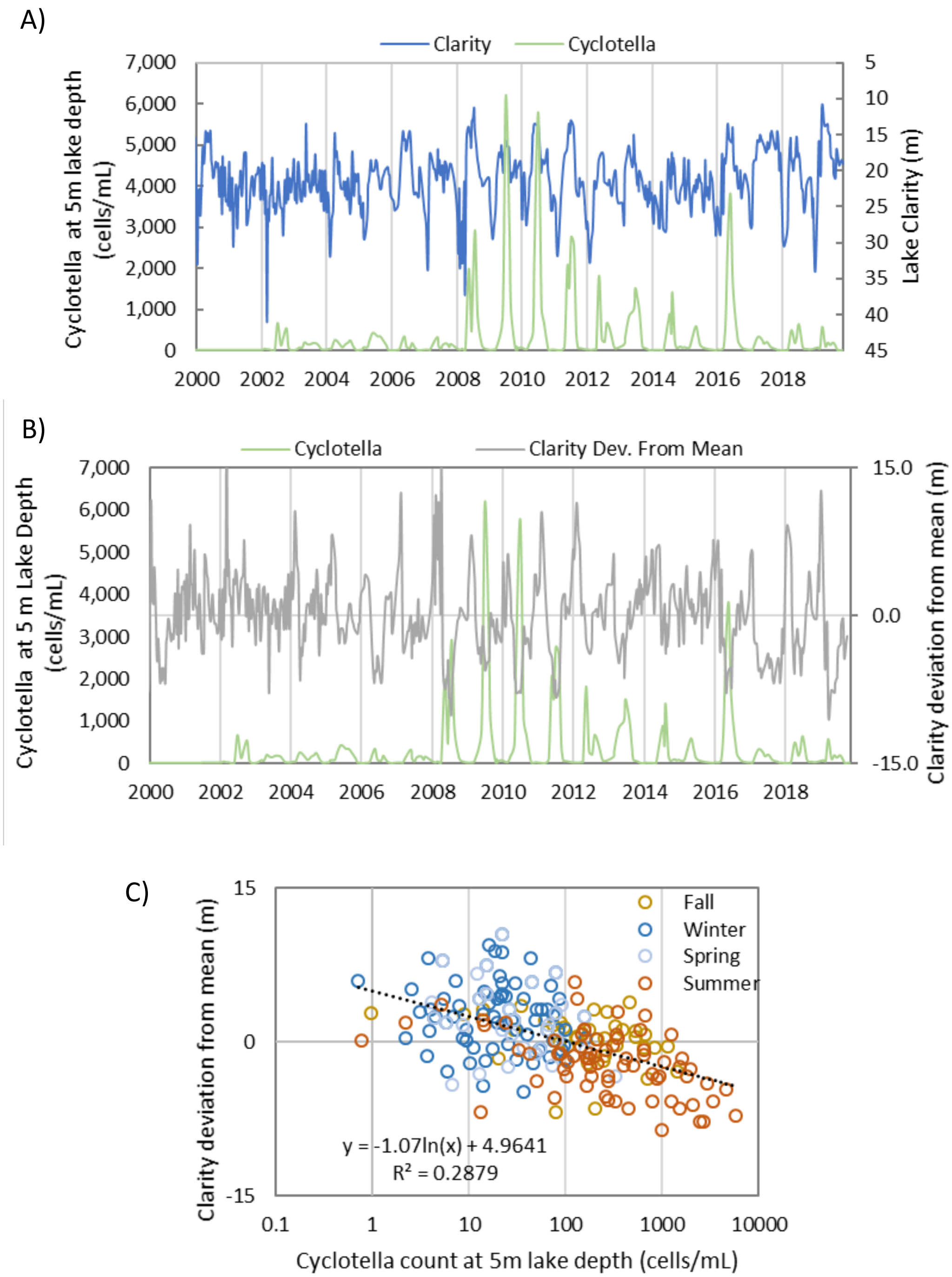

Figure 3.6. Time series of (A) clarity and abundance of *Cyclotella* in cells per mL, (B) clarity deviation from mean and *Cyclotella* abundance and (C) clarity deviation from mean vs. Log of *Cyclotella* abundance per season with the best-fit line through all data (black dash).

The particle abundance data include *Cyclotella* cells, both live and dead. Figure 3.7 shows time series of both the total particle abundance and estimated number of *Cyclotella* cells. At times in the past, the brief peaks in particle abundance have coincided with *Cyclotella* peaks, and reduced clarity. However, the high particle abundance in 2017-2019 do not appear to be correlated with the trend in *Cyclotella* at the 5 m depth. The order of magnitude increase in particle abundance (0.5-20 µm) that began in 2017 did not lead to a similarly dramatic decrease in clarity, lending support to the finding that particles of different sizes have different relative influences on clarity.

2017 featured exceptionally high stream inflows to Lake Tahoe. The four years of peak *Cyclotella* abundance (2008-2011) had the three lowest years of summer Secchi depth ever recorded. The next lowest Secchi depths were recorded in 2017 and 2019 when Cyclotella abundance was low, indicating the distinct roles of both inorganic and organic fine particles.

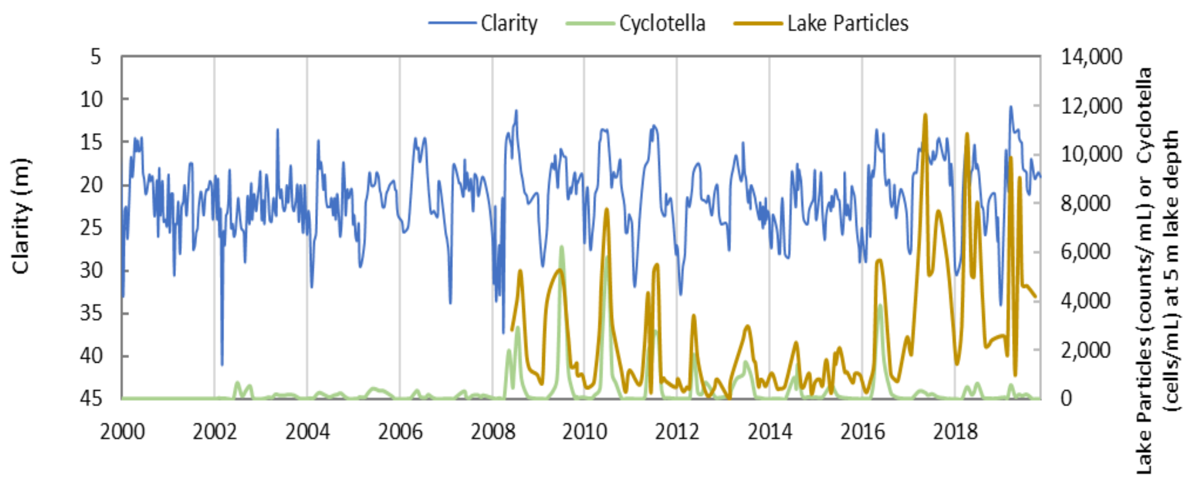

Figure 3.7. Time series of lake clarity with counts of total lake particles (1-4.76 µm) per mL and Cyclotella cells per mL at 5 m depth at LTP site.

There is a positive statistically significant correlation (p-values < 0.05) between the inverse of the Secchi disk depth and particle abundance, for different subsets of the sediment size range (Figure 3.8). The strongest regression is for the particle fraction larger than 1 µm, which is consistent with the earlier conclusion that both organic and inorganic particles below one µm exert little impact on clarity compared to those slightly larger.

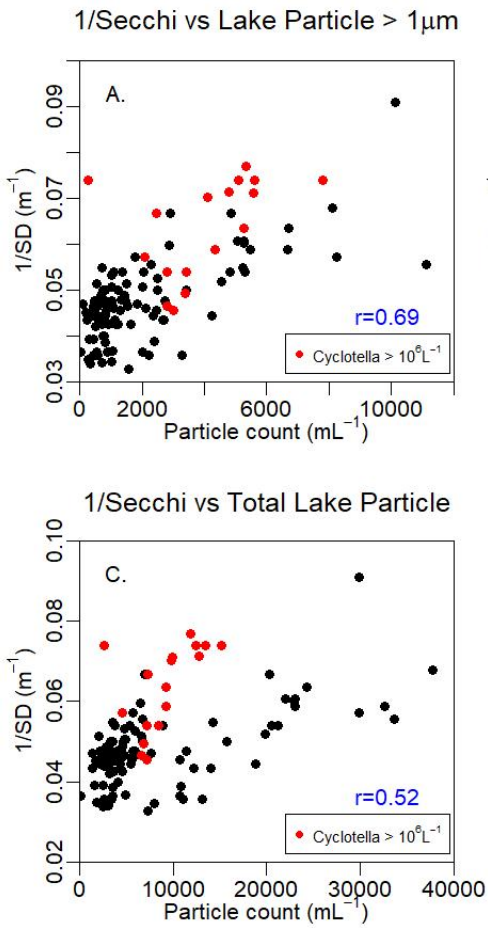

Figure 3.8. Inverse of Secchi disk depth (SD) vs. particle abundance for particles greater than (top left) and less than (top right) 1 µm, and for all size classes (bottom left). Observations featuring more than 1 million Cyclotella cells per liter at a 5 m depth are shown with red symbols.

3.5 Summary of Findings for Hypothesis 1

The hypothesis investigated in this section is restated here:

"**Clarity is controlled predominantly by the distribution and (volumetric) density of *fine particles in suspension*.**"

The evidence shown above, based on data for the period 2008-2019 and size range 0.5-20 µm, suggests that fine particles greater than 1 µm in size do exert a measurable influence on clarity, but that not all particle sizes contribute equally, and other factors also likely play a role. A large observed increase in the abundance of particles <1 µm in size, beginning in 2017 (with a brief high in summer 2016), did not result in a similarly abrupt reduction in clarity. The abundance of particles in the size range of 1.0-4.76 µm is more strongly correlated with Secchi depth, and high counts of Cyclotella tend to coincide with reduced Secchi depth. But decreases in Secchi depth are also evident at times when Cyclotella are only a small fraction of the particle distribution.

Considering all observed particle sizes 0.5-20 um, there was no statistically significant trend in annual lake particle abundance or mean particle size. The large increase in abundance observed in 2017 is likely the result of the high flows and sediment loads that occurred in 2017.

4. Hypothesis 2: The change in trend of winter clarity is a response to decreasing *fine suspended sediment concentrations* resulting from load reductions.

4.1 Background

Following reviews and discussions with agency representatives, investigation of this hypothesis required consideration of three questions:

1) Is there a statistically significant trend in the amount of fine suspended sediment in the lake?

2) Is there a trend in the loading of fine sediment to the lake? Potential sources include tributary streams, runoff from urbanized areas, and direct atmospheric deposition onto the lake's surface.

3) Is the fine sediment concentration in the lake correlated with in-lake clarity time series data?

The first and third of these questions have already been addressed to some degree in the discussion of the previous hypothesis, which was focused on all types of particles, not just those that are terrigenous in origin. Figure 3.7 includes a comparison of the estimated number of *Cyclotella* cells in suspension in the lake, compared to the number of particles in the 1-4.76 µm range, and shows that there have been times when these numbers have similar magnitudes. This has not been true since 2016, however. The relative abundance of fine sediment particles and *Cyclotella* varies by year and season. Also note that the data describing *Cyclotella* abundance are from the 5 m depth.

4.2 Data Sets

As with Hypothesis 1, this hypothesis was investigated by consideration of the fine particle data obtained by UC Davis at the two long-term, in-lake monitoring stations (MLTP, LPT).

Table 3.1. In-lake datasets used to investigate fine particle abundance and distribution within Lake Tahoe and from urban surface runoff measured by Tahoe Regional Stormwater Monitoring Program (RSWMP), where RSWMP provides estimates of total fine sediment particle (FSP) loads (0.5-16µm).

Site	LTP	MLTP	RSWMP
Start Date	7/2008	7/2008	10/2013
End Date	11/2019	11/2019	9/2019
Sampling Depths (m)	0,2,5,10,15,20,30,40,50	0,10,50	Surface runoff
Size Classes (µm)	1-4.76	1- 4.76	FSP (0.5-16µm)

4.3 Approach

Eleven years of data were available describing the abundance of fine particles (0.5-20 µm) in the lake and selected tributaries. The correlation between stream and lake particle counts was investigated with summer and winter subsets of the data. Fine sediment particle loads from the Upper Truckee River and urban loading derived from the seven RSWMP monitoring locations were inspected to reveal both the seasonal variations in loads and the overall trends in data. The six-year duration of data available for urban loads and the four-year period for pollution reduction credits was not long enough to demonstrate the influence of load reduction on winter clarity trends that have changed over the last 20 or more years.

4.4 Results

4.4.1 Lake and Stream Particles

Considering the full range of sediment sizes in the 0.5-20 µm range (2008-2019), there is no statistically significant trend of increasing or decreasing total number of particles at the two long-term lake monitoring stations, considering both annual values and winter values. This count contains both organic and inorganic particles.

Figure 4.1 shows summer particle counts at the monitored lake tributaries, which deliver water and sediment to the lake from primarily undeveloped sub-watersheds, and at monitoring stations within the lake (in-lake counts represent an average of the top 50 m of the lake). Particle count data are typically available no more than 2 times per month for the streams, and monthly for the lake, albeit at multiple depths. For each month of the respective records, a mean value of the particle count within the 1-4.76 µm range was determined. This resulted in a monthly time series of particle abundance for each site. The time series for the streams were compared to observations in the lake to evaluate the correlation between these values.

Figure 4.1 reveals a large increase in particle abundance at the monitored tributaries in the summer of 2017 (June-September). The abundance of particles increased in 2017 and a similar increase is evident at both in-lake monitoring stations. Figure 4.2 contains similar plots for the winter (Dec-Mar) months. Correlation between particle abundance at the tributaries and in the lake is high (Table 4.1). Similar results were obtained by Sunman (2004) and Rabidoux (2005) during the TMDL studies (Lahontan Regional Water Quality Control Board and NDEP, 2010).

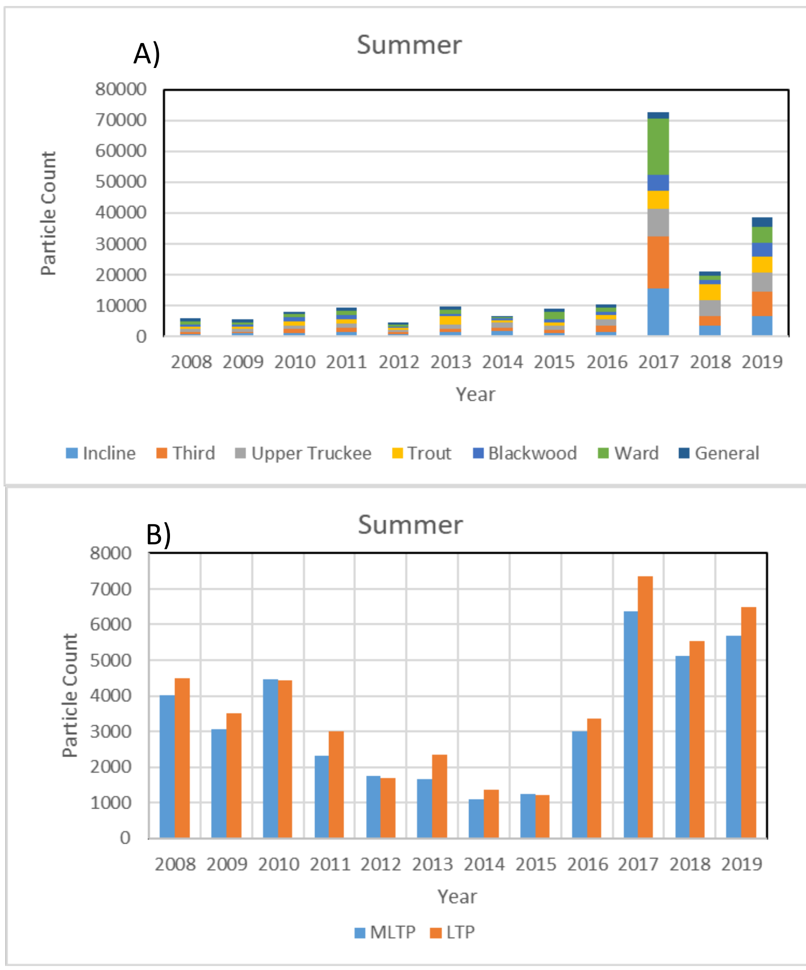

Figure 4.1. Summer particle counts at A) monitored tributaries to Lake Tahoe, and B) at the two in-lake monitoring stations LTP and MLTP. Particle counts are per milliliter and include all particles in the 1-4.76 µm size range. Mean monthly values were averaged to determine seasonal averages. In-lake values are vertically averaged over the top 50 m of the lake.

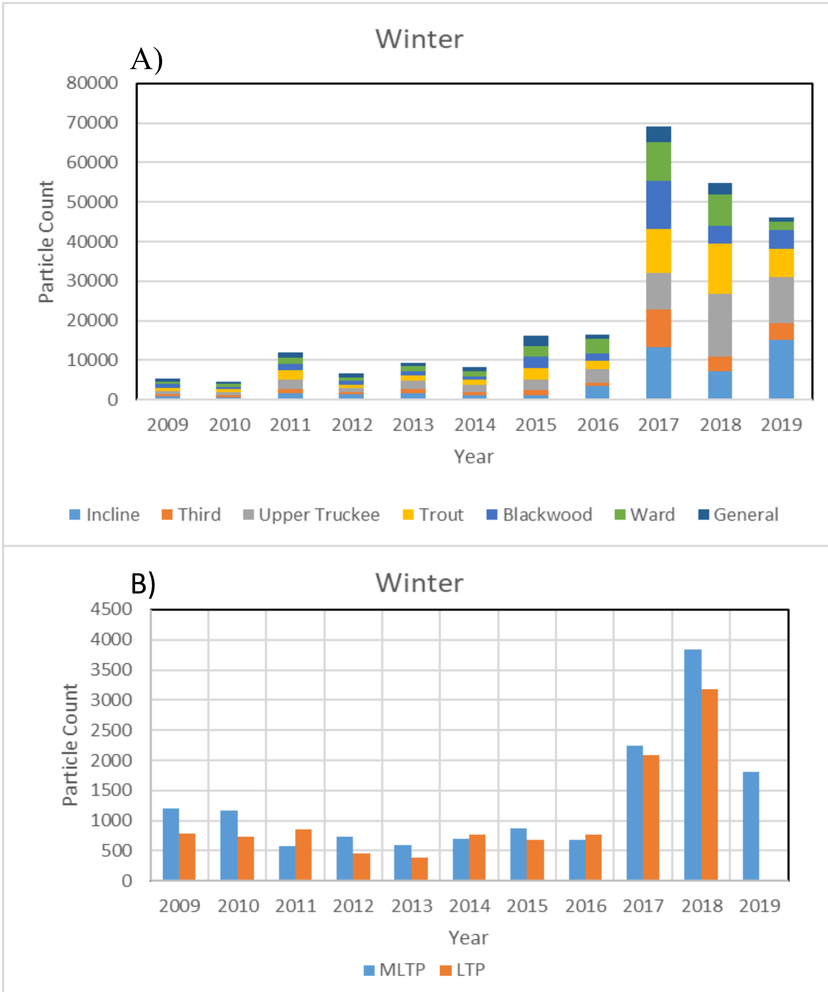

Figure 4.2. Winter (water year definition) particle counts at monitored tributaries A) to Lake Tahoe, and B) at the two in-lake monitoring stations LTP and MLTP (bottom). Particle counts are per milliliter and include all particles in the 1-4.76 µm size range. Mean monthly values were averaged to determine seasonal averages. In-lake values are vertically averaged over the top 50 m of the lake.

Particle data for most sites are typically available only two times per month; as a result, peak inflows could be missed, or in other cases overemphasized, in the total. Greater temporal resolution of data describing particles in streams is needed in order to have a clear picture of actual sediment loading. Another option is to convert more frequent turbidity data to suspended sediment concentration data and collect field samples to quantify the fine fraction. Quantifying sediment loading to the lake from streams also would be helpful but cannot be done with the available data.

Based on total precipitation during the water year, the three wettest years within the available record are 2011, 2017, and 2019. The last two of these years also feature very high numbers of particles at the tributaries and in the lake. Drier years feature lower numbers of particles in the tributaries, but the overall correlation of particle abundance in tributaries and in the lake is high (Table 4.1).

In winter, Upper Truckee River and Trout Creek have the highest correlation coefficients and are the best proxies for particle counts at the two lake observation stations. In summer, Trout Creek observations are the best proxy. Trout Creek is also the best proxy when the entire year is considered. This analysis compares simultaneous values, with no accounting for time that might be required for particles introduced at streams to reach the observation stations. Moreover, the particle counts at the in-lake stations include *Cyclotella* cells, whereas it is assumed that the stream counts do not.

Table 4.1. Correlation coefficients between in-lake particle counts and LTIMP tributary particle counts considering the 1-4.76 μm size range, 2009-2019. For example, the first number of 0.60 in the table is the correlation coefficient when comparing particle counts observed at Incline Creek in winter to the count observed at the MLTP station in winter. In the last column, BL+WRD+GN represents the sum of counts for Blackwood Creek, Ward Creek and General Creek, which are proximal to the LTP lake station.

Location	Incline Creek	Third Creek	Upper Truckee River	Trout Creek	Blackwood Creek	Ward Creek	General Creek	All LTIMP streams	BL+ WRD+ GN
	Winter Season								
MLTP	0.60	0.61	0.90	0.91	0.57	0.76	0.65	0.81	
LTP	0.76	0.66	0.97	0.96	0.64	0.86	0.76	0.88	0.77
Summer Season									
MLTP	0.70	0.72	0.77	0.97	0.75	0.63	0.75	0.74	
LTP	0.75	0.76	0.81	0.95	0.78	0.67	0.80	0.78	0.74
Annual									
MLTP	0.84	0.85	0.87	0.96	0.86	0.81	0.86	0.86	
LTP	0.83	0.84	0.87	0.93	0.83	0.78	0.85	0.84	0.81

4.4.2 Urban Fine Sediment Loads

The analysis above did not explicitly consider fine sediment loading to the lake from urbanized areas, although urban areas do contribute runoff to LTIMP streams as well as directly to the lake. Urban loading estimates are discussed in more detail below, but the correlations observed between particle abundance in streams and abundance in the lake suggests either that a) stream loading is dominant in controlling in-lake particle abundance, b) urban loading is closely synchronized in time with stream loading, or c) lake hydrodynamic processes are mixing or attenuating the relative influence of these sources. Figure 4.3 suggests that the timing of urban loads is similar to stream loading in the Upper Truckee River, as would be expected if urban loading is driven by the same hydrologic events that lead to high counts in the monitored river. Urban runoff is typically more variable than stream runoff, however, and the drainage area represented by urban monitoring is sparse. Only about 1.5% of total urban area in the Tahoe Basin is monitored by RSWMP, whereas the Upper Truckee River represents 18% of total land area in the Tahoe Basin and about 25% of annual stream discharge to the lake (Lahontan and NDEP 2010).

A major conclusion of the TMDL Technical Report (Lahontan and NDEP 2010) was that urban fine sediment particle (FSP) contributions represented approximately 80% of the total fine particle flux. Coincident with the large runoff year in 2017, and continuing in the two following years, there has been a pronounced increase in stream particle concentrations (Fig. 4.1 and 4.2), which manifests as a large absolute and relative increase in FSP loading from the Upper Truckee River compared to urban sites (Fig. 4.3). Also of note, many urban best management practices (BMPs) were implemented during the years following the 2003-2004 TMDL stormwater calibration, and benefits from these BMPs are now implicitly represented in RSWMP data collected from 2013 through 2019. Furthermore, precipitation for the 2003 and 2004 water years was below average (~83% of WYs 1981-2019). A tighter coordination between upland stream and urban monitoring programs could facilitate these comparative evaluations in the future.

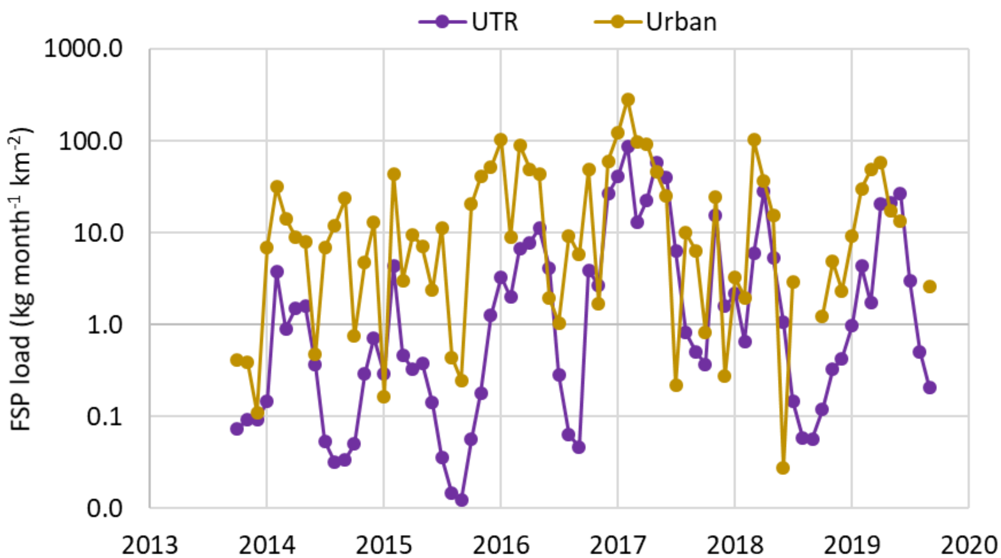

Figure 4.3. Comparison of fine sediment particle (FSP) loading to the lake based on Upper Truckee River (UTR) measurements and urban loading derived from the seven RSWMP monitoring locations identified in Table 4.2. Data are presented in terms of sediment mass, as consistent with reported FSP (0.5-16 μm) loads from RSWMP urban sites, normalized to area.

4.4.3 Contributions via Runoff from Urbanized Areas

The Tahoe Regional Stormwater Monitoring Program was developed to coordinate urban runoff monitoring across the Tahoe Basin for consistency of data acquisition, analysis and reporting. Specifically, it was implemented in support of the Tahoe TMDL (Total Maximum Daily Load) and it is used to meet jurisdictional permit requirements for the TMDL. Lake Clarity credits are a TMDL progress tracking tool based on modeled annual average load reductions acquired from aggregate BMP (Best Management Practice) implementations by each of the seven basin jurisdictions. These results are reported each year as part of the Lake Clarity Crediting Program (LCCP), which focuses on load reductions in the urban upland source category.

The most recent LCCP report summarizes TMDL implementation accomplishments through 2019 (LCCP, 2020). It presents progress with load reductions compared against baseline loading amounts, with the baseline representing 2004 conditions (Appendix 2). Annual load reductions are estimated from jurisdictional registrations within the LCCP Stormwater Tools accounting platform, which includes a Pollutant Load Reduction Model used to calculate reduced loadings (https://clarity.laketahoeinfo.org/Home/UrbanJurisdictions). Both the LCCP and RSWMP report loads in pounds (e.g., as lbs/yr from watershed or lbs/yr/ac). The LCCP estimates that one pound of fine sediment particles (FSP<16 μm) is approximately equivalent to 5×10^{13} particles (Appendix 2). RSWMP calculates FSP load from samples collected at RSWMP monitoring sites and analyzed for particle size distribution and mass (TRCD 2020).

Initial RSWMP monitoring sites were established in 2014, with several sites added subsequently and other sites discontinued (Table 4.2). Sites were selected to represent runoff from a range of land use categories, and for assessment of changes associated with BMP implementations within drainages from around the Tahoe Basin. Given the focus of this analysis on urban runoff association with clarity patterns, we removed sites from analysis that have been discontinued, are inflows to BMPs, or have less than five years of data. The remaining seven established monitoring sites represent a relatively short period of record (2014–2019) compared to Secchi clarity depth and most other watershed variables. Comprising this 6-year stormwater monitoring record are two initial years of severe drought, an extreme winter precipitation in 2017, and three years of average or above average precipitation.

Table 4.2. RSWMP urban monitoring stations. Site IDs of stations selected for statistical analysis in this report are shown in blue bold text (CO, JO, PO, SB, TV, TA, UT). The CICU category references mixed commercial, industrial, communications and utilities land use (TRCD 2020).

Station Name	Site ID	Latitude	Longitude	Drainage (acres)	Water Years on record	Dominant land use
Contech Inflow	CI	39.27436	-119.946	0.7	2014-2019	primary road (100%)
Contech Outflow	**CO**	39.27431	-119.947	0.7	2014-2019	primary road (100%)
Incline Village	IV	39.24028	-119.949	83.6	2014-2016	multi-family residential (38.2%)
Jellyfish Inflow	JI	39.27431	-119.947	0.7	2014-2019	primary road (100%)
Jellyfish Outflow	**JO**	39.27425	-119.947	0.7	2014-2019	primary road (100%)
Elks Club	EC	38.87345	-120.002	14.4	2018-2019	single family residential (50.0%)
Lakeshore	LS	39.24022	-119.946	97.8	2017-2019	multi-family residential (43.2%)
Pasadena Inflow	PI	38.94443	-119.981	78.8	2014-2017	single family residential (52.4%)
Pasadena Outflow	**PO**	38.94468	-119.981	78.8	2014-2019	single family residential (52.4%)
Rubicon	RI	39.01548	-120.118	13.8	2014-2015	single family residential (75.9%)
Speedboat	**SB**	39.2252	-120.01	39	2015-2019	single family residential (35.9%)
Tahoe Valley	**TV**	38.92064	-119.998	338.4	2015-2019	CICU (20.3%)
Tahoma	**TA**	39.06744	-120.126	49.5	2014-2019	single family residential (41.2%)
Upper Truckee	**UT**	38.92239	-119.99	10.5	2015-2019	CICU (39.3%)

4.4.4 RSWMP data analysis

RSWMP sites monitor runoff events and meteorological conditions throughout the year (TRCD 2020). Volumetric flow rates are calculated from transducer or bubbler stage readings continuously recorded throughout the water year at five- or ten-minute intervals. Runoff samples from selected events are collected by autosamplers at each site and used to create volume-weighted event mean composites (EMCs) for subsequent laboratory analysis of pollutant concentrations. When combined with runoff volumes these sample results produce reliable estimates of event loading amounts. The event loads are used to calculate annual, seasonal and monthly loads for each site (https://monitoring.laketahoeinfo.org/RSWMP). Data are presented in pounds of pollutant loads per month from the drainage for total phosphorus (TP), total nitrogen (TN) and fine sediment particles (FSP <16µm). Total suspended solids (TSS) are also analyzed for loading estimates. The data were converted from pounds to kilograms for our statistical evaluations.

Monthly loads were summed across RSWMP sites (Appendix 2), and then totaled by month over each water year (WY) of record for comparison to annual or seasonal Secchi clarity. Our analysis of trends and correlations with lake clarity and other water quality variables was applied to these data. In addition to site precipitation measurements, we also evaluated SNOTEL data from the Tahoe City Cross (TCX) station to represent Tahoe Basin precipitation at a slightly higher elevation (6797 ft). Association between variables was evaluated by Pearson product moment correlation. Trends analysis for precipitation-normalized loading by water year was conducted with a rank-based non-parametric approach, using Kendall's Tau for correlation (with associated probability) and a Theil-Sen estimator for best fit lines.

4.5 Results from urban data analysis

The year with highest average annual loads for RSWMP sites was WY 2017, an exceptional precipitation year, while low precipitation amounts during the drought years of 2014 and 2015 yielded correspondingly low annual loads (Table 4.3).

Table 4.3. Average annual loading of measured pollutants and precipitation from seven RSWMP urban sites by water year (WY). Annual precipitation from the Tahoe City Cross (TCX) SNOTEL site is also shown for these years.

WY	No. of Urban Sites	Avg WY TP (kg)	Avg WY TN (kg)	Avg WY TSS (kg)	Avg WY FSP (kg)	RSWMP Avg Precip (in)	TCX Precip (in)	WY Secchi Depth (m)
2014	4	2.2	3.5	719	384	18.26	24.6	23.8
2015	7	2.0	5.9	604	343	16.71	22.6	22.3
2016	7	7.4	15.9	1912	1515	25.16	41.8	21.2
2017	7	20.2	78.0	4549	2883	45.92	78.0	19.8
2018	7	5.9	21.4	1610	681	21.43	37.1	20.0
2019	7	5.8	22.6	1286	680	23.74	51.7	20.1

Amongst annual average pollutant loads from RSWMP sites, the highest Pearson's correlation coefficient for annual average Secchi clarity (Figure 4.5) was found with TN ($r = -0.67$), followed by TP ($r = -0.64$), TSS ($r = -0.63$) and FSP ($r = -0.55$). However, none of these correlations are statistically significant ($p > 0.05$). An equivalent analysis with annual winter Secchi clarity produced lower correlation coefficients and no statistically significant results.

Correlations of WY RSWMP average loads with calendar year (CY) Secchi are slightly stronger and are significant (p-value ≤ 0.05) for TN, RSWMP precipitation, and TCX, suggesting a potential carryover effect into fall (Oct-Dec). The association of monthly RSWMP data with Secchi clarity is not as strong as with the annual averages, but did show statistically significant correlations for FSP ($r = -0.40$, $p < 0.001$) and TP ($r = -0.39$, $p < 0.01$) with a four-month lag time relative to percent change in Secchi depth.

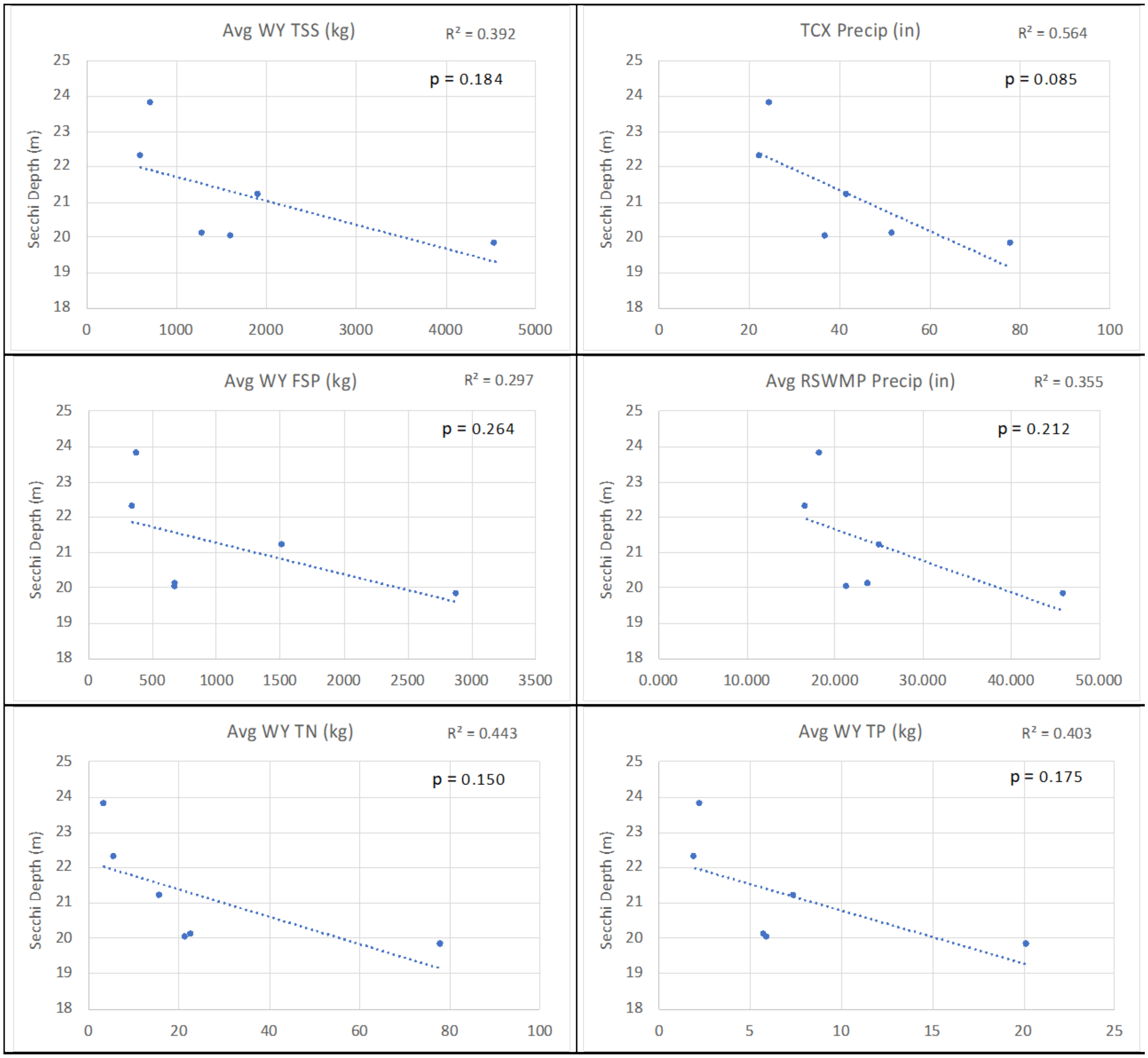

Figure 4.5. Annual average pollutant loads from RSWMP sites (Table 4.4). Secchi clarity at 23.8m represents WY 2014 data, during which only four of the seven monitoring sites were operational. Dashed lines show best-fit line through data points, with corresponding equation and R^2 value shown in each subplot. None of these relations between pollutant load and Secchi depth are statistically significant ($p > 0.05$).

Trend detection at monitoring sites is problematic with only six consecutive years of runoff data, especially given the variability of watershed processes among sites. Thus, it is not surprising that precipitation-normalized RSWMP results at sites through WY 2019 show no statistically significant trend, except at the Speedboat site where both TP and TN loads have apparently increased slightly over time (TRCD 2020).

Aggregating data from all seven RSWMP sites provides a broader perspective on loading trends within the Tahoe Basin, although still limited by the short period of record and number of sites. RSWMP average loading rates were calculated for each water year by taking the sum of all site loads and then normalizing to total drainage area and to average water year precipitation. These results are shown in Table 4.4.

Table 4.4. Average loading rates (kilograms per acre per inch of precipitation) for measured pollutants from RSWMP urban monitoring sites normalized to area and precipitation by water year (WY).

WY	No. of Urban Sites	Area of Drainages (ac)	TSS (kg/ac/in)	FSP (kg/ac/in)	TN (kg/ac/in)	TP (kg/ac/in)
2014	4	129.7	1.2146	0.6487	0.0059	0.0038
2015	7	517.6	0.4891	0.2774	0.0047	0.0016
2016	7	517.6	1.0277	0.8143	0.0086	0.0040
2017	7	517.6	1.3396	0.8489	0.0230	0.0059
2018	7	517.6	1.0159	0.4297	0.0135	0.0037
2019	7	517.6	0.7325	0.3875	0.0129	0.0033

Although normalization helps reduce some of the influence from variability introduced by differences in land use characteristics, drainage areas, and precipitation rates among sites, water year data remain quite scattered. Therefore, trends were assessed with non-parametric Kendall Tau correlation coefficients and Theil-Sen estimators for best-fit lines, which are more resistant to outliers than standard parametric techniques. Best-fit lines for annual average TSS and FSP normalized loading rates decrease over time, while TN increases, but none of these results are statistically significant (Figure 4.6). Notably, six data points represents a very short record for this type of evaluation, even with non-parametric techniques on normalized data, so continued data collection will be essential to support future trends analysis. Additional sites with appropriate representation and statistical sampling design would also improve the quality of these analyses.

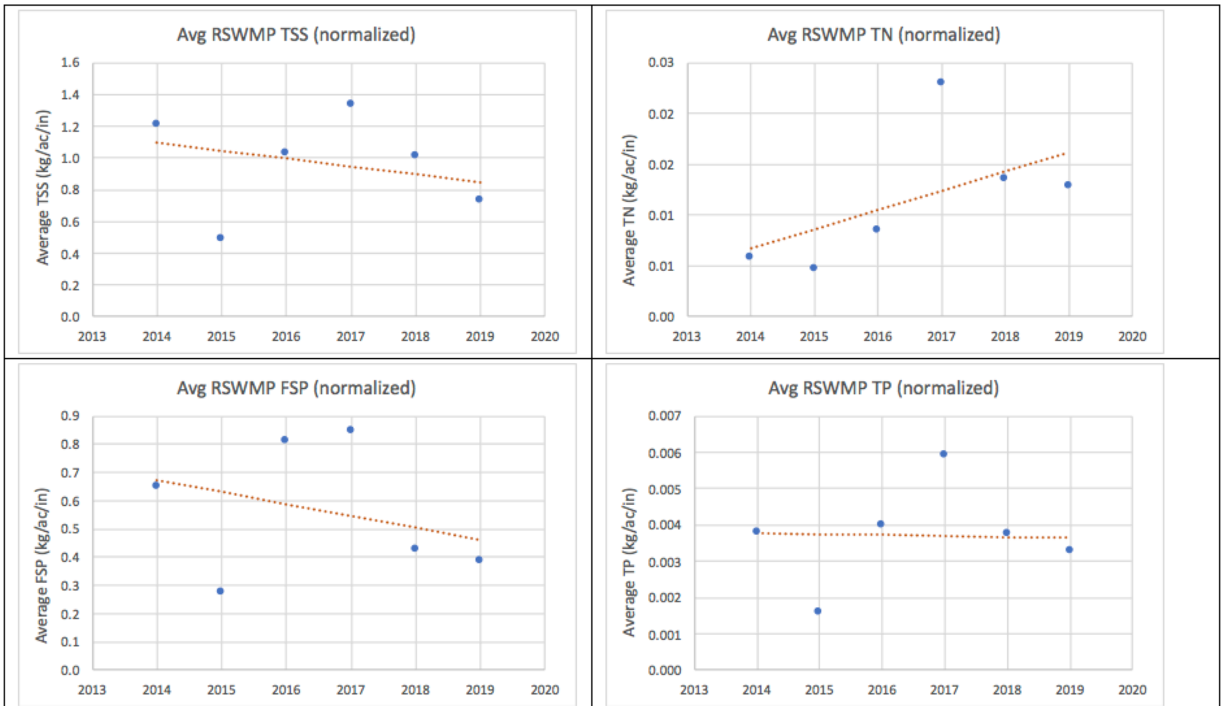

Theil-Sen (WYs 2014–2019)	RSWMP average **TSS** (kg/ac/in)	RSWMP average **FSP** (kg/ac/in)	RSWMP average **TN** (kg/ac/in)	RSWMP average **TP** (kg/ac/in)
Tau	-0.200	-0.067	0.467	-0.067
P-value for |Tau|	0.573	0.851	0.189	0.851
Slope	-0.0497	-0.0422	0.0019	-0.00003

Figure 4.6. Theil-Sen estimators of trend for normalized urban runoff loads at RSWMP sites. None of the non-parametric correlation coefficients (Tau) are significant, in part due to the short record of available data (WYs 2014-2019).

The Pollutant Load Reduction Model (PLRM) is a hydrologic and pollutant load generation model used to estimate annual average urban storm water pollutant loads in the Tahoe Basin for the Lake Clarity Crediting Program (NDEP 2020). Regional estimates of loading from urban catchments are derived from PLRM runs conducted by each jurisdiction as they register their improvements and BMP implementations for load reductions and corresponding Lake Clarity Credits. The existing PLRM uses precipitation and temperature time series data derived from extrapolation of local meteorological datasets available from 1988 through 2006. By design, therefore, surface runoff and pollutant loading results from the PLRM are based on an 18-year historical meteorological average, rather than on current WY measurements. Thus, substantial differences between PLRM estimates and measured values could be expected as annual precipitation and runoff characteristics vary from year to year. A recent evaluation of PLRM site loading estimates compared to RSWMP site-measured data for WY 2019 showed average and median differences of 899% and 455%, respectively, among the seven sites compared for FSP, TN and TP loading (TRCD 2020).

Although the time series of RSWMP monitoring site data are not yet adequate for reliable trends assessment, the LCCP reports that urban load reductions have occurred, based on PLRM estimates (see Appendix A2.2). Cumulative load reductions credited against 2004 (baseline) loading amounts estimated for the TMDL have hypothetically achieved an 19.7% reduction in FSP loading, a 15.5% reduction in TP loading, and a 11.7% reduction in TN loading.

We used average loading rates from RSWMP monitoring sites (in Table 4.4) to evaluate total urban loadings against the 2004 baseline levels. This evaluation included extrapolating to a total jurisdictional catchment area of around 40,000 acres from monitored drainage areas representing less than 1.5% of that total catchment. As a result, the accuracy of this evaluation is likely low and should be viewed more as an educated guess than a reliable estimate. Results summarized in Appendix 2 suggest that load reductions since 2004 could be represented already as part of the data from RSWMP monitoring that commenced in 2014. Longer-term data and many more sites would be needed to improve these estimates (Heyvaert 2011).

4.6 Summary of Findings for Hypothesis 2

Hypothesis 2 is restated here:

The change in trend of winter clarity is a response to decreasing fine suspended sediment concentrations resulting from load reductions.

Trend analysis performed on fine sediment loads for urban areas revealed no statistically significant trend. It is likely that load reduction activities that have taken place in the Tahoe Basin have resulted in nutrient and fine sediment reductions; however, the length of record is insufficient to reach a statistically meaningful conclusion.

Returning to the three questions that were posed at the beginning of this section:

1) Is there a statistically significant trend in the fine suspended sediment in the lake?

The results presented in the discussion of Hypothesis 1 reveal that while there was a large increase in the number of particles in the lake beginning in 2017, there is no statistically significant temporal trend in the number of particles observed at the two in-lake monitoring stations. The fraction of *Cyclotella* cells included in the counts of particle abundance contains some uncertainty and is not continuously available and we did not attempt to subtract *Cyclotella* counts from the total to determine a sediment-only time series.

2) Is there a trend in the loading of fine sediment to the lake? Potential sources include tributary streams, runoff from urbanized areas, and direct atmospheric deposition onto the lake's surface.

The available data do not allow for a definitive answer to this question. Data describing particle abundance at selected tributaries show close correlation with in-lake particle abundance. But these data are only available for selected periods that are insufficient to determine loading to the lake. Additionally, spatial coverage of streams is not complete, and the majority of watersheds remain unmonitored. As described below, climate change is altering lake stratification, hydrology and the timing of inflows, meaning that fine sediment loads may be inserted at different depths in the lake and thereby altering the impact of sediment loads on clarity.

The urban loading data are similarly problematic. Temporal span and resolution is limited, so uncertainty in the available data is high, and much of the urbanized area is not represented by the dataset. Consequently, the length of the record is not yet sufficient to perform trend analysis and extrapolation of limited monitoring sites would result in high uncertainty, even in the absence of these other concerns. Moreover, data are not yet available to estimate the relative importance of atmospheric deposition of insoluble particles directly onto the lake's surface.

3) Is the fine sediment concentration in the lake correlated with in-lake clarity time series data?

Figure 3.8 shows the correlation between the inverse of the Secchi depth and the particle abundance, with $R^2 = 0.49$. This assessment includes particles of all types, not only inorganic sediment. The *Cyclotella* counts contain enough uncertainty (due to enumeration, the short time scales of blooms relative to the sampling frequency, and the discrete depths sampled) that the true time series of sediment particle abundance in the optically important size range is not known. Clarity tends to be decreased when particle abundance is high, and the number of particles >1 μm is a better predictor than the total number of particles (>0.5 μm).

5.0 Hypothesis 3: *Changing hydrodynamic conditions* within the lake are increasing thermal stability and resistance to mixing.

5.1 Background

A lake's hydrodynamic characteristics and behavior depend on several factors, including size and shape, hydrology, and meteorological conditions. The latter two factors have been altered on account of climate change and are expected to continue changing at an accelerating rate for the same reason (Sahoo et al. 2015). Hydrodynamic processes and forcing, including thermal stratification, wind shear stress, vertical circulation, inflows and outflows, and gyres and seiches, play an important role in Lake Tahoe's hydrodynamics. Changes in hydrodynamic characteristics impact the distribution of chemical and biological solutes and particles, such as nutrients (nitrogen, phosphorous) and chlorophyll, among others (Hutchinson 1957).

5.2 Data Sets

We used physical, chemical and biological long-term time series of in-lake parameters measured by UC Davis at the two long-term sites from 1968 through 2019 (Table 5.1). We utilized data from the top 50 m of the water column at both sites, meaning we analyzed data from 9 depths at LTP (0, 2, 5, 10, 15, 20, 30, 40, 50 m) and 3 depths at MLTP (0, 10, 50 m).

Table 5.1. Long-term time series used to characterize the changes in hydrodynamic conditions in Lake Tahoe. MLTP = Mid-Lake Long-Term monitoring site (460 m); LTP = Long-Term monitoring site (120 m).

Parameter Category	Parameter	Site(s)	Period of Record	Frequency
Physical	Secchi depth	MLTP; LTP	4/1969-12/2019; 1967-present	Variable; typ. 1-2x/month
	Temperature (T)	MLTP; LTP	1969-1996; 1967-1996	monthly; every 10 days
	Profiling Temperature	MLTP; LTP	1996-2006	monthly; every 10 days
	Profiling Temperature (*Seabird*)	MLTP; LTP	2005-present	monthly; every 10 days
	Fine particle size distribution (FSD)	MLTP; LTP	2008-present	monthly; every 10 days
Chemical	Nitrate (NO_3)	MLTP; LTP	1970-present; 1968-present	monthly; every 10 days
	Total Kjeldahl nitrogen (TKN)	MLTP	1989-present	monthly
	Total hydrolyzable phosphorus (THP)	MLTP; LTP	1972-present; 1968-present	monthly; every 10 days

	Total Phosphorus (TP)	MLTP	1989 - 1992, 2000-present	monthly
Biological	Chlorophyll-a (Chl-a)	LTP	1974-1975; 1984-present	1974-1975: every 10 days; 1984-2006: monthly profiles with composites every 10 days; monthly (profile + composite) since 2007
		MLTP	1974-1975; 1984-present	monthly

5.3 Approach

To investigate Hypothesis 3, we first characterized the changes in thermal stratification (timing, intensity and duration) using long-term time series of lake temperatures to calculate indices that quantify the resistance to mixing across the thermocline and related the results to water *clarity*. Secondly, we evaluated trends of in-lake physical, chemical and biological variables (temperature, nutrients, chlorophyll, and fine particles) and flow discharge and also related them to *clarity*. Thirdly we investigated the periodicity of the different long-term time series described in this section and explored their correlations with *thermal stratification and clarity*. Finally, we propose potential explanations for the different periodicities in the time series and mechanisms underlying the variability in stratification and clarity.

We quantify the resistance to mixing across the thermocline using two indexes: stability index (SI, kg m^{-2}) and the buoyancy frequency (N, s^{-1}). The stability index measures the energy required to mix the upper 120 m of the lake when it is stratified (Sahoo et al. 2015) and it is computed as follows,

$$SI = \sum_{z=z_0}^{z=z_1} (z - \bar{z}) \rho_z$$

Here z is the depth of the water column from the surface, z_0 is the depth of the surface water (e.g. 0.5 m), z_1 is the maximum depth of the study water column, and $\bar{z}$ is the centroid or center of mass of the water column. Water density at depth z is ρ_z. A positive value for SI indicates stable stratification, and larger positive values indicate more stable stratification. The buoyancy frequency can be physically interpreted as the vertical frequency response excited by a displacement of a fluid parcel (i.e. resistance to mixing), and is calculated as,

$$N = \sqrt{\frac{g}{\rho_z} \frac{\partial \rho_z}{\partial z}}$$

where the vertical density gradient is $d\rho/dz$, and g is the acceleration due to gravity. A larger density gradient results in a higher buoyancy frequency, which indicates greater resistance to mixing. For this report, we evaluate the maximum values of both SI and N to characterize changes in hydrodynamic conditions in the upper waters of Lake Tahoe by first calculating these variables from the measured temperature profiles, and then identifying the depth at which the maxima occurred.

We quantified trends of the different data sets using the least square method to fit the time series to the best linear model (Molugaram and Rao 2017). T-tests were used to evaluate the statistical significance (p-values) of these trends. Correlation coefficients were calculated using the approach described in Press et al. (1992).

We computed the power spectrum for all the available long-term time series of parameters and depths above 50 m at the two sampling sites. We computed power spectral density (PSD) in the frequency domain using a fast Fourier transform and smoothing results with a cosine taper window [1,16] and a 95% confidence interval based on the chi-squared distribution (Bendat and Piersol 1986). Results from this analysis indicated the dominant periodicity or periodicities as peaks of the PSD expressed in years or fraction of year for each parameter. This analysis provides insight to the possible causes of the variance of specific time series.

5.4 Results

Changes in the thermal stratification of Lake Tahoe are the most straightforward observation of changes in the hydrodynamic conditions in the lake since 1968 (Figure 5.1).

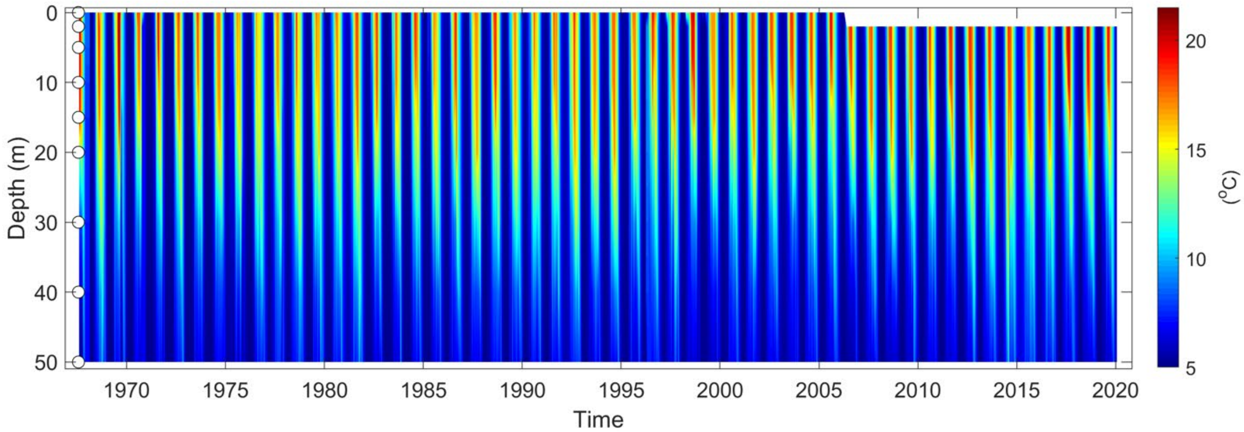

Figure 5.1. Time-depth time series of lake temperature at LTP. The circles adjacent to the depth axis indicate depths at which samples for water quality determination are collected.

The maximum annual values of indices that quantify the resistance to mixing across the thermocline show a linear increasing trend in the last 20 years (Figure 5.2). These values are always found during the summer season (June to September). The linear trends of stability index (SI) and buoyancy frequency (N) computed by the least squares method in the last 20 years are of order 10^{-3} kg-m^{-2} y^{-1} and 10^{-2} s^{-1} y^{-1} (R^2 = [0.54, 0.83], $p < 0.001$), respectively. We can draw several conclusions from these results: (1) both parameters define strength of stratification and are increasing over time, suggesting that stratification is becoming more significant, (2) buoyancy frequency may be a better index to quantify the changing hydrodynamic conditions in Lake Tahoe in the context of lake clarity since trend and root mean square values (R^2) are higher than for SI, and (3) suppressed mixing may be one of the factors affecting the reduction in clarity, particularly summer clarity.

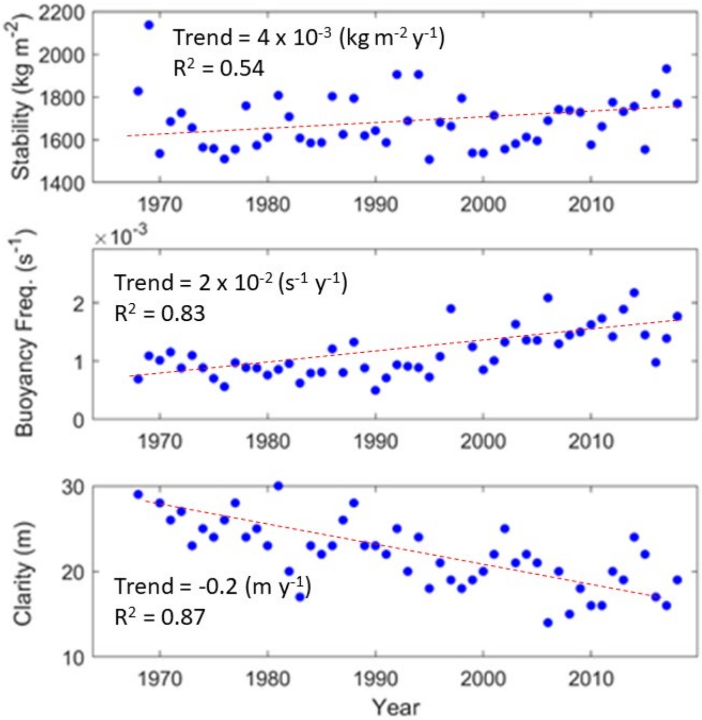

Figure 5.2. Time series of annual values of maximum stability index (SI) and buoyancy frequency (N) and mean summer clarity (m) (June - September) at LTP. Trends and root mean square (R^2) values are displayed for each variable. All trends were statistically significant ($p < 0.001$).

We also found a weak negative trend in the date when the deepest mixing occurred ($R^2 = 0.1$, $p = 0.028$, Figure 5.3). This may suggest that deep mixing is occurring earlier in spring, although the evaluation of the maximum mixing depth can only be made once a month, and therefore there is considerable uncertainty on the precise date (+/- 15 days). The key variable to analyze and relate to clarity may be the process of mixing in the spring. Deep mixing is known to be complex and believed to be strongly influenced by three-dimensional convective cooling from the relatively shallow shelves that are present at both the northern and southern ends of the lake. The analysis needed to understand that process is beyond the scope of this report.

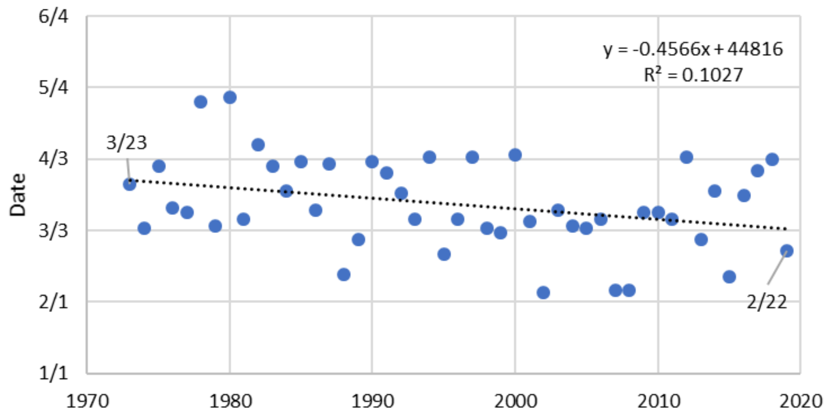

Figure 5.3. Time series of the date of maximum deep mixing at LTP ($p < 0.05$).

It is important to highlight the statistical assessment of the timing and duration of the lake stratification to complement our evaluation of stratification strength or resistance to mixing. We found statistically significant trends of order (10^{-1}) (R^2 = [0.71-0.83], $p < 0.001$) showing that earlier, prolonged and more intense stratification may be contributing to the decline in summer clarity (Figure 5.4). These trends are consistent with those presented in Sahoo et al. (2015) and as shown by Winder et al. (2008), such climate mediated effects are linked to an increasing occurrence of *Cyclotella*. This is one consequence that is consistent with decreasing clarity.

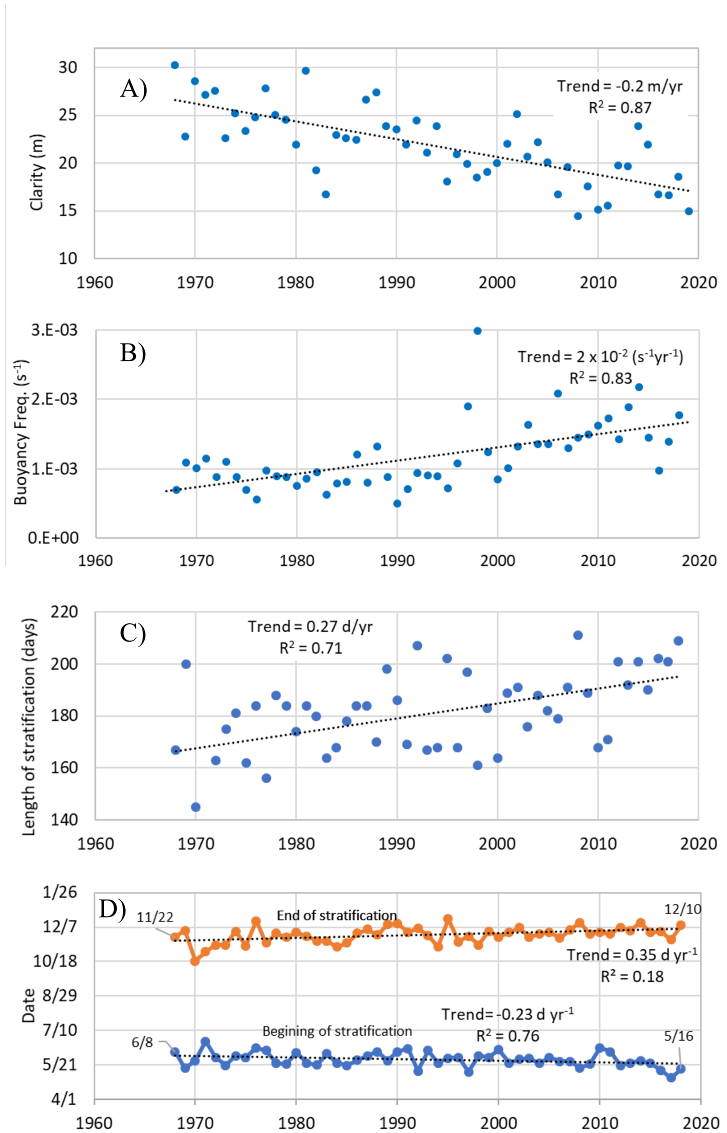

Figure 5.4. Time series of summer (June – September) trends of A) clarity, B) buoyancy frequency (N), C) length of stratification at LTP, d) dates of beginning and ending stratification. Trends and root mean square (R^2) values are also plotted for each variable. All trends were statistically significant ($p < 0.001$).

The lake's hydrodynamic conditions are changing over time, but determination of the impact of stratification on other variables is not straight forward. Linear trend analysis over the last 18 years shows that with the exception of clarity, nutrients and fine particle concentrations have displayed negligible trends. Overall, no strong trends emerged except for summer clarity ($R^2 > 0.8$). Appendix 3 contains plots with all the long-term time series used in our analysis of trends. Clarity is decreasing over time (Table 5.2). Total Phosphorous at the MLTP site shows an increasing trend overall, but for the first half of the record it was decreasing. Chlorophyll shows a negligible trend, however this may disguise the fact that smaller species (that impact clarity) have been increasing in concentration relative to larger species that do not impact clarity. The actual change in chlorophyll concentration is small, thus disguising what may be an important trend. Trends of the variables in Table 5.2 at different depths had less than 2% variability from the mean. A large peak in the upper lake concentration of fine particles occurred in 2017, the year of record high inflows. Fine particle concentrations in the lake increased by a factor of three to four times (see also Fig. 3.3). The values remained elevated for the next two years. This three-year period of time appeared to cause the linear trend to increase, but the trend was not significant. Prior to this time, fine particle concentrations were relatively unchanging if not decreasing, although the available record is relatively short. Trends of the other variables were negligible over the same time period, although visually the trend appeared to vary over multi-year periods.

Table 5.2. Linear trends computed by the least square method, goodness of fit (R^2), and standard deviation of the mean values in depth of the time series analyzed for this hypothesis. Each in-lake variable was measured at two sites in the lake (LTP and MLTP) albeit at different depths. Variables in bold are showing negative trends. All trends were statistically significant ($p < 0.001$). Trend Units: clarity in ($m\ yr^{-1}$), fine sediment particle concentration (FSP) in ($counts\ ml^{-1}\ yr^{-1}$) and total phosphorous (TP) concentration in ($\mu g\ L^{-1}\ yr^{-1}$).

Variable	Site	Trend	R^2	Std in depth
Annual clarity	**LTP**	-4×10^{-4}	0.2	-
Annual clarity	**MLTP**	-4×10^{-4}	0.1	-
Summer clarity	**LTP**	-2×10^{-1}	0.9	-
Summer clarity	**MLTP**	-2×10^{-1}	0.8	-
Lake temperature	LTP	-	negligible	-
Lake temperature	MLTP	-	negligible	-
FSP	LTP	-	negligible	1%
FSP	MLTP	-	negligible	2%
Chl-a	LTP	-	negligible	-
Chl-a	MLTP	-	negligible	-

NO_3	LTP	-	negligible	-
NO_3	MLTP	-	negligible	-
THP	LTP	-	negligible	-
THP	MLTP	-	negligible	-
TKN	MLTP	-	negligible	-
TP	MLTP	6×10^{-4}	0.1	1%
Blackwood flow	Blackwood	-	negligible	-

We investigated the periodicity inherent in the long-term time series and explored their relationships with thermal stratification and clarity. Results from the power spectral analysis provided the dominant periodicity or periodicities as peaks of the power spectral density (PSD) expressed in years or fraction of year for each parameter. This approach provides some insights into the processes that may be driving change. For example, the periodicity of lake temperatures at LTP was dominated by one-year periodicity (10^0) at all depths down to 50 m. Six-month periodicity was significant at the surface, whereas longer six-year periodicity was only evident at 50 m. (Figure 5.6). This may suggest that deep mixing events have an impact on temperature at this depth but that the surface heat fluxes dominate at shallower depths. Summer clarity has a range of periodicity varying from 1 year to 10 years, depending on the measurement site. These longer periodicities indicate that sub-decadal meteorological changes as well as long-term climate change may be playing a role. The six-month periodicity represents seasonality. Further analysis of periodicity was beyond the scope of this project.

A summary of the periodicities of all variables from both LTP and MLTP is presented in Figure 5.6. Periodicities in clarity appear to be similar to those for the load of fine particles (flow multiplied by number of fine particles), nitrate and lake temperature values. This does not establish causality. Rather, it points to a common set of drivers that could be explored further. Thus, changes in lake stratification expressed (e.g. more resistance to mixing) and higher concentrations of fine particles (both organic and inorganic) appear to be impacting the reduced clarity in Lake Tahoe.

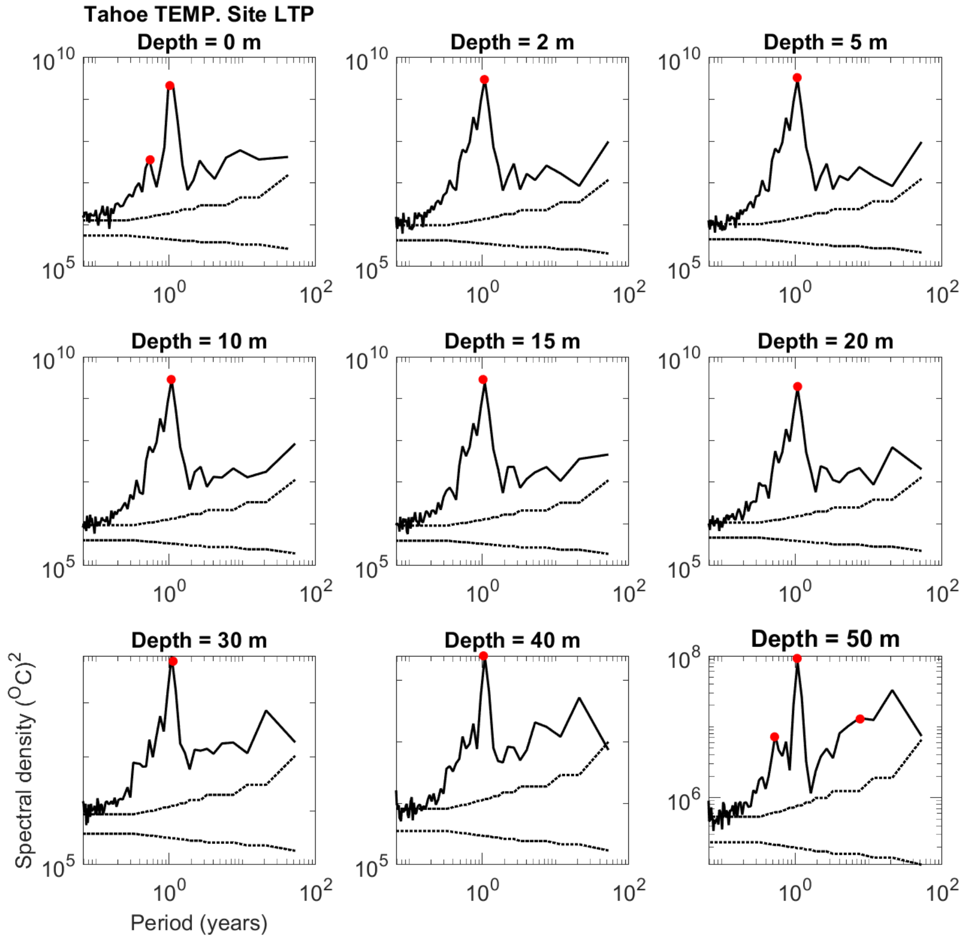

Figure 5.5. Power spectral density (PSD) of lake temperature at LTP at 9 depths (sub-plots). Statistically significant periodicity or peaks in frequency (in years) are marked on each plot with red dots. Dashed lines represent the 95% confidence intervals outside which we identify peaks in frequency content.

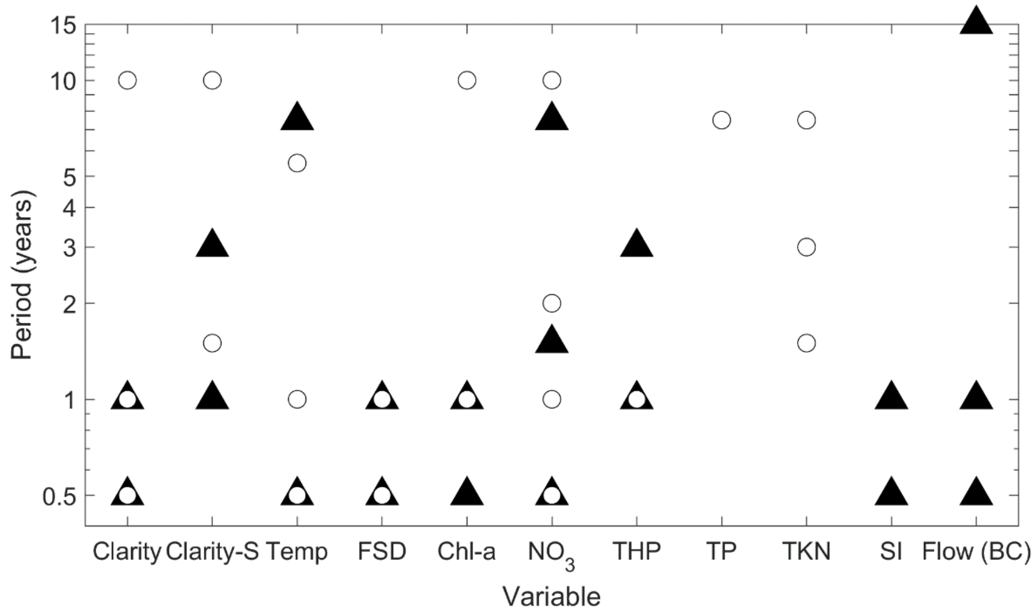

Figure 5.6. Periodicity (in years) of the different long-term time series. Each variable was measured at two sites in the lake (LTP and MLTP). Triangles represent LTP, and hollow circles show MLTP. Clarity-S refers to summer clarity, FSD indicates the fine sediment particle number, Flow (BC) is at mouth of Blackwood Creek.

5.5 Summary of Findings for Hypothesis 3

Hypothesis 3 is repeated here:

Changing hydrodynamic conditions within the lake are increasing thermal stability and resistance to mixing.

The hypothesis posed required a statistical evaluation of the trends in thermal stratification variables. We found statistically significant trends that support earlier, prolonged and more intense stratification as a contributing factor to the decline in summer clarity ($R^2 > 0.71$, $p < 0.001$). These are factors that have already been shown to be linked to climate change (Winder et al. 2008; Sahoo et al. 2015). Our analysis shows that the maximum annual values of buoyancy frequency and resistance to mixing show an increasing linear trend of order 10^{-2} s^{-1} y^{-1}($R^2 = 0.83$, $p < 0.001$), Winder et al. (2008) linked this trend to an increase in Cyclotella, and hence to the clarity of the lake. The following Section looks at the effect of these changing stratification conditions on the insertion depth of inflows, another potential cause of clarity decline

In-lake solutes and particles are also changing, following different patterns, some of them probably related to the modified lake mixing dynamics. Most of these changes are small, although the 18 year record was limiting.

Periodicity of long-term time series of in-lake variables reveal patterns (0.5- and 1-year periods) driven by annual and seasonal changes in meteorological conditions and hydrological conditions. Longer periodicities such as 3, 7 and 10 year are present in our long-term records. Some potential explanations for these longer periods of more than one year include climatological phenomena such as El Niño/ENSO, etc. and their hydrological consequences, interactions between different trophic levels and nutrients**,** and ecological impacts of invasive species introductions

6.0 Hypothesis 4: The trend in summer clarity is a result of earlier, prolonged, and *more intense stratification*.

6.1 Background

The previous section revealed trends indicating long-term increases in stability index, buoyancy frequency, and duration of stratification, and a trend toward earlier onset of stratification. Hypothesis 4 is focused on summer clarity and its relationship to stratification.

Table 6.1 reveals the relationships between summer clarity and 1) buoyancy frequency (N), the date of onset of stratification, and the duration of stratification. Earlier stratification would in most cases be expected to lead to stronger (higher buoyancy frequency), longer-duration stratification, and the results are consistent with this idea.

Summer clarity and buoyancy frequency were negatively correlated, as were summer clarity and duration of stratification. Earlier stratification was correlated with reduced summer clarity. The trends revealed show that when stratification is stronger, commences earlier, or extends longer, summer clarity is reduced. These are all trends that have previously been identified (Sahoo et al. 2015). These relationships do not necessarily reveal cause and effect. It is more likely that changes in stratification are affecting other processes that directly influence clarity.

Table 6.1. Correlation coefficients (r) and p-values for the relationships between decreasing summer clarity and stratification variables magnitude of buoyancy frequency, earlier stratification, and increased length of stratification).

Variables	**Correlation coefficients**	**p-value**
Clarity – Magnitude of N	-0.46	0.0007
Clarity - Earlier stratification	0.26	0.0426
Clarity - Length of stratification	-0.34	0.0167

Considering "summer" to be the period of stratification, and "winter" to be the period of no stratification (as opposed to the calendar-based definitions used for summer and winter clarity), the counterpart to longer summers is a reduction in the length of the winter period when vertical mixing occurs. Through the process of deep mixing, there is a vertical transfer of water quality variables. The deep water is typically high in nutrients (e.g. NO_3) but low in particle concentration. However, data suggest that shorter winter periods do not directly impact clarity. Clarity during winter tended to decline at different rates until early 2000, but the rate of change in clarity has been stable or slowly rising during winter in the last 20 years (Fig. 2.1, Section 2 of this report). Deep mixing may, however, impact summer clarity both because of the nutrients it transfers to the euphotic zone that may be used to stimulate spring algal blooms and the fact that the occurrence of deep mixing is immediately followed by the onset of stratification. Understanding of the process of the vertical mixing in Lake Tahoe over the winter would be useful to develop robust correlations with clarity but is beyond the scope of this report.

Other in-lake processes may be altered by an earlier onset of stratification and the changes in magnitude and duration of this period, which may be directly impacting the lake clarity. Longer and stronger stratification periods has the potential to alter particle settling rates. However, our trend analysis of in-lake solutes and particles in the upper 50 m has shown little spatial variability in the vertical (normalized standard deviation < 7%, Table 6.1). These results do not suggest changed settling rates in the water column as a result of stronger stratification.

The interaction of the stream water with the ambient lake stratification could impact the stream insertion depth (depth of stream insertion in the lake, once its level of neutral buoyancy has been attained) and dilution of fine particles and nutrients from streams (and urban discharges from culverts). This process was recently shown to be important and highly responsive to climate change by Roberts et al. (2018). Changes in the onset and extent of the summer stratification period (in combination with changing stream temperatures) impact the stream intrusion depth.

Streams entering a stratified water body may form plunging flows when the inflowing stream is denser than the ambient water, or form overflows near the lake surface when stream water is less dense than the ambient water (Figure 6.1). The distribution of lake density changes throughout the day and throughout the summer stratified period. Stream temperatures can vary by up to 8 ºC over the day-night cycle. Given the potential for stream loads to impact clarity if they insert at shallow depths, we explore the impact of the depth distribution of stream load insertion.

Overflows will reduce clarity, since river-borne fine particles are trapped in the near-surface, while plunging flows or underflows that are inserted below the Secchi depth may not affect the clarity observation. Here we describe a simplified analytical model to evaluate the timing of overflows, the interannual variability, and the relationship with lake clarity. This simplified model only requires basic stream and lake physical properties.

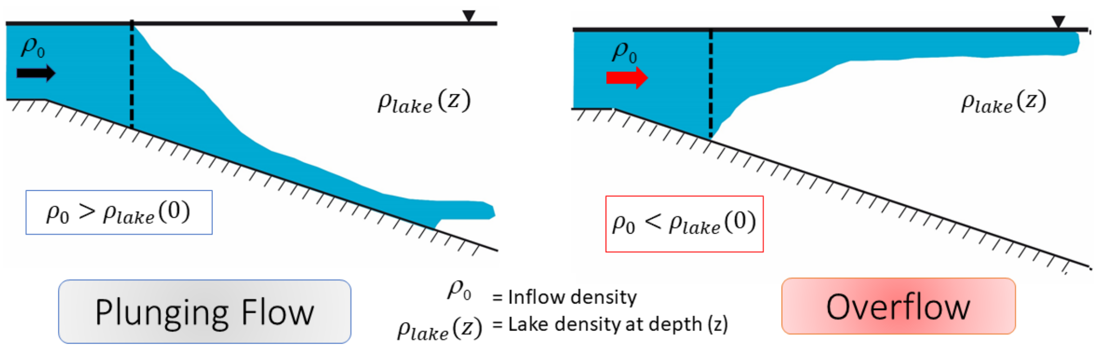

Figure 6.1. Idealized inflow dynamics of streams entering a stratified water body.

6.2 Data Sets

We used the **lake temperature** time series measured in the top 5.5 m every 2 min at the NASA/UC Davis buoys deployed in Lake Tahoe. Sensors were vertically spaced at approximately every 1 m in depth. Our period of analysis extends from January 2015 to May 2020.

We also used the 15-minute **stream temperature, flow rate, and stage** data provided by the U.S. Geological Survey at two of the inflowing streams (Upper Truckee and Blackwood) for the same period. For each stream, we computed a continuous time series of **width at the mouth** as a function of stream flow.

6.3 Approach

We developed a dimensionless number to characterize the nature of the overflows entering Lake Tahoe as a function of time, using a balance between the strength of the inflow and the strength of the lake stratification in the upper 5.5 m. This "Buoyancy Number" (BN), is defined as

$$BN = \frac{IBF_0^{2/3}}{(N\ H)^2}$$

Here IBF_0 is the inflow buoyancy flux per unit width, H is the thickness of the upper lake layer (assumed to be 5.5 m), and N is the buoyancy frequency. The inflow buoyancy flux per unit width can be estimated as,

$$IBF_0 = \frac{gp_0\ Q_0}{W_0}\ [m^3 s^{-3}]$$

where Q_0 is the stream flow discharge, W_0 is the stream width at the mouth, and gp_0 is the reduced gravity, which is calculated as,

$$gp_0 = g\frac{\rho_0 - \rho_{lake}(0)}{\rho_{lake}(0)}\ [m\ s^{-2}]$$

Here ρ_0 is the stream density, $\rho_{\text{lake}}(0)$ is the lake surface density, and g is the acceleration due to gravity. Finally, we characterize the strength of the lake stratification in the top 5 m using the buoyancy frequency (N),

$$N = \frac{g}{\rho}\frac{\Delta\rho}{dz}\ [s^{-1}]$$

where the vertical density gradient is $d\rho/dz$. The stratification in the top 5.5 m was evaluated because high spatial and temporal resolution temperature data are only available at the buoy sites.

The physical significance of the Buoyancy Number is that it indicates the likelihood of overflows to occur (rather than plunging inflows). If BN > 5, the inflow buoyancy flux dominates and the stream water overflows at the lake surface. If the BN < 5, lake stratification dominates, inflow momentum gets arrested by the ambient stratification and plunges below the surface flowing down the lakebed as a plunging flow or underflow before insertion at its level of neutral buoyancy.

6.4 Results

Changes in surface water temperature and buoyancy frequency were delineated at time scales that ranged from hourly to inter-annually between 2015 and 2020 (Figure 6.2). These results show the impact of the warmer summers that occurred after 2017. Buoyancy frequency (N), indicative of the strength of the stratification, was as high as 0.06 s^{-1} in the summer, and approaching zero in the winter. However, it is important to note that large departures of hourly values of N from the daily values can occur at all times of year, showing the propensity for short-term thermal stratification to affect the fate of stream-borne particles and nutrients throughout the year. Hourly values of N were almost double the daily mean values.

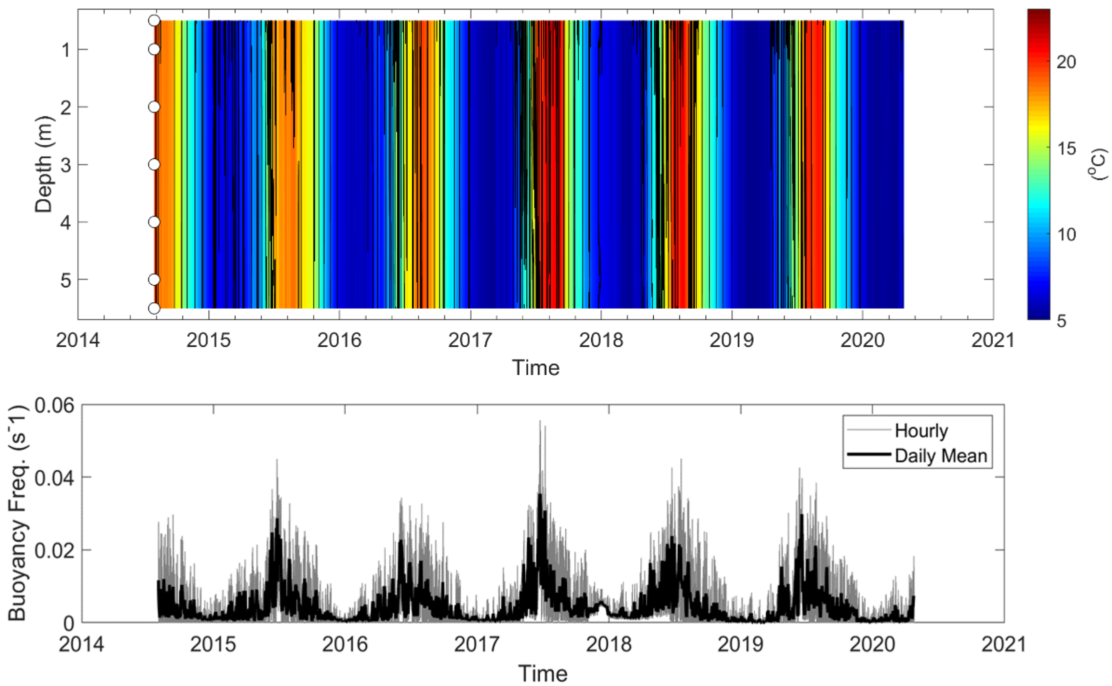

Figure 6.2. Lake temperature time-depth series and buoyancy frequency (hourly and daily values) of the upper 5.5 m in Lake Tahoe between 2015 and 2020.

Stream properties also were delineated on an hourly, daily, seasonal and annual basis (Figure 6.3). Blackwood Creek was used as representative of streams in this analysis. Generally, stream temperatures were colder than the lake surface, except for short periods in summers. These temperature differences produced large density differences between the stream and lake surface (i.e. large gp_0). Stream temperatures oscillated up to 8°C between day and night, particularly during spring and early summer, when snowmelt was a dominant component of the streamflow. Lowest stream temperatures occurred early in the day, and warmest temperatures were late in the day, with precise timing varying with factors such as watershed size, aspect and daily meteorology. The values of gp_0 indicate the difference between the stream and lake surface densities. As indicated previously, the daily average values indicate that the stream is generally denser (i.e. colder) than the lake surface with values of gp_0 being positive. However, the hourly values show that during spring and summer the stream can become less dense during the day (negative gp_0). These are conditions that increase the possibility of overflows occuring. Of note, 2017 and 2019 had virtually no such negative gp_0 conditions for Blackwood Creek. Stream velocity (based on measured stream flow and stage height, together with calculate stream width) was highest during the spring, when snowmelt was at its peak. In 2017 stream velocity remained high (0.4 m s^{-1}) for much of the year due to the high snowmelt and streamflow during that year (discussed previously).

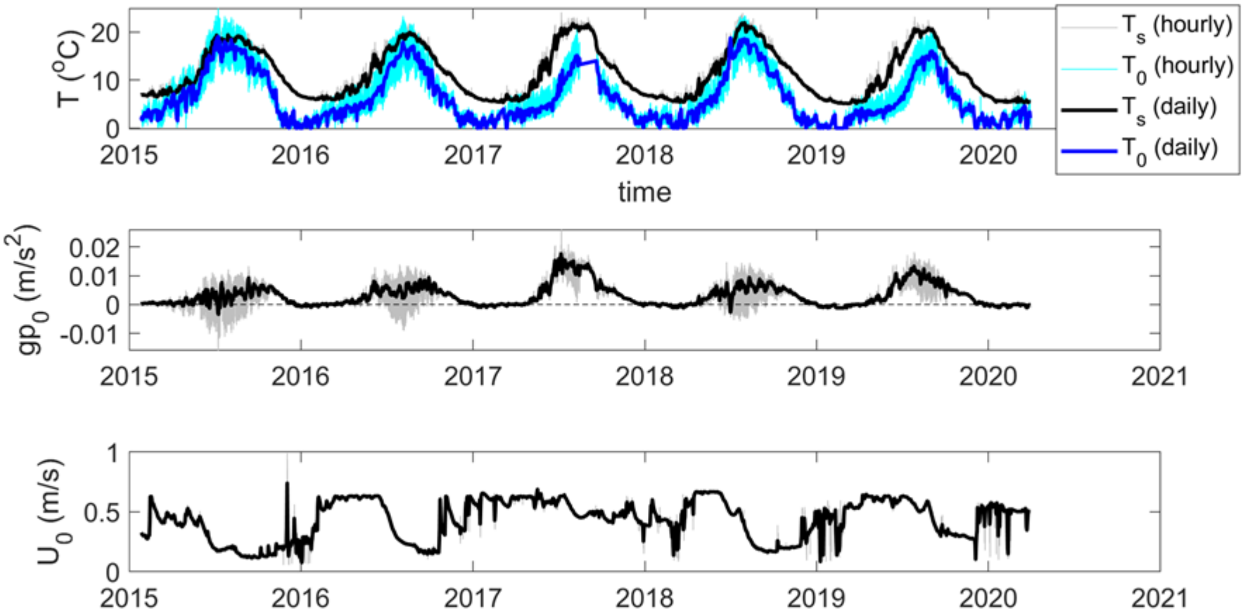

Figure 6.3. Blackwood Creek: Time series of inflow temperature (0) shown in dark and light blue and lake surface (S) temperature shown in black and gray at hourly and daily time scales between 2015 and 2020; reduced gravity of the stream (gp_0) indicating the density difference between the stream and the lake surface; and the calculated stream velocity (U_0).

Buoyancy Numbers were computed and are displayed in Figure 6.4. Overflow conditions (BN > 5) can be seen to be occurring more in winter, spring, and early summer (both on a daily average and an hourly basis, while underflows (BN < 5) tended to occur more during the fall. The fall is often a time of low particle flux. Because of the high diurnal fluctuations, the Buoyancy Number could change in sign throughout the year, meaning that overflows (particle fluxes being introduced above the Secchi depth) could occur at any time of year, depending on specific storm event and the lake conditions.

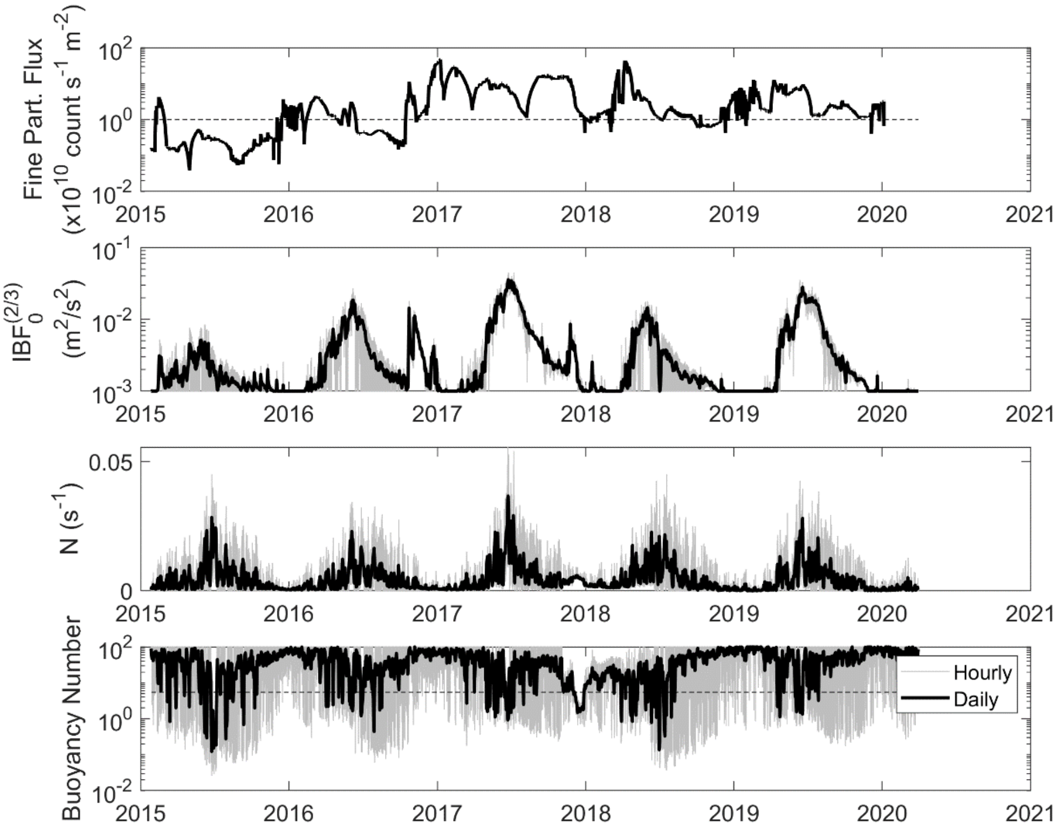

Figure 6.4. Time series of fine particle flux (x10^{10} counts s^{-1} m^{-2}) between 2015 and 2020 from Blackwood Creek; inflow buoyancy flux per unit width (IBF_0); lake buoyancy frequency (N); Buoyancy Number values, where the dashed line marks the critical value of 5.

Interesting inter-annual variability occurred in the Buoyancy Number values between 2015 and 2019 (Table 6.2). The minimum annual value of the Buoyancy Number occurred in 2015, which means that underflows were more likely to happen in that year. Higher values of Buoyancy Number during the summer occur after 2016, suggesting more frequent overflows at the lake surface that likely influence summer lake clarity. In addition, both the buoyancy flux (IBF_0) and the fine particle flux from the stream appear to be consistently higher after 2016 (fig. 6.4).

It is extremely important that the length of this record and the particular conditions that prevailed during this five-year period be borne in mind when drawing conclusions. The first two years represented the end of a drought of historic proportion, when streamflows and accompanying particle fluxes were very low. 2017 was a year with historically high precipitation, streamflows and particle fluxes, and the two years since have both been above average in precipitation and streamflow, and shown well above average particle fluxes (see earlier sections of this report).

Table 6.2. Seasonal and annual values of Buoyancy Number and lake clarity.

	Buoyancy Number (s^{-1})				
Period	**2015**	**2016**	**2017**	**2018**	**2019**
Winter (D-M)	46	66	66	12	81
Summer (J-S)	20	24	30	31	39
Annual	36	48	45	39	44

	Clarity (m)				
Period	**2015**	**2016**	**2017**	**2018**	**2019**
Winter (D-M)	21.8	25.4	24	22.4	24.7
Summer (J-S)	22.3	17.2	16.3	18.8	16.1
Annual	22.3	21.1	18.4	21.6	19.1

Finally, we evaluated the effect of using a different surface lake temperature definition (0 m vs mean of the top 5.5 m, dT = 0.15 ºC) when computing Buoyancy Numbers. Results only changed 0.12-0.17%. We also explored the effect of spatial variability comparing results from two streams (Blackwood and Upper Truckee). Upper Truckee tended to have more buoyancy, but Buoyancy Numbers only changed ~5.2% between both streams. This suggests that the approach taken is both robust in terms of the data used, and may be used as a guide to what to expect for other streams in the Tahoe basin.

6.5 Summary of Findings for Hypothesis 4

Hypothesis 4 is repeated here:
The trend in summer clarity is a result of earlier, prolonged, and more intense stratification.

Declining summer clarity is correlated with earlier, prolonged, and more intense stratification, thus factors that change the distribution of clarity-reducing need to be increasing as a result of those changes. To fully test this hypothesis would require modeling of both the fate of fine inorganic particles and of fine algae over time, a major undertaking. To at least partially explore the hypothesis, we focused on the insertion depth of stream flows for the period of time when high resolution lake surface stratification data were available. It is to be expected that the higher the frequency of surface insertions, rather than plunging insertions, the greater the reduction in clarity.

Using a Buoyancy Number to evaluate the occurrence of overflows, its interannual variability, and its relationship with lake clarity, we confirmed that higher frequency occurrences of insertion overflows coincide with reductions in clarity. Overflows, with high concentrations of fine particles, occurred more frequently in years of poorer lake clarity, and particularly during summers after 2016 with higher Buoyancy Numbers. As a caveat on these findings, the five years available for the analysis were far from "average" years. The first two were extreme drought years, and the last three were heavily impacted by the extreme wet year of 2017.

These finding are similar to those from Roberts et al. (2018). They explored the impacts of changing snowpack conditions as well as changing lake stratificatiom. They concluded that "…lower snowpack has caused inflows to enter Lake Tahoe earlier relative to the onset of thermal stratification and with more positive buoyancy. With projections of warming air temperatures and a reduction in snowpack, inflow mixing conditions are likely to increasingly favor nearshore and near-surface mixing".

Other processes affecting clarity that could be impacted by longer, more strongly stratified summer periods may include bloom dynamics of small phytoplankton cells, the depth of lake mixing in early spring (which can transfer nutrients to the euphotic zone), and changes in settling rates as density gradients increase and suppress turbulent mixing.

7. Hypothesis 5: Ecological (food web) interactions are causing changes in the trends of seasonal or annual clarity.

7.1 Background

Long term data on food web interactions at Lake Tahoe do not exist, so a narrative assessment of this hypothesis is provided. The findings of this hypothesis were summarized from a draft publication by Schladow et al., 2020 (in-review). To support this narrative assessment there are data from both Lake Tahoe and its embayment, Emerald Bay. We do not attempt to evaluate the relationship of the entire Lake Tahoe food web to lake clarity. Rather, we focus specifically on the relationship between the introduced *Mysis* shrimp, the native cladocerans (*Daphnia* and *Bosmina*) that were largely eliminated following *Mysis* introduction, and the impact on particulates within Lake Tahoe. Here particulates are taken to include both free floating phytoplankton and inorganic particles of terrigenous origin. This is motivated by the recent observation (between 2011-2016) that when *Mysis* disappeared from Emerald Bay, cladocerans returned, and clarity increased by 11 m in 18 months. When *Mysis* returned the cladocerans largely disappeared again and clarity fell to its previous level.

The impacts of *Mysis* on lakes, in general, are discussed, the events in Emerald Bay from 2011-2016 are described, the long-term Tahoe phytoplankton record is reviewed in light of the impacts of cladocerans on fine particles, and then the results are summarized. Specific questions posed by Agency representatives are addressed at the end of this section.

The decline of the clarity of Lake Tahoe has been attributed to land use change spurred by rapid development and population growth in the Lake Tahoe basin starting in the 1950s (Goldman 1988), as well as by enhanced atmospheric deposition of nitrogen from vehicle emissions and other sources (Jassby et al. 1994). Through the TMDL studies (LRWQCB and NDEP 2010), it was found that fine particulates had a larger impact on lake clarity than nutrients (Jassby et al. 2003; Swift et al. 2006). Consequently, most restoration efforts have been targeted at remediating legacy development projects and their impacts on fine particle and nutrient additions (EIP 2018).

From 1963 to 1964, coincident with the period of rapid development, the non-native opossum shrimp, *Mysis diluviana* (formerly *M. relicta*, hereafter referred to as *Mysis*) was introduced to Lake Tahoe and Emerald Bay. The population of newly introduced mysids took several years to establish lake-wide, but by 1970 they were a large part of the diet of deep living lake trout (Richards et al. 1975). Once established, *Mysis* quickly altered the aquatic food web. By selectively feeding on native cladoceran species (*Bosmina longirostris*, *Daphnia rosea* and *D. pulex*; Cooper and Goldman 1980; Threlkeld 1981), they effectively depressed the abundances of all three species within Lake Tahoe by 1973 (Richards et al. 1975). Stomach contents analysis of *Mysis* identified remains of all of the non-cladoceran zooplankton (Threlkeld et al. 1980), highlighting the role of *Mysis* in altering the structure of the native zooplankton community. The resulting pelagic zooplankton assemblage became dominated by copepods *Epischura nevadensis, Diaptomus tyrrelli* and the rotifer *Kellicottia longispina*.

Zooplankton community structure can be a strong selective pressure affecting phytoplankton assemblages. Copepods are less efficient grazers than cladocerans (Wu and Culver 1991) and can reduce predation on smaller algae species by selectively grazing on larger forms of phytoplankton, thereby enhancing the pelagic biomass of small-sized algae (Sommer and Sommer 2006). Evidence of such a shift was found in Tahoe, where a concomitant increase in the occurrence of the small diatom genus, *Cyclotella spp.* followed the loss of cladoceran species (Richards et al. 1975). More recently Winder and Hunter (2008) reported a trend that among diatoms, *Cyclotella spp.* is the only genus that increased significantly in concentration over the period of 1982-2006. They attributed the increased abundance primarily to climate change and increased thermal stratification (Winder and Hunter 2008).

The shift towards an increase in small-sized planktonic diatom abundance is a contributing factor in the decline in lake clarity (Schladow 2011;2012; 2013; 2014; 2015; 2016; 2017; 2018; 2019; 2020). Suspended particles (be they organic or inorganic) attenuate a fraction of light impinging on them via scattering, with a much smaller loss due to absorption. This fraction, the attenuation efficiency, varies in a complex manner with particle size and composition. van de Hulst (1957) showed theoretically that the attenuation efficiency is maximum at a particle diameter of 1.7 µm for inorganic particles such as quartz, and about 6.5 µm for organic particles. At larger particle sizes, the attenuation rapidly decreases. Diatoms, being both an organic particle and possessing a silica frustule, may be expected to reflect the characteristics of both particle types, and given the size range of those commonly observed in Lake Tahoe, be expected to scatter light at similar efficiencies.

The extent to which *Mysis* in Lake Tahoe may be linked to declines in water clarity went unnoticed for decades. In 2011, an unprecedented, near-total disappearance of *Mysis* was observed in Emerald Bay, leading to a large and sustained increase in water clarity for over three years. Records of water clarity in Emerald Bay (1962 – present, non-continuous) confirm its clarity has always been less than that of the main body of Lake Tahoe.

Emerald Bay was sampled over the five-year period following the decline in *Mysis* to characterize the ecosystem-level effects. The sampling results strongly suggest that the decline in water clarity within Lake Tahoe was in part a result of the alteration to food web structure set in motion by the loss of cladocerans through the introduction of *Mysis*. This seminal action is what lowered Lake Tahoe's resilience to the impacts of watershed degradation produced through rapid urban development.

7.2 Data Sets

The data used in this analysis are indicated in the Table 7.1.

Table 7.1. Sampled variable, sites, date range for record, frequency and standard deviation for long term data. Discrete indicates samples at specific depths. Composite indicates a prescribed mixture of water from specific depths. Profile indicates continuous measurements with depth. Station designations are EB= Emerald Bay; LTP=long term monitoring station; MLTP = mid-lake, long-term monitoring station; SS= south shore site

Variable	Site	Sample Type	Sampling Dates	Frequency (SD) in days
Mysis	19 Tahoe stations	Vertical tow	1979-1986	1-3 events/year
	11 Tahoe stations	Vertical tow	1987-1995	1-4 events/year
	LTP	Vertical tow	Nov 2011 - Nov 2016	80.1 (30.6)
	MLTP	Vertical tow	Nov 2011 - Nov 2016	84.0 (29.5)

	SS	Vertical tow	Nov 2011 - Nov 2016	82.7 (29.8)
	EB	Vertical tow	1979-1985	1-6 events/year
	EB	Vertical tow	Nov 2011 - Nov 2016	81.0 (30.6)
Zooplankton	LTP	Vertical tow	Aug 1967 - Nov 2019	monthly
	MLTP	Vertical tow	Apr 1980 - Nov 2019	monthly
	EB	Vertical tow	Jul 1983 - Dec 1985	monthly
	EB	Vertical tow	Nov 2011 - Nov 2016	monthly
Phytoplankton	LTP	Discrete	Aug 1967 - Nov 1989	13.6 (28.0)
	LTP	Discrete	Jan 2002 - Nov 2016	31.8 (14.4)
	LTP	Composite	Oct 1984 - Nov 1989	11.5 (2.31)
	MLTP	Discrete	Sep 1998 - Dec 2015	30.4 (18.2)
	MLTP	Composite	Feb 1992 – Dec 2014	32.3 (15.4)
	EB	Discrete	Dec 2013 - Dec 2016	
Chlorophyll-*a*	LTP	Discrete	Nov 1983 - Nov 2016	32.1 (11.7)
	MLTP	Discrete	Mar 1992 - Nov 2016	31.8 (12.3)
	EB	Surface	Dec 2013 - Nov 2016	91.1 (28.8)
Primary Prod.	LTP	Discrete	Jun 1970 - Dec 2006	11.4 (4.1)
	LTP	Discrete	Jan 2007 - Nov 2016	40.6 (32.5)
NO3/NO2 and THP	LTP	Discrete	Aug 1967 - Dec 1991	10.8 (4.1)

	LTP	Discrete	Jan 1992 - Nov 2016	31.0 (12.6)
	MLTP	Discrete	Apr 1980 - Nov 2016	28.2 (18.7)
Temperature	LTP	Profile	Aug 1967 - Nov 2016	11.7 (4.9)
	MLTP	Profile	Mar 1969 - Nov 2016	27.9 (17.8)
	EB	Profile	Jan 2011 - Nov 2016	35.1 (30.1)
Secchi Depth	LTP		Jul 1967 - Nov 2016	12.8 (6.6)
	MLTP		Apr 1980 - Nov 2016	28.4 (12.5)
	EB		Jan 2011 - Nov 2016	35.1 (30.1)

7.3 Methods

7.3.1 The Emerald Bay Perturbation - The range of relevant data from Emerald Bay and Lake Tahoe are shown in Fig. 7.1. When sampled in November 2011, *Mysis* density was < 1 individual(ind.) m^{-2} (Fig. 7B), and remained low until mid-2014, after which values increased to a peak of approximately 150 ind. m^{-2}. For reference, *Mysis* densities ranged from 21-292 ind. m^{-2} with an average of 120 ind. m^{-2} between July 1979 and June 1985.

Values of Secchi depth for Emerald Bay (Fig. 7.1A) increased by over 11 m during the 2012 to 2013 period. This is particularly noteworthy, as a positive change of clarity within either Emerald Bay or Lake Tahoe of this magnitude has never been observed, except for the response to very brief (days) upwelling events (for example, Schladow et al. 2004) or after complete mixing to the bottom of Lake Tahoe (weeks).

Small bodied zooplankton such as copepods and rotifers, while present in large numbers, fluctuated with no apparent relation to changes in water clarity (Figure 7.1C). Declines in their abundance associated with increases in *Mysis* density suggest they are being grazed by *Mysis*. In the absence of *Mysis*, the abundance of large bodied zooplankton increased substantially. *Bosmina* abundance responded fastest to declines in *Mysis*, with an initial peak exceeding 3,000 ind. m^{-3} occurring in July 2012. By November 2012, *Daphnia* concentrations overtook *Bosmina*, and it remained the dominant cladoceran until August 2016. The cladoceran populations fluctuated, usually 180 degrees out of phase with *Mysis* values, but for the period from November 2012 through August 2016 the mean *Daphnia* population was 1,112 ind. m^{-3}. By mid-

2014, with *Mysis* abundance again increasing, cladocerans declined and Secchi depth was consistently below 20 m.

The correlation between Secchi depth and Mysis concentration for the 2011 – 2016 period shown was r=-0.42 (p=0.434, n = 23). Note that Mysis samples are not taken concurrently with Secchi depth, as the former are sampled at night. Correlating the large zooplankton (the cladocerans) with Secchi depth shows a high level of significance, with r = 0.72 ($p < 0.01$, n = 36).

The same set of measurements for Lake Tahoe over the same period (Fig. 7.2) provide a context for the Emerald Bay data. The annual average Secchi depth in 2012 through 2014 was close to the long-term trend for Lake Tahoe (Schladow 2015), although early 2012 had some high Secchi depth readings due to upwelling events. In 2013, the annual average Secchi depth in Lake Tahoe was 21.4 m, only slighter higher than what was observed in Emerald Bay (19.8 m). *Mysis* concentrations remained high in Lake Tahoe, with the summer and fall of 2012 having exceptionally high values (in the range of 400 ind. m^{-2}), the very opposite to what was being observed in Emerald Bay. Copepods and rotifers were more than a factor of five lower than values in Emerald Bay. Cladocerans were at even lower numbers relative to Emerald Bay, with the exception of large *Bosmina* numbers in late 2012. Running the same correlations for Lake Tahoe itself is meaningless, as the cladocerans are essentially zero.

7.3.2 Lake Tahoe *long-term data* - Since 1968 annual average clarity has generally decreased, albeit with a slowing trend in the last 20 years (Figure 7.3). The period of decrease, as noted earlier, coincided with both rapid development in the Tahoe basin and the introduction and establishment of *Mysis*.

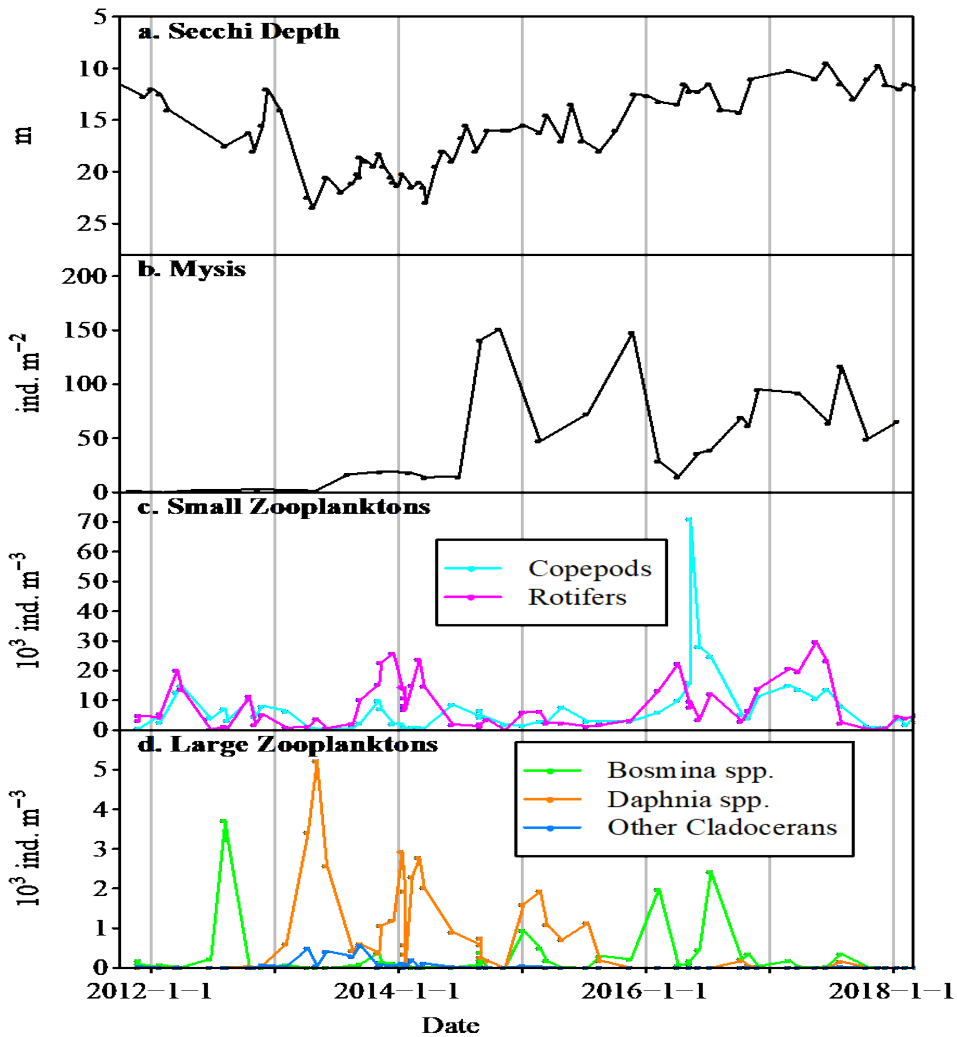

Figure 7.1. Secchi depth, *Mysis* and zooplankton abundance in Emerald Bay. a: Secchi depth (m), b. *Mysis* concentration (ind. m^{-2}), c. Cladocerans (ind. m^{-3}), and d. Copepods, Cladocerans and Rotifers (ind. m^{-3}). Note the different axis ranges in c. and d.

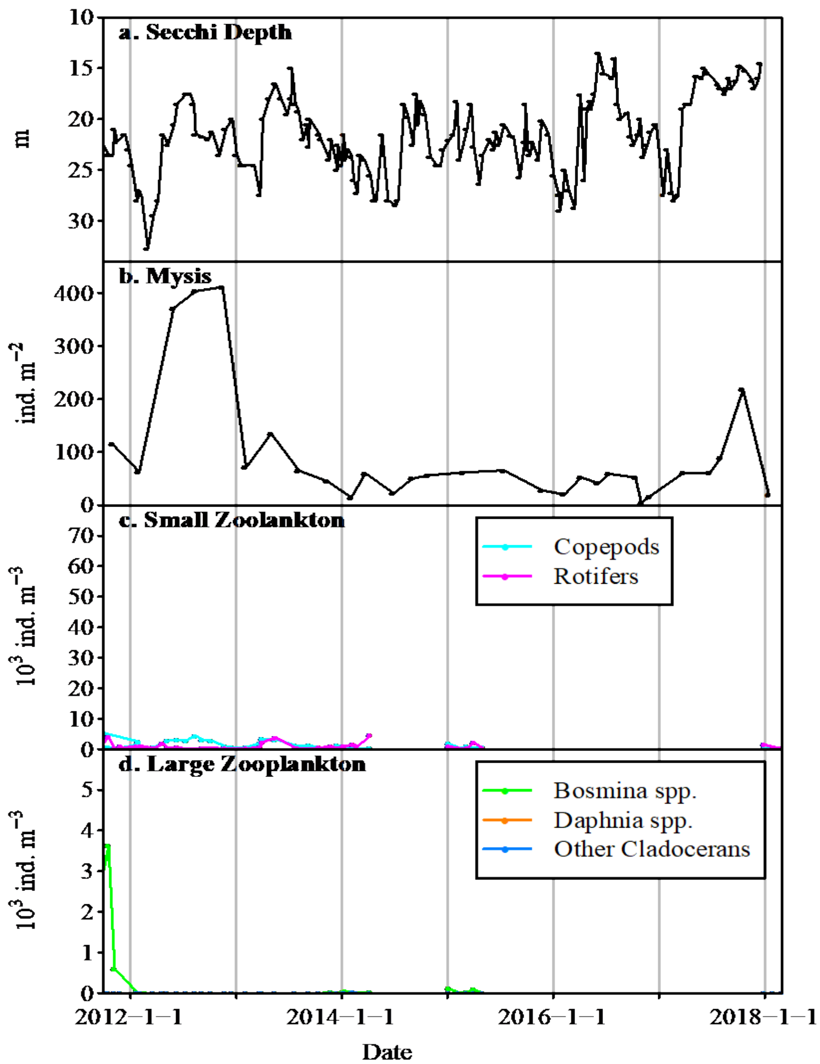

Figure 7.2. Measurements from the LTP site in Lake Tahoe. a. Secchi depth (m), b. *Mysis* concentration (ind. m^{-2}), c. Cladocerans (ind. m^{-3}), and d. Copepods, Cladocerans and Rotifers (ind. m^{-3}). Note the different axis ranges in c. and d.

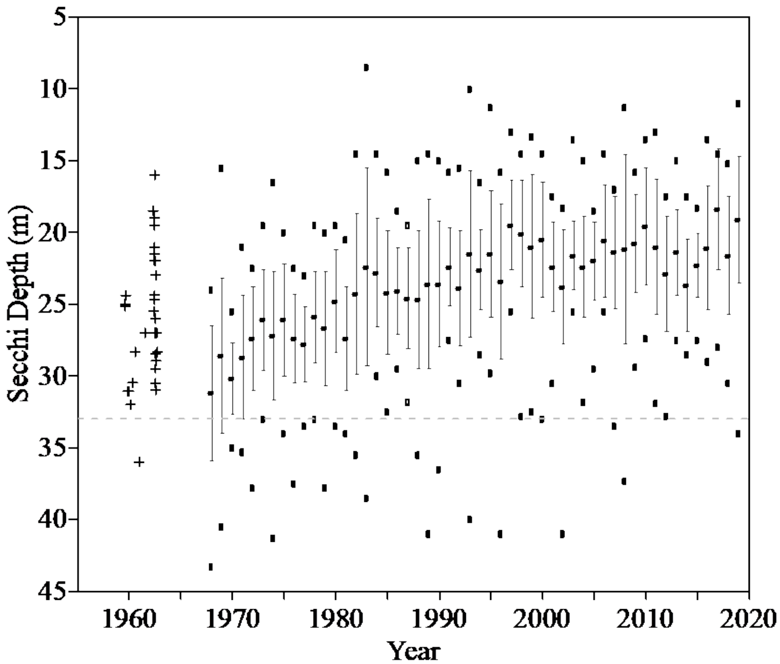

Figure 7.3. Long-term Secchi depth data for Lake Tahoe LTP station. Solid circles are annual average values with standard deviation as error bar for the period 1968 to 2019. Hollow circles indicate the highest and lowest values recorded in each year. Crosses are the individual measurements taken during the period 1959 to 1962 when measurements were episodic. Gray dashed line shows Secchi depth measured by LeConte on June 9, 1873.

While the pre-1982 phytoplankton data record has some quantitative uncertainties within a factor of two (relating primarily to the uncertainties of the counting of live or dead diatom cells) making them suspect for long-term trend analysis, here they are being used in a presence-absence mode. As such the 50-year phytoplankton record shows clear evidence of the impact of *Mysis*. Diatoms have always been the dominant component of the phytoplankton assemblage in Lake Tahoe, however, their composition and size structure have changed substantially over time. The large sized, colonial diatom species *Fragilaria crotonensis* was a major component of the algal community during the first years of Lake Tahoe monitoring. This species was consistently dominant both in abundance (number of cells mL^{-1}) and biomass (as cell volume). Prior to 1970, *F. crotonensis* population increased in January and February, reached a peak of over 150 cells mL^{-1} in March and April before declining to a mid-fall minimum. Time series data from two water depths (5 m and 20 m) for *Fragilaria crotonensis* are shown in Fig. 7.4 for the period 1967 –2018 (excluded 1989 - 2001). The individual elements of *F. crotonensis* have a length range of 60-72 µm and a width range of 2-3 µm (Morales et al. 2013). A colony of *F. crotonensis* is shown in Fig. 7.5a. Since 1976, *F. crotonensis* had declined steadily to extremely low densities, and after 1980 it has been an infrequent species in pelagic areas of Lake Tahoe.

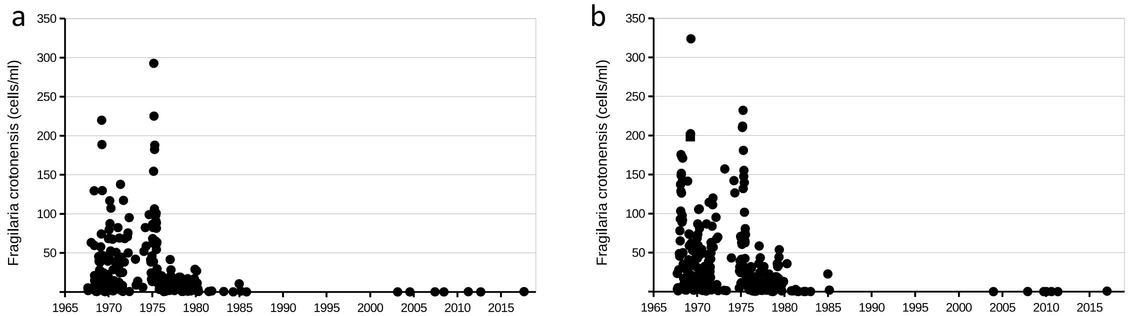

Figure 7.4. Cells per ml of *Fragilaria crotonensis* at depths of (a) 5 m and (b) 20 m at LTP station. Note the dramatic decline in occurrence after the mid-1970s that has continue to the present. No data available between from1988 through 2001. For all other years a zero reading indicates a total absence of Fragilaria.

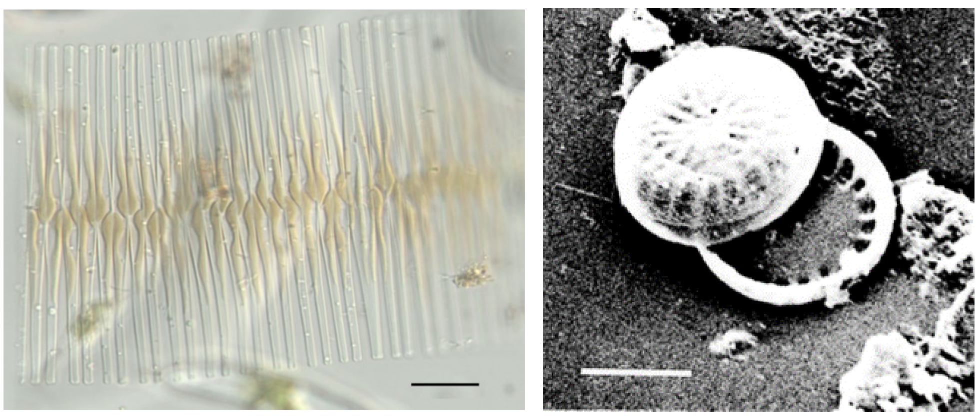

Figure 7.5. (a) *Fragilaria crotonensis* with scale bar = 20 µm (photo L. Tanaka); b. *Cyclotella gordonensis* with scale bar = 2 µm (photo Kling and Håkansson).

Data for the uni-cellular, centric diatom *Cyclotella* are shown in Figure 7.6. *Cyclotella* in Lake Tahoe are generally small and are difficult to correctly distinguish individual species, particularly with the lower resolution microscopes available during the early decades of the Tahoe phytoplankton record. The species of *Cyclotella* represented likely include *C. ocellate* (3.7-15 µm), *C. stelligera* (3.7 – 13.8 µm), *C. glomerata* (3 - 10 µm), *C. comensis* (5-12 µm), *C. kuetzingiana* (6.3-16.5 µm) and *C. gordonensis* (< 5 µm). Size ranges are provided by https://diatoms.org/species/ and by Kling and Håkansson (1988).

As discussed previously, light scattering by particulate material is highest in the range of about 1.7- 6.5 µm, depending on whether the material is organic or inorganic. Diatoms possess the attributes of both material types and the nature of their scattering properties is not well understood. The replacement of the dominant diatom with a colony size of 70 µm, with a unicellular diatom with a diameter of between 2-10 µm, would have had a large impact on light scattering.

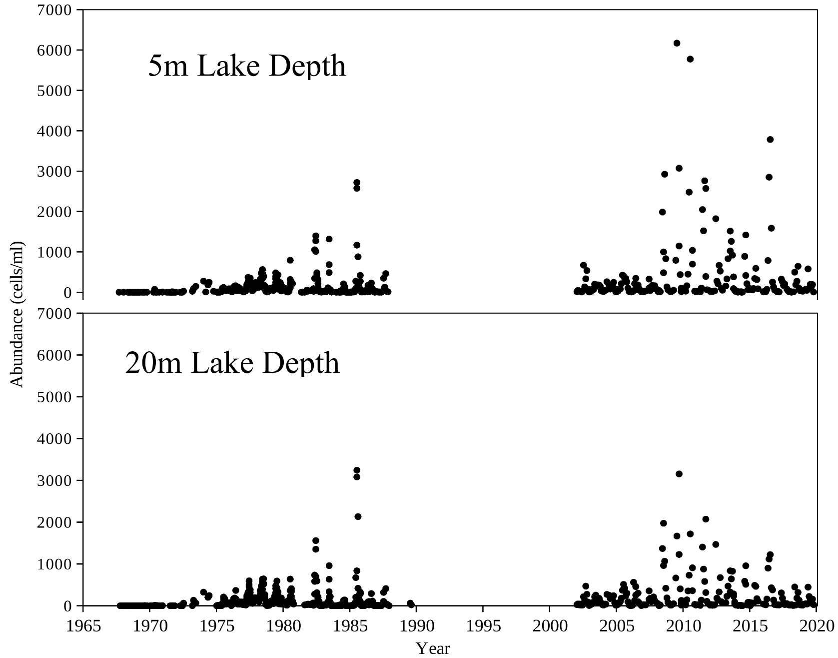

Figure 7.6. Long-term trend in abundance of *Cyclotella sensulato* from LTP from 1967 to 2019. No data available between late-1980s through 2001.

The phytoplankton community for four separate years (1969, 1985, 2002 and 2018) were sorted into two size classes. that in 2009, 2010 and 2016 the small Cyclotella cell counts were in excess of 4000 cells/ml (higher than in 1985). The first category includes organisms smaller than 20 µm in length or diameter (excluded picoplankton, 0.2–2.0 µm). All phytoplankton species larger than 20 µm were assigned to the large phytoplankton cells category. Some consistent patterns have emerged. Large sized species made up over 86 percent of the phytoplankton cell counts throughout 1969, but this ratio changed drastically by 1985, when the small sized species dominated numerically (consistently 80-100 % of the cells). The number of cells decrease a factor of five from 1985 to 2002. As shown in Fig. 3.7, there are other years where the abundance of small cells is high. For example, in 2009, 2010 and 2016 the small Cyclotella cell counts were in excess of 4000 cells/ml (higher than in 1985). In general, *Cyclotella spp*. account for the major fraction of the small celled phytoplankton.

Looking specifically at *Cyclotella spp*. in Figure 7.8, the evolution in both total number of cells and annual distribution is evident. From a negligible presence throughout the year in the pre-*Mysis* period, to a large presence initially in just one summer month, but in more recent years to spring, summer and fall in the post-Mysis period. This observation coincides with the recently observed trend in declining summer and fall clarity at Lake Tahoe (Schladow 2019).

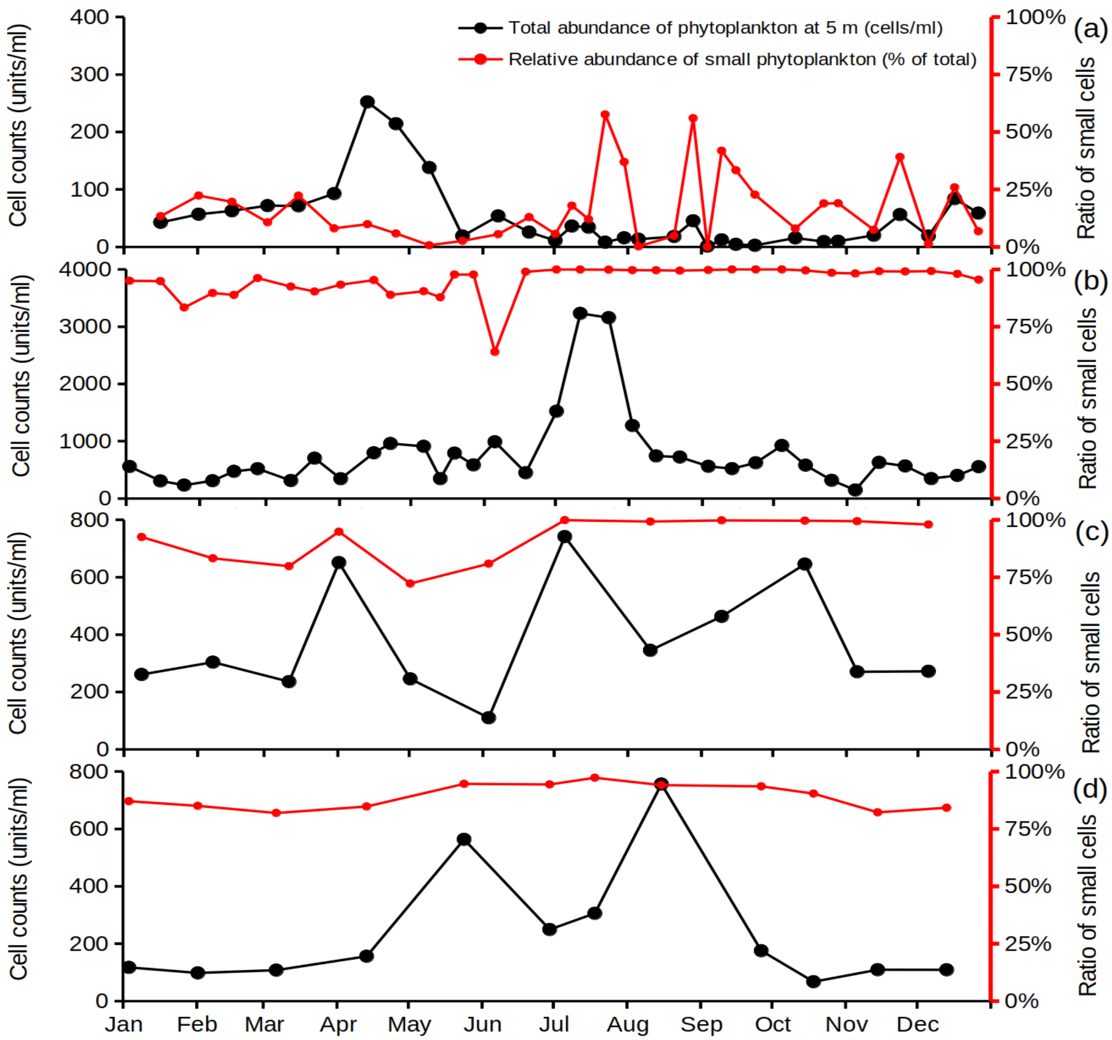

Figure 7.7. Temporal changes in distribution of phytoplankton assemblages at 5 m depth for four years (a) 1969, (b) 1985, (c) 2002 and (d) 2018, LTP station. Left axis is total phytoplankton abundance (cell counts) estimated from enumeration using light microscopy. Right axis is the percentage abundance of the small size fraction (ca. 2-16 µm) of the phytoplankton assemblage. Note that the left vertical axis changes scale between panels.

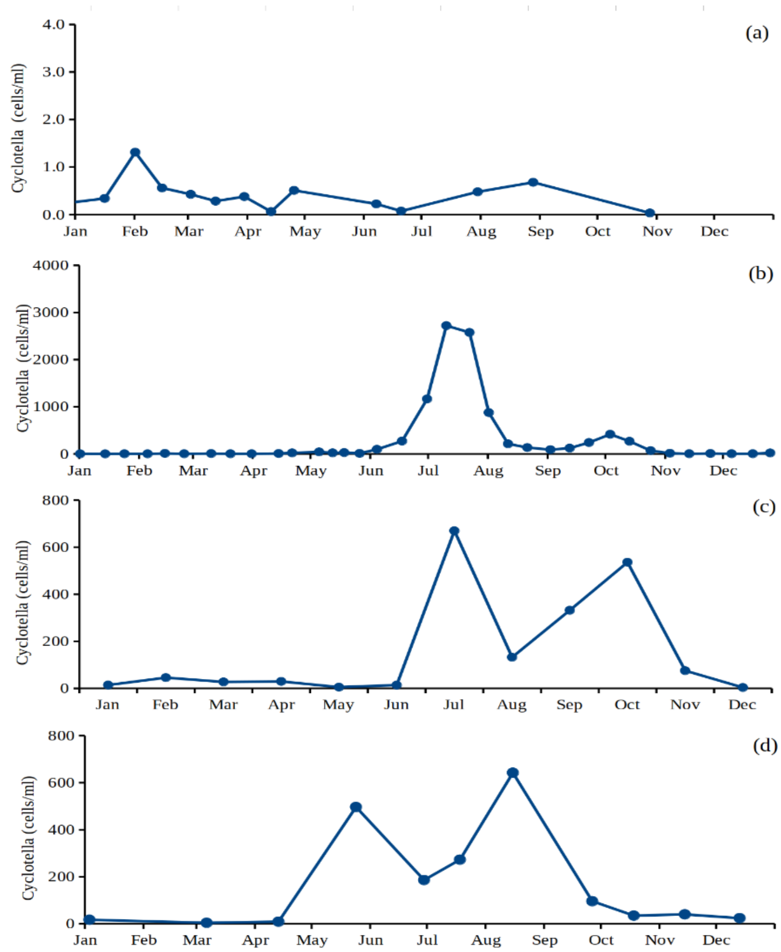

Figure 7.8. Temporal changes in distribution of *Cyclotella* spp. at 5 m depth during (a) 1969, (b) 1985, (c) 2002 and (d) 2018. Unit: cells/ml.

7.4 Results

The introduction of *Mysis* into Lake Tahoe and Emerald Bay altered zooplankton community structure by causing the large-bodied native cladocerans, *Daphnia* and *Bosmina,* to decline. As a result, the long-term Tahoe phytoplankton data suggests these changes resulted in a substantial shift in the phytoplankton assemblage favoring smaller cell sizes which are known to reduce clarity. Part of this latter alteration may have been due to the grazing by *Mysis* themselves.

Stable isotope analysis and gut content analysis of *Mysis* in other lakes showed that diatoms or algal material formed between 25% and 50% of the assimilated diet depending on the season (Stalberg 1933; Larkin 1948; Johannsson et al. 2001). This is consistent with the feeding habits of *Mysis*, which can both filter feed on suspended particles and undertake raptorial feeding on larger organisms (Grossnickle 1981). Given the feeding behavior of *Mysis* in other systems, it seems likely that larger diatoms in Lake Tahoe, such as *Fragilaria*, made up at least a portion of their diet, and may fully account for the disappearance of the larger native diatoms after *Mysis* introduction. It seems highly unlikely that *Mysis* could control the emerging population of small *Cyclotella* given that observed *Mysis* gut contents typically are at least one to two orders of magnitude larger than this. Cyclotella.

Could *Daphnia* and *Bosmina* species have been effectively controlling the presently emergent small celled *Cyclotella*, and did the decline of large bodied cladocerans in Lake Tahoe contribute to the long-term trend of decreasing water clarity? It appears that a combination of the absence of grazing cladocerans, the lack of competition for nutrients with the larger diatoms on account of *Mysis* grazing, plus the effect of climate change favoring small species (Winder et al. 2008), has allowed *Cyclotella* abundance to increase through time, and likely contribute to declining water clarity, especially during the summer months when *Cyclotella* concentrations are at their highest.

Could *Daphnia* grazing rates control *Cyclotella*? Burns and Rigler (1967) showed *D. rosea* feeding rates of up to 10^5 cells/*Daphnia*/hr. The cells in that case were yeast, with a length scale of about 4.2 microns. Currently measurements of *Cyclotella* density can reach as high as $6x10^3$ cells/ml in Tahoe (Fig. 3.7).

Why wouldn't *Daphnia* have also eaten the larger diatoms that the long-term data suggests have declined since *Mysis* introduction? Burns (1968) showed that there is a linear relationship between filter feeding cladocera size (including *Daphnia*) and the size of their prey. *Bosmina longirostris* is 0.4-0.6 mm long and *Daphnia pulex* 0.2-3.0 mm long. Cladocerans up to 2 mm in length (the maximum size of *D. rosea*) do not prey on phytoplankton larger than 40 µm. That would eliminate the *Fragileria* as *Daphnia* prey and explains why large diatoms were dominant before the introduction of *Mysis* because they were released from grazing pressure due to their size. Consequently, the subsequent decline in large diatoms is likely due to direct grazing by *Mysis*.

Another important issue is whether *Daphnia* could also remove fine inorganic particles (such as those introduced by stream and urban loading), in addition to small *Cyclotella* cells. Fine inorganic particles have previously been identified as are confirmed in this report to be a significant contributor to declining clarity in Lake Tahoe (Lahontan 2010). Most experiments to determine *Daphnia* filtering rates use inorganic particles, such as glass beads (Burns 1968) and polystyrene beads (Gophen and Geller 1984). The latter found that *Daphnia* would solely ingest polystyrene particles larger than their filter meshes (0.4 – 0.7 µm). They used particle concentrations of order $10^4 – 10^8$ ml^{-1} for the size range 0.5 – 5 µm, the particle size range important for light scattering and clarity loss (Van de Hulst 1957; Davis-Colley and Smith 2001). Thus, *Daphnia* could readily clear inorganic particles in this size range, which exist at concentrations of 10^3 to 10^5 particles/ml in Lake Tahoe (Schladow 2019).

7.6 Summary of Findings for Hypothesis 5

Hypothesis 5 is repeated here:

Ecological (food web) interactions are causing changes in the trends of seasonal or annual clarity.

With the disappearance of *Mysis* from Emerald Bay and the subsequent return of cladocerans coinciding with an unprecedented increase in Secchi depth of 11 m, researchers were able to witness the potential for restoration of at least a part of the Lake Tahoe food web. While the relationship between *Mysis* and cladocerans at Tahoe and elsewhere has long been known, the impact on clarity is new and offers an additional tool for clarity restoration.

The long-term record from Lake Tahoe indicates that a key impact was the change to the phytoplankton assemblage, where larger diatoms disappeared due to *Mysis* grazing only to be replaced by order-of-magnitude smaller *Cyclotella spp*. Cells in this latter group were too small to be grazed by *Mysis* and other Tahoe zooplankton, and benefited from both reduced competition for nutrients and a more density-stable water column. *Daphnia and Bosmina*, the copepods long known to have been almost eliminated by *Mysis*, are known to feed at high rates on particulates in the size range of both *Cyclotella* and fine terrigenous particles. Both *Cyclotella* and fine inorganic particles are known to impact clarity in Lake Tahoe through their high light scattering efficiency.

Insofar as the specific hypothesis that "*Ecological (food web) interactions are causing changes in the trends of seasonal or annual clarity*" the answer would be yes to both (for seasonal and annual clarity). The loss of cladocerans, the "internal cleaners" of the lake, coincided with the long, sustained period of annual clarity decline from about 1970, and a mechanistic explanation of the process of decline exists through the published literature.

The seasonal nature of these food web impacts is more complex. The loads of fine particles to the lake from the watershed are typically highest in spring and summer. Likewise blooms of *Cyclotella*, when they occur, are increasingly in the spring, summer and fall. Thus, the loss of internal cleaners would be expected to show a maximal impact in these seasons. There are, however, other factors such as changing meteorology, hydrology and lake stratification as described in this report that also contribute to decreased clarity outside of winter. Many of those factors are beyond the control of Agency actions. However, actions that restore *Daphnia* and *Bosmina* to Lake Tahoe (through control of *Mysis*), would complement existing actions that seek to control external loading and growth of small algae.

8. Variables that Influence Winter and Summer Lake Clarity

This work focused on specific hypotheses and questions raised by agencies. To the extent that other variables are important, a more comprehensive list of applicable variables were evaluated as it relates to summer and winter clarity. Thus, winter and summer clarity data were evaluated by non-parametric Spearman's rank order correlation with many additional variables beyond what agencies were requesting. This univariate correlation analysis is intended to evaluate the broad suite of measured and calculated variables related to watershed and in-lake processes that may influence lake clarity. It is not intended to draw definitive conclusions, but rather highlight the multiple variables that are likely contributing to changes in clarity that are outside of the list of hypothesis questions. We are also cautious not to conclude that strong correlation leads to causation. For example, streamflow inputs from Upper Truckee and Blackwood creek were used as surrogates for all stream inputs in both timing of streamflow and fine sediments. A more comprehensive evaluation of stream inputs could be evaluated to determine individual gaged basin influence on clarity. Additional exploration of other important variables that may drive seasonal clarity will be examined further in the upcoming *Lake Tahoe Data Synthesis and Analysis* project. Description of variables used in winter and summer correlation assessment are defined in Appendix 4. Variables used in winter and summer correlation assessment are defined in Appendix 4.

8.1 Winter Clarity and Summer Variables

Correlation between winter clarity was evaluated against thirty-four variables monitored over winter months (Dec to Mar) and summer months (Fig. 8.1a). Variables monitored during winter months were statistically evaluated but did not provide significant correlations to winter clarity, which implies processes in other seasons are likely driving winter clarity. Therefore, a more comprehensive evaluation including summer variables was necessary to provide insight into winter clarity trends. Five summer variables were found to be statistically significant that either negatively or positively correlated to winter clarity (Fig 8.1b). These results suggest that winter clarity is influenced by internal lake processes and watershed processes that typically peak during seasons outside of the December to March winter period. Winter clarity was found to be negatively correlated ($p<0.05$) with median values of summer peak and maximum buoyancy frequency, and positively correlated with maximum snow water equivalent (SWE), summer total phosphorus from Blackwood Creek, and beginning stratification day. Correlations not statistically significant ($P > 0.05$) are not shown in Figure 8.1b.

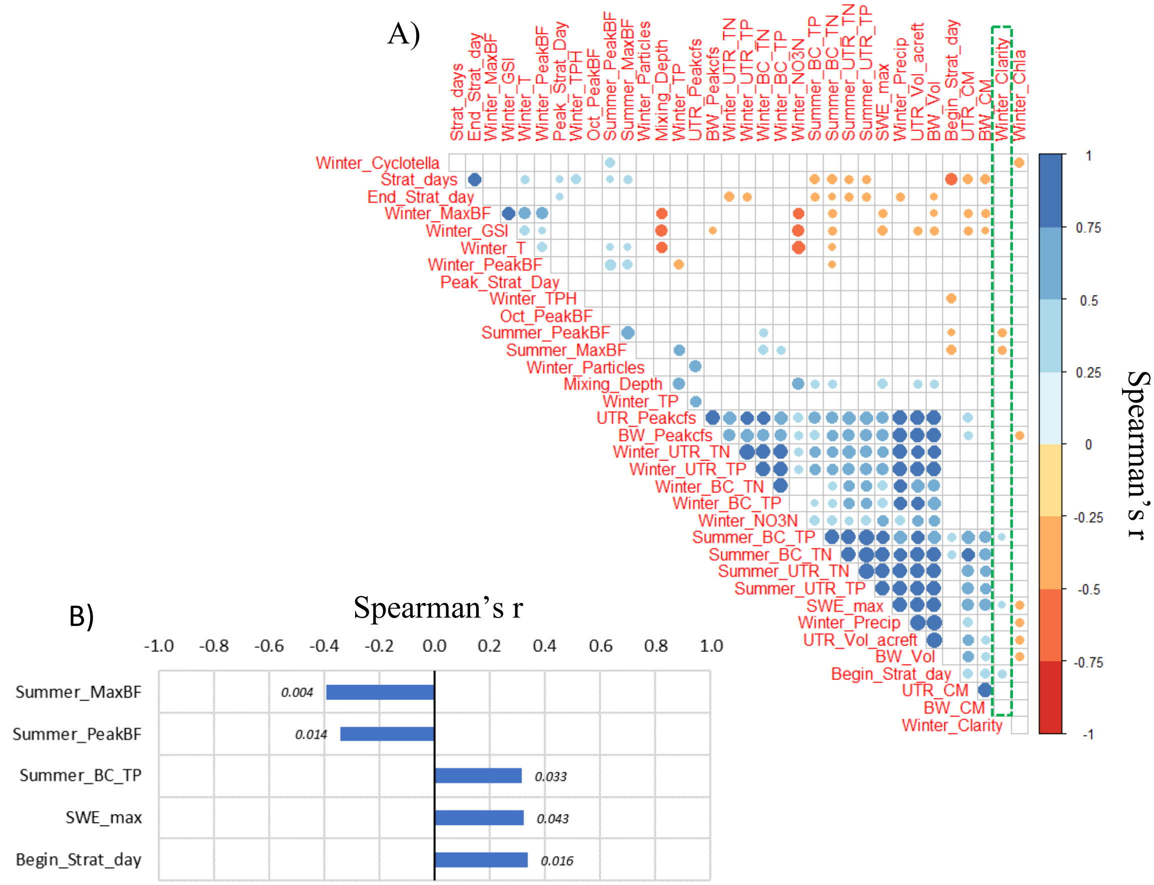

Figure 8.1 Spearman’s rank-order correlation coefficient for A) thirty-four variables of summer and winter processes, and B) summer variables significantly ($p<0.05$) correlated to winter clarity. The five variables correlated to winter clarity were summer maximum buoyancy frequency (maxBF) and summer peak buoyancy frequency (peakBF), summer total phosphorus from Blackwood Creek (BC_TP), maximum snow water equivalent (SWE_max) and beginning stratification day (Begin_Strat_day). In A), correlations not statistically significant ($P > 0.05$) are blank and in B) p-values corresponding to each variable are displayed in italics.

Winter clarity improves during the winter months because winter mixing dilutes light attenuating particles (Jassby et al., 1999). However, the timing and influence of mixing on lake clarity is difficult to describe based on metrics other than mixing depth or temperature, which were found not to be statistically significant. However, it has been widely recognized for Lake Tahoe that deep mixing brings clearer water from depth to the near surface during isothermal conditions that commonly occur during February or March (Jassby et al., 1999). As an example, in 2019 the highest individual clarity reading of 34 m occurred on February 19, coincident with the onset of vertical mixing to 450 m. During mixing events, nitrate concentrations also change throughout the water column as hypolimnetic waters have higher concentration than epilimnetic waters. Nitrate concentration was considered a better surrogate for mixing than temperature, given that isothermal conditions may not always result in mixing (Paerl et al., 1975), and because past temperature instruments before 1975 could typically resolve only 0.01 deg C. Using time-series nitrate concentrations at 10 m lake depth as a tracer for mixing events provides a visual positive correlation with seasonal lake clarity (Fig 8.2A). During seasonal periods of mixing, nitrate concentrations increase and correspond to seasonal highs in lake clarity (Fig. 8.2B). The improvement in clarity resulting from mixing is more pronounced during spring and winter but appears to be insignificant in summer months (Fig. 8.2C).

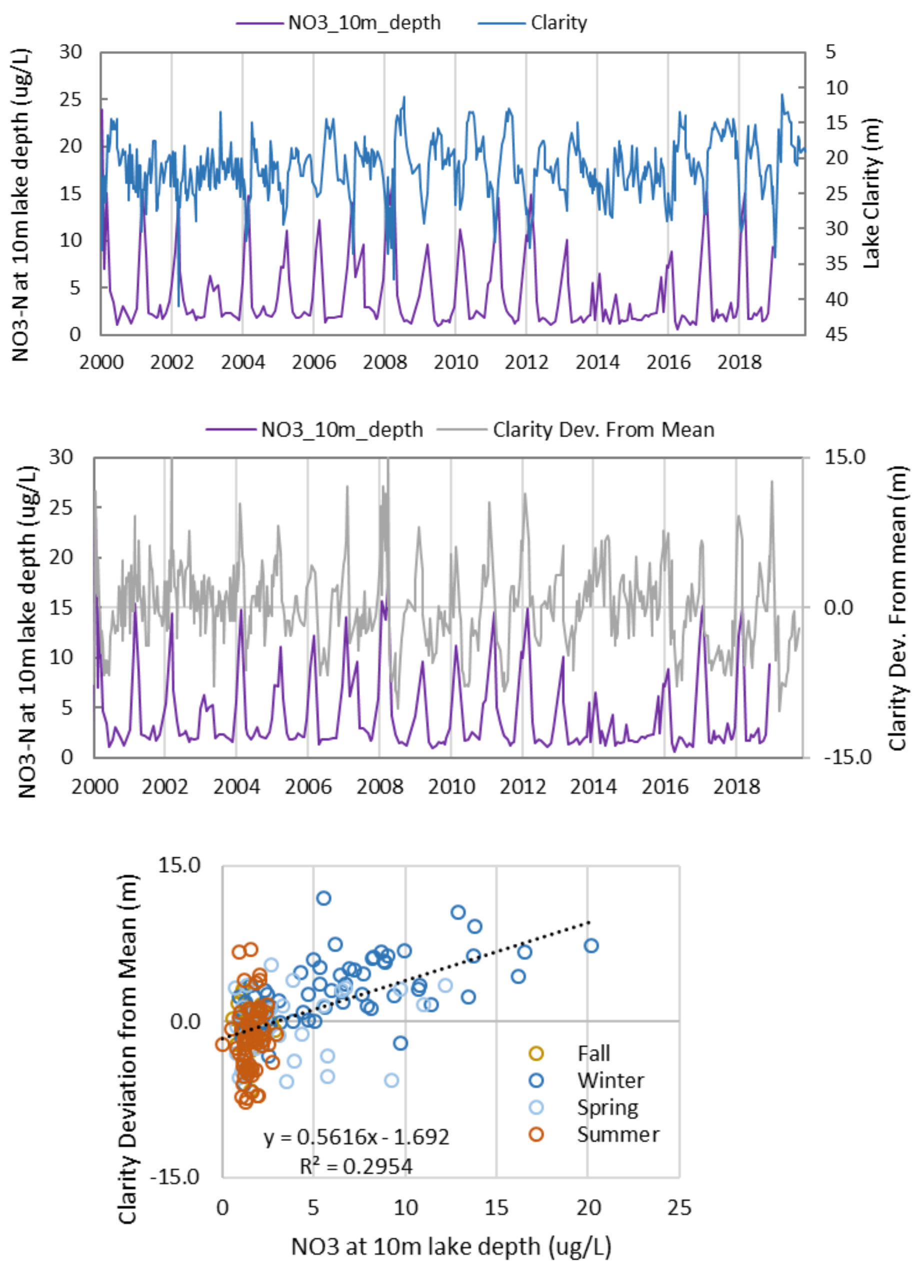

Figure 8.2 Time series of (A) lake nitrate (NO_3-N) concentrations at 10m lake depth with clarity, (B) clarity deviation from mean, and (C) seasonal variations in nitrate. Deep lake mixing results in rapid improvements in clarity along with substantial changes in NO_3-N levels at shallow depths.

8.2 Summer Clarity and Summer Variables

To examine important variables influential in summer clarity, univariate correlations of twenty-six summer variables were evaluated (Fig. 8.4A). Fifteen variables representing various watershed and lake processes were found to be negatively correlated ($p<0.05$) to summer clarity (Fig 8.4B). For watershed processes, stream peak flow, volume, and center of mass were found to be negatively correlated to summer clarity. In-lake processes such as lake particles, *Cyclotella*, and resistance to mixing (MaxBF) were also negatively correlated. Additionally, streamflow nutrients such as nitrogen and phosphorous from Upper Truckee and Blackwood creek were also found to be negatively correlated to summer clarity. The summer univariate analysis clearly shows the drivers of summer clarity to be driven by both watershed and in-lake processes.

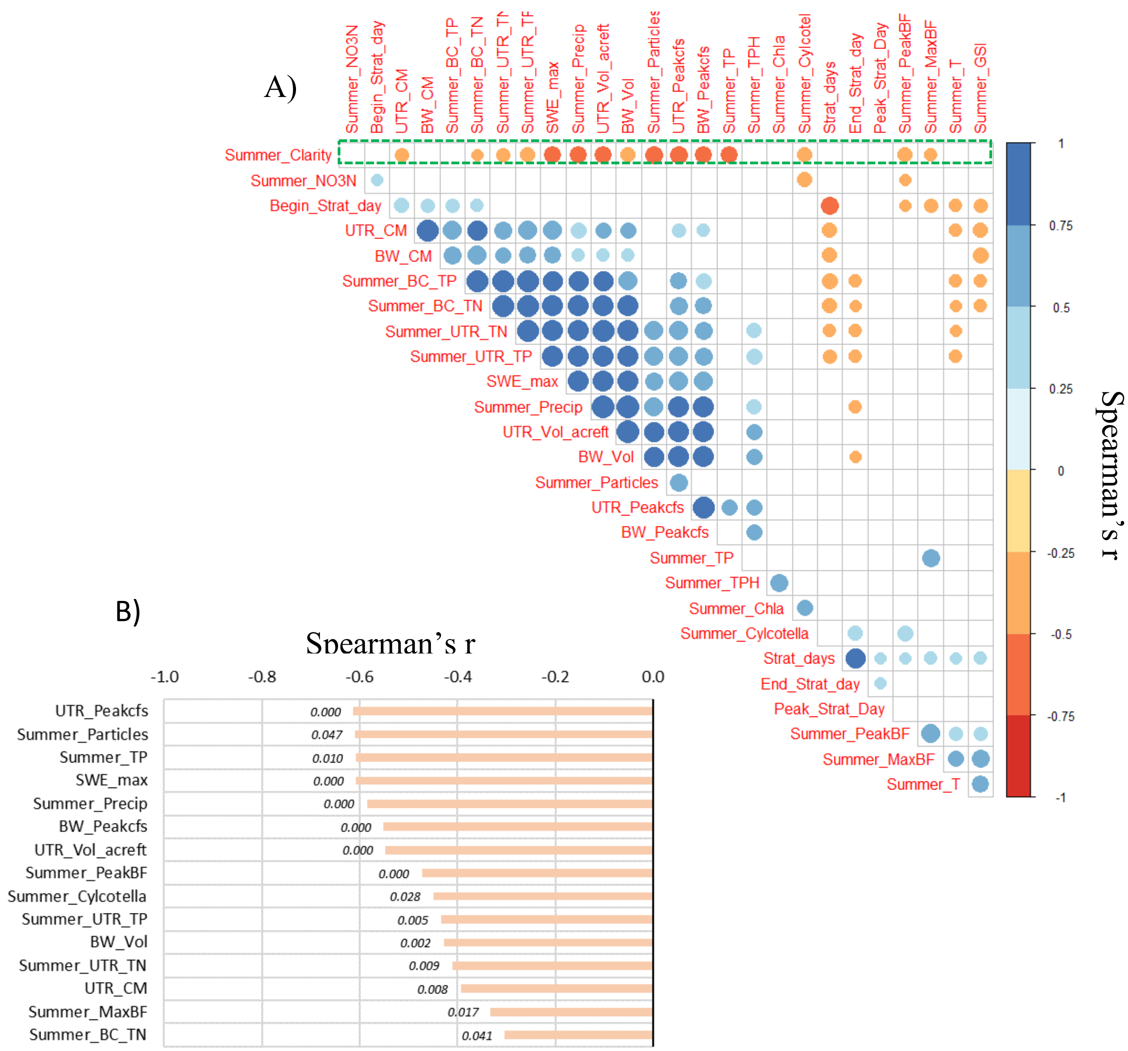

Figure 8.4. Spearman's rank-order correlation coefficient for A) twenty-six variables of summer processes, and B) those variables that were found to be significantly (p<0.05) correlated to summer clarity. The 15 variables found to be negatively correlated to summer clarity were Upper Truckee River peak flow (UTR_peakcfs), summer lake particles, summer total phosphorus (TP), maximum snow water equivalent (SWE_max), summer precipitation (Precip), Blackwood peak flow BW_peakcfs), Upper Truckee River total

volume of flow (UTR_Vol_acreft), summer peak buoyancy (PeakBF), summer *Cyclotella*, summer Upper Truckee River total phosphorus (UTR_TP), Blackwood creek volume of streamflow (BW_Vol), summer Upper Truckee River total nitrogen (UTR_TN) and center of streamflow mass (UTR_CM), summer maximum buoyancy frequency (MaxBF) and summer Blackwood Creek total nitrogen (TN). In A), correlations not statistically significant (P > 0.05) are blank and in B) p-values corresponding to each variable are displayed in italics.

8.2 Lake Clarity and Climate Change

The results of the trend analysis during 2000-2019 period indicate lake clarity during fall and winter months is no longer decreasing. During this same period, the Tahoe basin has experienced a series of persistent droughts followed by above average precipitation periods. Using streamflow records from the Upper Truckee River, lake clarity values were grouped according to streamflow timing and volume based on water year and season (Figure 8.3).

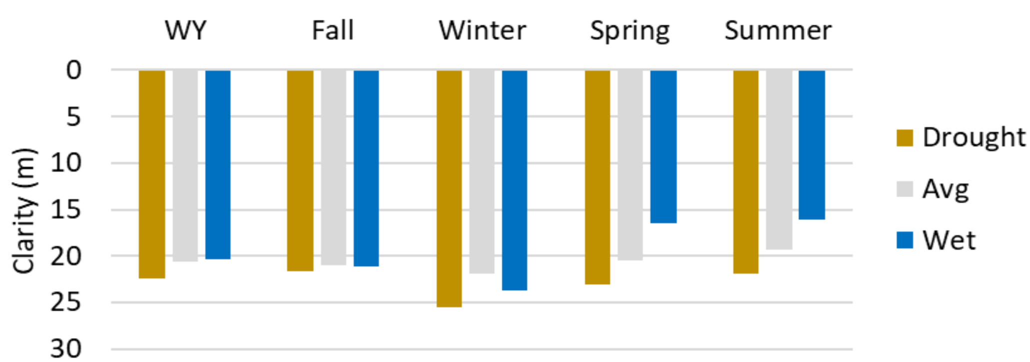

Figure 8.3. The role of climate conditions such as drought, average (avg) and above average conditions (wet) on seasonal clarity values measured from 2000-2019. Drought, average, and wet were defined by analyzing streamflow records from Upper Truckee River. Average water-year streamflow volumes for drought, average and wet are 39,000, 65,000 and 137,000 acre-ft, respectively. During this period, drought, average and above average streamflow conditions occurred 50%, 30%, and 20% of the time, respectively.

Since 2000, 50% of the water years have resulted in less than average streamflow conditions (drought). During drought conditions, lake clarity for each season and annually is higher than average or wet precipitation conditions (Fig. 8.3). Moreover, the highest lake clarity occurs during winter months of drought or wet precipitation conditions when sediment influx to the lake is lowest. During drought years, reduced snowpack, runoff, and associated sediment influx to the lake is less. During wet years, precipitation is stored as a high-volume snowpack or high snow-water equivalent (SWE) that usually results in less runoff during winter months and more runoff during spring and early summer months. The univariate analysis (fig. 8.1A) indicates that winter lake clarity as positively correlated to SWE ($p<0.05$). Moreover, given that drought has occurred during much of the last 20 years of record, the reduction in the rate of clarity decline identified in the trend analysis for winter and fall may be a consequence of reduced stream sediment inflows caused by lower than average SWE, streamflow, and subsequent sediment influx into the lake.

9. Limitations

Some limitations related to the available datasets and past research became apparent during this investigation. These are listed here in no particular order, in the interest of providing input to future monitoring and research efforts:

- Obtain data on the size distribution of *Cyclotella* cells in suspension, recognizing that the species present may be changing year-to-year and even season-to-season. This would help to assess how much of the clarity problem in a particular year can be attributed to *Cyclotella* as opposed to terrigenous particles.
- Continue to monitor fine particle loading to the lake from urban areas, and resolve the efficiency at which numbers of particles from 1–5 µm are being trapped or removed by BMPs (with a focus on particle counts in that range). Current estimates of loading from monitoring sites are highly variable, and only represent a small fraction of the total urban watershed.
- Designed as a planning tool for long-term average loading estimation, the Pollutant Load Reduction Model cannot currently resolve loading estimates at the higher temporal resolutions represented by typical site monitoring efforts for event, seasonal or annual periods. Results, therefore, are not directly comparable.
- Additional focus on methods will be needed to ensure that fine sediment particle numbers >1.0 µm are accurately represented by site monitoring and modeling results for urban and tributary loading.
- Improve the ability to estimate loading of fine sediment particles to the lake from streams, and to account for those that are not monitored.
- Coordinate stream and urban monitoring programs to assure that comparable data are collected and reported for improved comparative evaluations of fine sediment particles and nutrient loading estimates.
- Collect data describing atmospheric deposition of insoluble particles.
- The assessments of in-lake conditions are limited to once-per-month and at a small number of discrete depths, limiting the ability to see the actual changes in water column variables. Continuous sampling is now technologically feasible.
- Better understand the insertion depths of inflows from both streams and stormwater culverts, and the ultimate fate of the nutrients and particle loads.
- Clarity data are not collected on the same day as other important variables, thereby limiting interpretations.
- Short-term fine sediment data from streams and urban areas are insufficient to draw conclusions on the efficacy of EIP actions on load reductions.

- Climate change will continue to be a factor on clarity trends given the extreme variation in seasonal runoff and sediment loads. Given that many of the important processes that influence clarity are becoming less predictable, clarity variations due to climate change may need periodic assessments.

10. Conclusions

The work described in this report was intended to reveal trends in Lake Tahoe water clarity as defined by Secchi disk depth, differences between summer and winter clarity, and relationships between clarity and other observed variables. It also included the collation of the various datasets used in the analysis. Data that were not already publicly available online have been assembled into a Microsoft Excel spreadsheet and are being provided as a project deliverable.

The analysis of clarity trends indicates that over the period of record, annual mean lake clarity has declined, meaning lower Secchi disk readings and reduced clarity. However, over the last 20 years, clarity reductions per year have improved from statistically significant negative trends to no trend. Since 2000, mean monthly clarity for 10 out of 12 months did not significantly decrease. This is an improvement from the period 1980-1999, where one month in every season or 4 out of 12 months were significantly decreasing. July and August are the only months during the most recent period where statistically significant declining trends are identified.

Of the five hypotheses that were investigated in this effort, the first focused on the abundance of fine particles within the lake and their impact on water clarity. Data to reveal particle abundance within the lake date from 2008 to present and have been collected on a nominal basis of twice per month. The data are obtained by a laser diffraction device that reveals the abundance and size distribution of suspended particles in the 0.5-20 μm range.

Based on light scattering theory, the influence of particles depends on both their size and composition. For inorganic (sediment) particle sizes in the range of 1.2 - 1.7 μm, scattering efficiency is maximized and such particles should exert a far greater impact on clarity than smaller and larger terrigenous particles. The species of *Cyclotella* most prevalent in Lake Tahoe (*Cyclotella gordonensis*) are in the size range of 2-5 μm. However, due to the presence of a silica frustule the size of these alga that maximizes light scattering is not precisely known.

Available data on particle size for the lake indicate that sizes of less than 1 μm represented at least 2/3 of the total number of particles in suspension, and these smaller particles are believed to have a negligible impact on lake clarity. A large increase in particle abundance was observed in 2016-2017 that may be partially attributable to an extreme winter snowpack following the end of a long period of drought. Similar increases in particle abundance were not observed in datasets for other wet years in the precipitation record.

Correlation analysis was performed to investigate the relationships between water clarity and several different measures of particle abundance: all particles, particles < 1 μm, particles > 1 μm, and *Cyclotella* particles of all sizes. In all cases, a negative correlation was found, as has been found by many previous observers, and as predicted by light scattering theory. The strongest correlation with declining lake clarity was for particles > 1 μm, and this finding is consistent with light scattering theory indicating that terrigenous particles in the 1-2 μm range will have the greatest negative impact on clarity. The analysis for *Cyclotella* particles showed a similar but less defined relationship. Particle abundance and *Cyclotella* abundance are time-dependent (algal blooms tend to be highly episodic at Lake Tahoe)and this condition adds to the difficulty of assigning a relative importance for each process on lake clarity; however, correlations presented in this report suggest that both processes likely influence lake clarity.

A second hypothesis focused on sediment loading to the lake, but this effort was hampered by data limitations. Trend analysis on fine sediment loads from urban areas revealed no statistically significant trend, but this could be a result of the short length of the data (derived from modeling efforts) describing this loading. Loading via streams is limited by temporal resolution, with fine particles measured only one or two times per month beginning in 2008. This allowed for inspection of trends in particle abundance but is insufficient for quantification of loading when stream discharge can vary greatly over time scales not resolved in the particle measurement effort.

The was no statistically significant trend in particle abundance within the lake, or in streams, for the 2008-2019 period considered. High correlation between abundance in the streams and within the lake was observed, and a large increase was observed beginning in 2016-17. This time period marked the end of a major drought, and the beginning of a very wet year.

Hypotheses 3 and 4 considered the changes in hydrodynamics and thermodynamics of the lake and their impact on water clarity. The resulting investigation included trend analysis of time series describing buoyancy frequency, the date of the onset of stratification, and the duration of stratification. Statistically significant trends were identified that reveal that stratification is starting earlier and lasting longer than in the past, increasing resistance to mixing. Most years observed peak clarity occurs closely in time with maximum mixing. The current trend of decreasing summer clarity was concluded to be a result of earlier, prolonged, and more intense stratification.

Periodicity of long-term time series of in-lake variables was also investigated, revealing 0.5- and 1-year periods corresponding to annual and seasonal changes in meteorological conditions and hydrological conditions. Longer periodicities such as 3, 7 and 10 years are also present in long-term records. Some potential explanations for these longer periods of more than one year include climatological phenomena such as El Niño/ENSO and the hydrological consequences, interactions between different trophic levels and nutrients, and ecological impacts of invasive species introductions.

Hypothesis 5 focused on impacts of ecological changes and events and their impact on clarity. Observed changes in both *Mysis* abundance and clarity in Emerald Bay within the lake suggest a strong linkage between these variables.

Long-term records from the lake reveal the disappearance of larger diatoms and their replacement by much smaller *Cyclotella spp*, closer to the particle size that maximizes light scattering in water. *Cyclotella* are unlikely to be grazed by Tahoe zooplankton, and benefited from both reduced competition for nutrients and a more density-stable water column. The introduction of *Mysis* resulted in drastic reduction of the *Daphnia and Bosmina* populations, both of which feed on particulates in the size range of both *Cyclotella* and fine terrigenous particles.

These ecological changes are also linked to physical changes in the lake that influence the timing and strength of stratification, controlling mixing events. Cyclotella blooms are typically observed in spring, summer, and fall, and the timing of these seasons, as reflected by stratification data, is changing. The longer stratification and greater resistance to mixing that is revealed by the long-term dataset has both physical and ecological implications.

While not envisioned at the onset of this study, an additional analysis was performed to look at correlation of clarity with a very large set of monitored, modeled, or derived parameters, and to consider both their winter and summer values. This dataset included water chemistry parameters and atmospheric, meteorological, and hydrological variables. The reader is referred to section 8 of this report for details, but the results reveal that summer clarity is strongly dependent on inflow-driven and stratification-based parameters, whereas there is no clear parameter or group of winter parameters that exerts strong control over winter clarity.

There is a long history of data collection and research at Lake Tahoe and the multi-decadal datasets utilized in this report were invaluable, as were the multitude of previous investigations of lake processes and ecology. As the understanding of the lake and the issues affecting it have evolved, so have the programs yielding the data for subsequent analysis. In some cases, these programs have not been in place long enough to allow for the assessment of statistically significant trends, but with long enough records, this will become possible.

References Cited

Abbott, M.R., Powell, T.M. and Richerson, P.J. 1982. The relationship of environmental variability to the spatial patterns of phytoplankton biomass in Lake Tahoe. Journal of Plankton Research, 4(4), 927-941.

Allen, B., B. Berry, A. Liston, S. Hackley, T. Hammell, K. Senft, S. Sesma, R. Townsend, S. Watanabe, G. Schladow, undated. Lake Tahoe Pelagic Monitoring, Calendar Years 2016-2018 Data Report and Summary Analysis. Project report to Tahoe Regional Planning Agency. UC Davis Tahoe Environmental Research Center, 29 pp.

Bendat, J.S. and Piersol, A.G., 1986. Random data: analysis and measurement procedures. 2nd ed., John Wiley and Sons, 566 pp.

Bürgi, H.R., J.J. Elser, R.C. Richards, and C.R. Goldman. 1993. Zooplankton patchiness in Lake Tahoe and Castle Lake, USA. Verh. Internat. Verein. Limnol. 25:378-382.

Burns, C.W. and Rigler, F.H. 1967. Comparison of filtering rates of *Daphnia rosea* in lake water and in suspensions of yeast. Limnology and Oceanography, 12(3), 492-502.

Burns, C.W. 1968. The relationship between body size of filter feeding *Cladocera* and the maximum size of particle ingested. Limnology and Oceanography 13(4), 675-678.

Byron, E.R., Folt, C.L. and Goldman, C.R. 1984. Copepod and cladoceran success in an oligotrophic lake, J. Plankton Res., 6, 45-65.

Byron, E.R., Sawyer, P.E. and Goldman, C.R. 1986. The recurrence of *Daphnia rosea* in Lake Tahoe: analysis of a population pulse. J. Plankton Research, 8(4), 771-783.

Cayan DR, Maurer EP, Dettinger MD, Tyree M, Hayhoe K (2008) Climate change scenarios for the California region. Clim Chang 87(Suppl 1):S21–S42. doi:10.1007/s10584-007-9377-6

Cayan DR, Tyree M, Dettinger M, Hidalgo H, Das T, Maurer E, Bromirski P, Graham N, Flick R (2009)Carney, H.J. and Elser, J.J. 1990. Strength of Zooplankton-Phytoplankton Coupling in Relation to Lake Trophic State. In: Tilzer M.M., Serruya C. (eds) Large Lakes. Brock/Springer Series in Contemporary Bioscience. Springer, Berlin, Heidelberg.

Coats R (2010) Climate change in the Tahoe Basin: regional trends, impacts and drivers. Climate Change 102:435–466. doi:10.1007/s10584-010-9828-3.

Coats, R., M. Costa-Cabral, J. Riverson, J. Reuter, G. Sahoo, G. Schladow and B. Wolfe. 2013. Projected 21st century trends in hydroclimatology of the Tahoe basin. Climatic Change. DOI:10.1007/s10584-012-0425-5.

Coats R, Costa-Cabral M, Riverson J, Reuter J, Sahoo G, Schladow G,Wolfe B (2012) Projected 21st century trends in hydro climatology of the Tahoe basin. Climatic Change 2013 116, 51–69 (2013). https://doi.org/10.1007/s10584-012-0425-5

Coats, R., Sahoo, G., Riverson, J., Costa-Cabral, M., Dettinger, M., Wolfe, B., Reuter, J., Schladow, G., and Goldman, C.R. (2013). Historic and likely future impacts of climate change on Lake Tahoe, California-Nevada, USA. In Goldman, C., Kumagai, M., and Robarts, R. (Eds.), Climatic change and global warming of inland waters: Impacts and mitigation for ecosystems and societies. Hoboken, NJ: John Wiley and Sons.

Coats, R., J. Lewis, N. Alvarez, and P. Arneson. 2016. Temporal and Spatial Trends in Nutrient and Sediment Loading to Lake Tahoe, California-Nevada, USA. Journal of the American Water Resources Association (JAWRA) 1-19. DOI: 10.111/1752-1688.12461.

Cooper, S.D. and Goldman, C.R. 1980. Opossum Shrimp (*Mysis relicta*) predation on zooplankton. Canadian Journal of Fisheries and Aquatic Sciences, 37(6): 909-919.

Davies-Colley, R.J. and Smith, D.G., 2001. Turbidity, suspended sediment, and water clarity: A review. JAWRA Journal of the American Water Resources Association, 37: 1085-1101. doi:10.1111/j.1752-1688.2001.tb03624.x.

Dettinger, M.D. (2013) Projections and downscaling of 21st century temperatures, precipitation, radiative fluxes, and winds for Southwestern US, with a focus on Lake Tahoe Climate Change 116:17-33 DOI 10.1007/s10584-012-0501-x

Dettinger, M.D and Cayan, D.R. (1995) Large-scale atmospheric forcing of recent trends toward early snowmelt runoff in California. J. Climate, 8, 606–623, https://doi.org/10.1175/1520-0442(1995)008<0606:LSAFOR>2.0.CO;2.

Deamer, D.W., H. Paerl, C.R. Goldman and R. Leonard. 1975. Tahoe's troubled waters. Natural History 84:60-67.

Ellis, B.K, Stanford, B.A., Goodman, D. Stafford, C.P., Gustafson, D.L., Beauchamp, D.A., Chess, D.W., Craft, J.A., Deleray, M.A. and Hansen, B.S. 2011. Long-term effects of a trophic cascade in a large lake ecosystem. PNAS 108(3), 1070-1075.

Elser, J.J. and Goldman, C.R. 1991. Zooplankton effects on phytoplankton in lakes of contrasting trophic status. Limnol. Oceanogr., 36(l), 64-90.

Environmental Improvement Program (EIP), 2018. Accomplishments and a look ahead. 2019. Tahoe Regional Planning Agency. (https://eip.laketahoeinfo.org/FileResource/DisplayResource/d098819e-8ea6-4595-bc6e-b99cf73fcd8a)

Gevertz, A.K., Tucker, A.J., Bowling, A.M., Williamson, C.E. and Oris, J.T, 2012. Differential tolerance of native and nonnative fish exposed to ultraviolet radiation and fluoranthene in Lake Tahoe (California/Nevada), USA. Environmental Toxicology and Chemistry, 31(5), pp 1129-1135.

Goldman, C. R. 1963. The measurement of primary productivity and limiting factors in freshwater with carbon-14. Pages 103-113 in M. S. Doty, editor. Proceedings of the conference on primary productivity measurements, marine and freshwater. United States Atomic Energy Commission, Division of Technical Information, Washington, DC.

Goldman, C.R., Morgan, M.D., Threlkeld, S.T. and Angeli, N. 1979. A population dynamics analysis of the cladoceran disappearance from Lake Tahoe, California-Nevada. Limnol. Oceanogr., 24, 289—297.

Goldman, C.R. 1981. Lake Tahoe: two decades of change in a nitrogen deficient oligotrophic lake. Internationale Vereinigung für theoretische und angewandte Limnologie: Verhandlungen, 21:1, 45-70, DOI: 10.1080/03680770.1980.11896960.

Goldman, C.R. 1988. Primary productivity, nutrients, and transparency during the early onset of eutrophication in ultra-oligotrophic Lake Tahoe, California-Nevada. Limnol. Oceanogr. 33(6), 1321-1333.

Gophen, M. and Geller, W. 1984. Filter mesh size and food particle uptake by *Daphnia.* Oecologia (Berlin) 64: 408-412.

Griffiths, D. 2007. Effects of climatic change and eutrophication on the glacial relict, *Mysis relicta*, in Lough Neagh. Freshwater Biology, 52, 1957–1967.

Grossnickle N.E. 1982. Feeding habits of *Mysis relicta* - an overview. In: Morgan M.D. (eds) Ecology of Mysidacea. Developments in Hydrobiology, vol 10. Springer, Dordrecht

Hansen, J. A., 1966. Final introduction of the opossum shrimp (*Mysis relicta Loven*) into California and Nevada. Cal. Fish Game 52 (3), 220.

Hansen J, Sato M, Ruedy R, Lo K, Lea DW, Medina-Elizade M (2006) Global temperature change. Proc Natl Acad Sci USA 103:14288–14293Helsel, D.R., and Hirsch, R.M., 2002. Statistical Methods in Water Resources. Techniques of Water-Resources Investigations 04-A3, https://doi.org/10.3133/twri04A3.

Heyvaert, A., J. Reuter, J. Thomas. 2011. Tahoe Regional Stormwater Monitoring Program Quality Assurance Project Plan and Sampling and Analysis Plan. Final report submitted to the USDA Forest Service. May 2011. 129 pp.

Hunter, D.A., Goldman, C.R. and Byron, E.R. 1990. Changes in the phytoplankton community structure in Lake Tahoe, California-Nevada Verh. Internat. Verein. Limnol. 24(1), 505-508.

Hutchinson, G.E. 1957. A Treatise on Limnology, Volume I: Geography, Physics, Chemistry.

Jassby, A.D., Goldman, C.R. and Powell, T.M. 1992. Trend, seasonality, cycle, and irregular fluctuations in primary productivity at Lake Tahoe, California-Nevada, USA. Hydrobiologia 246: 195-203.

Jassby, A.D., Reuter, J.E., Axler, R.P., Goldman, C.R. and Hackley, S.H. 1994. Atmospheric deposition of nitrogen and phosphorus in the annual nutrient load of Lake Tahoe (California-Nevada). Water Resources Research, V.30(7), pp 2207-2216.

Jassby, A.D., Goldman, C.R., Reuter, J.E., and Richards, R.C., 1999. Origins and scale dependence of temporal variability in the transparency of Lake Tahoe, California–Nevada. *Limnol Oceanogr*, 44(2), 282–294.

Jassby, A.D., C.R. Goldman, J.E. Reuter and R.C. Richards. 2000. Biostatistical evaluation of long-term lake clarity record. Verh. Internat. Verein. Limnol. 27:2634-2635.

Jassby, A.D., J.E. Reuter and C.R. Goldman. 2003. Determining long-term water quality change in the presence of climatic variability: Lake Tahoe (USA). Can. J. Fish. Aquat. Sci. 60:1452-1461.

Johannsson, O.E., Leggett, M.F., Rudstam, L.G., Servos, M.R., Mohammadian, M.A., Gal, G., Dermott, R.M. and Hesslein, R.H. 2001. Diet of *Mysis relicta* in Lake Ontario as revealed by stable isotope and gut content analysis. Can. J. Fish. Aquat. Sci. 58: 1975–1986.

Kivivuori, L.A. and Lahdes, E.O. 1996. How to measure the thermal death of Daphnia? A comparison of different heat tests and effects of heat injury. Therm. Biol. Vol. 21(5/6), 305-311.

Kling H. and Håkansson 1988. A light and electron microscope study of *Cyclotella* species (Bacillariophyceae) from Central and Northern Canadian lakes. Diatom Research Vol. 3(l), 55-82.

Koksvik, J.I., Reinertsen, H. and Koksvik, J. 2009. Plankton development in Lake Jonsvatn, Norway, after introduction of *Mysis relicta*: a long-term study. Aquatic Biology, Vol. 5: 293–304.

Lahontan Regional Water Quality Control Board (LRWQCB) and Nevada Division of Environmental Protection (NDEP). 2010. Final Lake Tahoe Total Maximum Daily Load (TMDL) Report. November 2010.

Larkin, P. A. 1948. *Pontoporeia* and *Mysis* in Athabaska, Great Bear, and Great Slave Lakes. Bull. Fish. Res. Bd Can. 78: 1–33.

Lebo, M.E. and J.E. Reuter. 1995. Evidence for sediment resuspension in a large, deep lake: Implications for phosphorus cycling. Marine and Freshwater Research. 46: 321-326.

LeConte, J. 1883. Physical studies of Lake Tahoe – I. Overland Monthly and Out West Magazine. Vol. II, No.11

Linn, J.D., and T.C. Frantz. 1965. Introduction of the opossum shrimp (*Mysis relicta Loven*) in California and Nevada. California Fish and Game 51:48-51.

Marjanovic, P. 1989. Mathematical modeling of eutrophication processes in Lake Tahoe: Water budget, nutrient budget and model development. PhD Dissertation, University of California, Davis.

McCoy, A. K., 2015. An Assessment of the Impact of Non-Native Lake Trout *Salvelinus namaycush* and *Mysis diluviana* on the Growth and Survival of Pelagic Planktivores in Lake Tahoe (Doctoral dissertation).

Molugaram, K, and Rao, G. S., 2017. Statistical Techniques for Engineers. 2nd ed. Elsevier

Morales, E., Rosen, B., Spaulding, S. 2013. *Fragilaria crotonensis*. In Diatoms of North America. Retrieved December 28, 2019, from https://diatoms.org/species/fragilaria_crotonensis

Morgan, M.D., and A.M. Beeton. 1978. Life history and abundance of *Mysis relicta* in Lake Michigan. *Journal of the Fisheries Board of Canada*, *35*(9), pp.1165-1170.

Morgan, M. D. 1979. The dynamics of an introduced population of *Mysis relicta* (Loven) in Emerald Bay and Lake Tahoe, California-Nevada. Dissertation. University of California, Davis, California, USA.

Nevada Division of Environmental Protection and the Lahontan Regional Water Quality Control Board, 2020. Lake Clarity Crediting Program (LCCP). 2020. Lake Tahoe TMDL Program 2019 Performance Report. January 2020.

Nevada Tahoe Conservation District, 2016. PLRM V2.1 Recalculated Baseline Pollutant Loads for Washoe County and the Nevada Department of Transportation. https://ndep.nv.gov/uploads/water-tahoe-docs/Washoe_Co__NDOT_Bseline_Report.pdf

Paerl, H.W., Richards, R.C., Leonard, R.L. and C. Goldman 1975. Seasonal nitrate cycling as evidence for complete vertical mixing in Lake Tahoe, California-Nevada. *Limnology and Oceanography* vol. 20 (1), 1-8.

Press, W.H., Teukolsky, S.A., Vetterling, W.T., and Flannery, B.P., 1992. Numerical Recipes in C, 2nd ed., Cambridge University Press.

Rabidoux, A.A. 2005. Spatial and Temporal Distribution of Fine Particles and Elemental Concentrations in Suspended Sediments in Lake Tahoe Streams, California-Nevada.Master of Science in Civil Engineering, UC Davis.

Reardon, K.E., P.A. Moreno-Casas, F.A. Bombardelli, and S.G. Schladow. 2016. Seasonal nearshore sediment resuspension and water clarity at Lake Tahoe, Lake and Reservoir Management, 32(2), 132-145, DOI:10.1080/10402381.2015.1136013.

Reuter, J.E. and Miller, W. 2000. Aquatic resources, water quality, and limnology of Lake Tahoe and its upland watershed. In: Murphy, D.D and C.M. Knopp (Technical Editors.) Lake Tahoe Watershed Assessment: Volume I. Gen. Tech. Rep. PSW-GTR-175. Albany, CA: Pacific Southwest Research Station, Forest Service, US Department of Agriculture; 753p.

Richards, R.C, Goldman, C.R., Frantz.T.C. and Wickwire. R. 1975. Where have all the *Daphnia* gone? The decline of a major cladoceran in Lake Tahoe, California-Nevada. Verh. Int. Verein. Limnol., 19, 835-842.

Riverson, J., R. Coats, M. Costa-Cabral, M. Dettinger, J. Reuter, G. Sahoo and G. Schladow. 2013. Modeling the transport of nutrients and sediment loads into Lake Tahoe under projected climatic changes. Climatic Change. DOI:10.1007/s10584-012-0629-8.

Roberts, D.C., Forrest, A.L., Sahoo, G.B., Hook, S.J., and S.G. Schladow. 2018. Snowmelt timing as a determinant of lake inflow mixing. Water Resources Research. 10.1002/2017WR0219177.

Rose, K., C. E. Williamson, S. G. Schladow and M. Winder. 2009. Patterns of Spatial and Temporal Variability of Transparency in Lake Tahoe, CA/NV. JGR Biogeosciences, 114: G00D03.

Rowe, T.G., 2000. Lake Tahoe Interagency Monitoring Program: Tributary Sampling Design, Sites, and Periods of Record. USGS Fact Sheet 138-00, U.S. Geological Survey, October 2000, 4 pp.

Rudstam, R.G., Hetherington, A.L. and Mohammadian, A.M. 1999. Effect of temperature on feeding and survival of *Mysis relicta*. J. Great Lakes Res. 25(2):363–371.

Rudstam, R.G. and Johannsson, O.E. 2009. Introduction: Advances in the ecology of freshwater mysids. Aquatic Biology, Vol. 5: 246–248.

Rybock, J. T., 1978. *Mysis relicta Loven* in Lake Tahoe: vertical distribution and nocturnal predation. Ph.D. dissertation. Univ. California, Davis, 116 pp.

Sahoo, G. B., S. G. Schladow and J. E. Reuter. 2010. Effect of sediment and nutrient loading on Lake Tahoe optical conditions and restoration opportunities using a newly developed lake clarity model, Water Resources Res., 46, W10505, DOI:10.1029/2009WR008447.

Sahoo, G.B., D.M. Nover, J.E. Reuter, A.C. Heyvaert, J. Riverson and S.G. Schladow. 2013. Nutrient and particle load estimates to Lake Tahoe (CA-NV, USA) for Total Maximum Daily Load establishment. Science of the Total Environment 444 (2013) 579–590.

Sahoo, G.B., Forrest, A.L., Schladow, S.G., Reuter, J.E., Coats, R. and Dettinger, M., 2015. Climate change impacts on lake thermal dynamics and ecosystem vulnerabilities. Limnology and Oceanography, doi: 10.1002/lno.10228.

Sahoo, G.B., Schladow, S.G., Reuter, J.E. et al. The response of Lake Tahoe to climate change. Climatic Change 116, 71–95 (2013). https://doi.org/10.1007/s10584-012-0600-8

Sawyer, P.E. 1985. The Predatory Behavior and Distribution of *Mysis relicta* in Lake Tahoe, California—Nevada. MS Thesis, University of California, Davis.

Schladow, S.G., Palmarsson, S.O., Steissberg, T.E., Hook, S.J. and Prata, F.E. 2004. An extraordinary upwelling event in a deep thermally stratified lake. Geophysical Research Letters, Vol. 31, L15504, doi:10.1029/2004GL020392.

Schladow, S.G. (Ed.) 2015. Tahoe: State of the Lake Report: 2015. Report of the UC Davis Tahoe Environmental Research Center. https://tahoe.ucdavis.edu/sites/g/files/dgvnsk4286/files/inline-files/complete-2015-sotl_low.pdf

Schladow, S.G. (Ed.) 2019. Tahoe: State of the Lake Report: 2019. Report of the UC Davis Tahoe Environmental Research Center. https://tahoe.ucdavis.edu/sites/g/files/dgvnsk4286/files/inline-files/SOTL2019_reduced.pdf

Schladow, S.G., Allen, B.C., Senft, K.J., de Souza Cardoso, L., Forrest, A. L., Sadro, S., Watanabe, S., Tanaka, L.L., Gamble, A.E. and Richards, R.C. 2020. Rethinking the causes of clarity loss at Lake Tahoe. Under Journal Review

Sommer, U. and Sommer, F. 2006. Cladocerans versus copepods: The cause of contrasting top-down controls on freshwater and marine phytoplankton. Oecologia. 147. 183-94. 10.1007/s00442-005-0320-0.

Stafford, C.P., Stanford, J.A., Hauer, F.R. and Brothers, E.E. 2002. Changes in Lake Trout growth associated with *Mysis relicta* establishment: A retrospective analysis using otoliths. Transactions of the American Fisheries Society 131:994–1003.

Stalberg, G. 1933. Beitrag zur Kenntnis der Biologie von *Mysis relicta* des Vättern. Arkiv. Zool. 26A: 1–29.

Stubblefield, A.P., J.E. Reuter, R.A. Dahlgren and C.R. Goldman. 2007. Use of turbidometry to characterize suspended sediment and phosphorus fluxes in the Lake Tahoe basin, California, USA. Hydrological Processes 21:281-291.

Sunman, B. 2004. Spatial and Temporal Distribution of Particle Concentration and Composition in Lake Tahoe, California-Nevada. Master of Science in Chemical Engineering, UC Davis.

Swift, T.J., Perez-Losada, J., Schladow, S.G., Reuter, J.E., Jassby, A.D., and Goldman, C.R., 2006. Aquat. Sci. 68, 1 – 15, 1015-1621/06/010001-15, DOI 10.1007/s00027-005-0798-x.

Tahoe Environmental Research Center, 2019. State of the Lake Report 2019. University of California-Davis, 97 pp.

Tahoe Resource Conservation District (TRCD), 2020. Annual Stormwater Monitoring Report, Water Year 2019. Prepared for the Implementers' Monitoring Program (IMP) component of the Regional Stormwater Monitoring Program (RSWMP). Submitted to the Lahontan Regional Water Quality Control Board and the Nevada Division of Environmental Protection, March 15, 2020.

Threlkeld, S.T. 1981. The recolonization of Lake Tahoe by Bosmina longirostris: evaluating the importance of reduced *Mysis relicta* populations. Limnol. Oceanogr., 26, 433—444.

Threlkeld, S.T., Rybock, J.T., Morgan. M.D., Folt, C.L. and Goldman, C.R. 1980. The effects of an introduced invertebrate predator and food resource variation on zooplankton dynamics in an oligotrophic lake, in Kerfoot.W.C. (ed.), *Evolution and Ecology of Zooplankton Communities, New England Press*, pp. 555-56.

Tilzer, M.M., C.R. Goldman, R.C. Richards and R.C. Wrigley. 1976. Influence of sediment inflow on phytoplankton primary productivity in Lake Tahoe (California-Nevada). Internat. Revue der gesamten Hydrobiologie 61:169-182.

Tucker, A.J., Williamson, C.E., Rose, K.C., Oris, J.T., Connelly, S.J., Olson, M.J. and Mitchell, D.L. 2010. Ultraviolet radiation affects invasibility of lake ecosystems by warm-water fish. Ecology Vol.91(3), pp. 882-890.

van de Hulst, H.C., 1957. Light scattering by small particles. New York (John Wiley and Sons), London (Chapman and Hall). Pp. xiii, 470; 103 Figs.; 46 Tables. 96s. Q.J.R. Meteorol. Soc., 84: 198-199. doi:10.1002/qj.49708436025

Watanabe, S., Vincent, W.F., Reuter, J., Hook, S.J., and Schladow, S.G., 2016. A quantitative blueness index for oligotrophic waters: Application to Lake Tahoe, California–Nevada. Limnol. Oceanogr.: Methods 14, 2016, 100–109. doi: 10.1002/lom3.10074

Winder, M. and Hunter, D. A. 2008. Temporal organization of phytoplankton communities linked to physical forcing. Oecologia, 156:179–192.

Winder, M., Reuter, J.E. and Schladow, S.G. 2008. Lake warming favours small-sized planktonic diatom species. Proc. R. Soc. B, 276, 427–435.

Wood, S. N. 2006. Generalized Additive Models: An Introduction with R. Vol. 66. CRC Press.

Wu, L. and Culver, D.A. 1991. Zooplankton grazing and phytoplankton abundance: an assessment before and after invasion of *Dreissena Polymorpha*. Journal of Great Lakes Research, 17(4), Pages 425-436.

Supplemental Information

Appendix 1 Data Availability

LTP = Long-term monitoring site
MLTP = Mid-Lake long-term monitoring site

Parameter Category	Parameter	Site(s)	Period of Record	Locations	Frequency	Notes
Physical	Secchi depth	MLTP; LTP	4/1969-12/2019; 1967-present		Variable; typ. 1-2x/month	
	Temperature	MLTP; LTP	1969-1996; 1967-1996	11 depths from 0-450 m; 10-30 depths from 0-98 m	monthly; every 10 days	Technology and resolution varied over the years.
	Continuous Temperature	MLTP; LTP	1996-2006	Continuous 0→200 m; Continuous 0→150 m	monthly; every 14 days	LTP and MLTP RBR temp. profiles began 9/96
	Temperature	4 buoys	2000-present	0 m	continuous	

	Temp. (+conductivity, depth, DO, pH, turbidity, PAR, light transmission)	MLTP; LTP	2005-present	Continuous 0→450 m; Continuous 0→150 m	monthly; every 14 days	Seabird data collection began 10/05
	Fine particle size distribution	MLTP; LTP	2008-present	0, 10, 50 m; 9 depths from 0-50m	monthly; every 14 days	14 size classes spanning 0.5-20 micron size range
Chemical	Nitrogen (NO3)	MLTP; LTP	1970-present; 1968-present	0, 10, 50 m; 9depth from 0-50m	monthly; every 14 days	
	Nitrogen (TKN)	MLTP	1989-present	0, 10, 50 m;	monthly	
	Phosphorus (THP)	MLTP; LTP	1996-present; 1996-present	0, 10, 50 m; 9depth from 0-50 m	monthly; every 10 days	Data prior to 1996 were not usable.
	Phosphorus (TP)	MLTP	1989 - 1992, 2000-present	0, 10, 50m;	monthly	
Biological	Primary production	LTP	1967-present	13 depths from 0-105m	twice monthly; every 10	

					days, monthly since 2007	
	Chlorophyll a	LTP	1984-present	9 depths from 0-50m	1984-2006: monthly profiles with composites every 10 days; monthly (profile + composite) since 2007	
	Chlorophyll a	MLTP	1984-present	0, 10, 50m	monthly	
	Chlorophyll a, fluorescence	MLTP, LTP	2005-present	Continuous 0→450m; Continuous 0→150m	monthly; every 14 days	Availability depends on instrumentation on Seabird instrument

	PhytoP ident. & enum.	MLTP, LTP	1980-present; 1969-present	**MLTP-->**; 2/1992-9/2006: 0-100 m composites; 10/2006-present: 0-100 m, **LTP-->**1969-1991: 13 depths from 0-105 m; 1992-present: 5,20,40,60,75,90 m; 1984-3/1990: 0-105 m composite; 3/1990-1/2007: 0-20 m & 0-105m composites; 2/2007-present: 0-105 m composite	monthly; every 10 days, monthly since 2007	
	Zoop - crustaceans	MLTP, LTP	1967-present	0→150m tow; 0-30,30-60,60-150m since 2007	monthly; every 10 days,monthly since 2007	
	Rotifers	MLTP, LTP	1967-present	0→150m tow	monthly; every 10 days,monthly since 2007	
Streams	Flow	10 streams *	1986-present *	depth integrated samples **?**	continuous	* ~30 active locations sampled regularly;

						some site began late 60s-early 70s
	Nutrients (N&P), Fe	10 streams *	1986-present *	depth integrated samples	approx 25 per year	* ~30 active locations sampled regularly; some site began late 60s-early 70s
	SSC	10 streams *	1986-present *	depth integrated samples	approx 25 per year	* ~30 active locations sampled regularly; some site began late 60s-early 70s
Atmos. Dep.						

	Nutrients/bkt volume	Mid-lake buoy	1984-89; 91-96; 98-present	Dry-bulk (buoy bucket); also snow tube portion of pds	approx. 7-10 days	**gaps due weather & contam.**
	Nutrients/bkt volume	TB-4 buoy	2003-present	Dry-bulk (buoy bucket)	approx. 7-10 days	**gaps due weather & contam.**
	Nutrients/bkt volume	South Lake buoy	1984-88 only	Dry-bulk (buoy bucket)	approx. 7-10 days	**gaps due weather & contam.**
	Nutrients/bkt volume	Crystal Bay buoy	1984 only	Dry-bulk (buoy bucket)	approx. 7-10 days	**gaps due weather & contam.**
	Nutrients/bkt volume	West Lake buoy	1989-90	Dry-bulk (buoy bucket); also snow tube portion of pds	approx. 7-10 days	**gaps due weather & contam.**
	Nutrients/bkt volume	Interm ed. Buoy	1989-90	Dry-bulk (buoy bucket); also snow tube portion of pds	approx. 7-10 days	**gaps due weather & contam.**

Meteorology						
	wind, temp, RH, rad, precip	USCG Tahoe City	2000-present	N/A	every 10 min.	

Appendix 2 Supplemental information on Hypothesis 2

A.2.1 Seasonal Variations in Inorganic Particles, Organic Particles and Lake Clarity

Seasonal variations in lake particles (inorganic) and Cyclotella (organic particles) and lake clarity are shown by 5, 50th (median) and 95th percentiles (Figure A2.1). Seasonally, median lake particles are relatively constant of 1,000 counts/mL during Fall (Oct-Nov) and Winter (Dec-Mar) periods. Increases in median particles occur during Spring (April-May and Summer months (June-Sept) about 5,000 particles. Median Cyclotella counts are decrease from 100 counts/mL during the Fall and to a seasonal low of 20 counts/mL during the Winter months. This order of magnitude decrease is then followed by an increase through late summer to 300 counts/mL close to observations in the Fall. Clarity is relatively constant during the Fall, then increases during the winter months (note y-axis is reversed). Median clarity values decrease during the Spring and remain relatively constant during summer months around 20m.

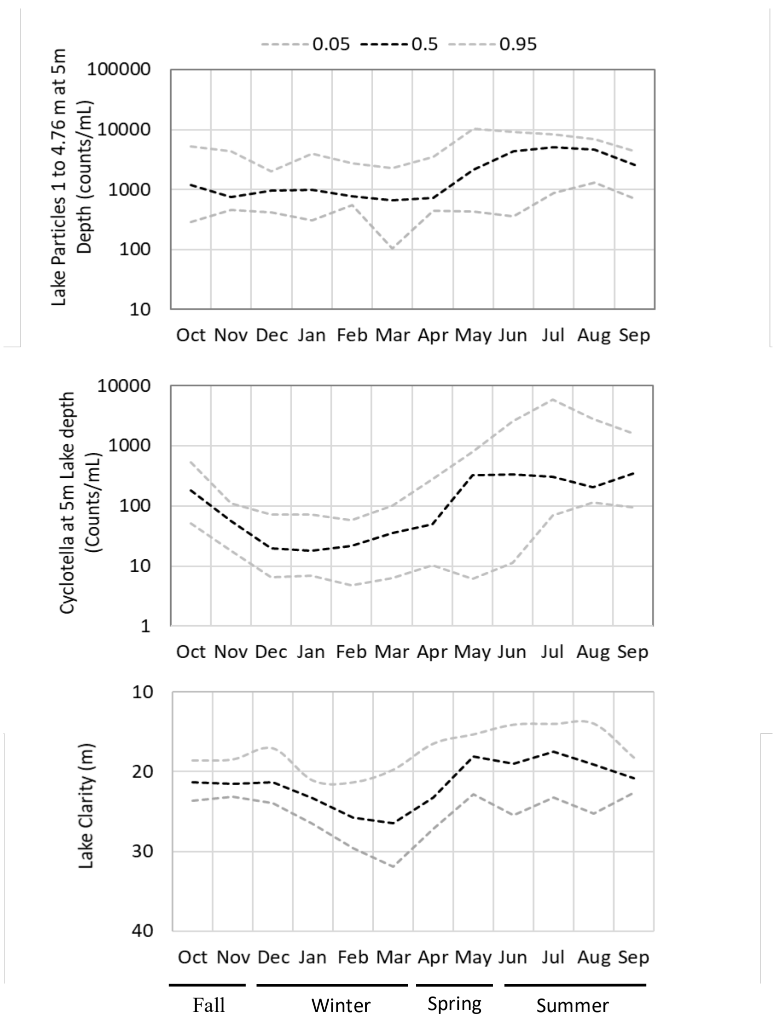

Figure A2.1 Seasonal variation in lake particles (2008-2019), Cyclotella (1981-2019), and lake Clarity (2000-2019). Lines represent the 5th, 50th (median) and 95% percentiles. Based on analysis in Section 4, values lake particle counts greater than 1,000 and Cyclotella counts greater than 100 have a linear negative affect on clarity.

A2.2 Urban Loading Data

Baseline loads, cumulative load reductions and clarity credits for Tahoe TMDL Program. Results are based on Pollutant Load Reduction Model (PLRM) results through WY 2019.

Table A2.1. Baseline average annual pollutant loads, representing 2004 estimated loads. Note: one pound of fine sediment particles (FSP<16 µm) is approximately equivalent to 5E+13 particles (LCCP 2020).

Jurisdiction	FSP		TP	TN
	#particles/yr	(lbs/yr)	(lbs/yr)	(lbs/yr)
CalTrans	3.10E+19	617,600	1,720	5,370
CSLT	2.44E+19	488,138	2,063	8,185
Douglas	4.80E+18	96,000	374	1,530
ElDorado	1.63E+19	326,960	1,170	4,170
NDOT	1.03E+19	205,006	564	1,704
Placer	2.64E+19	528,500	2,280	8,860
Washoe	1.45E+19	290,412	1,228	4,722
Basinwide	**1.28E+20**	**2.55E+06**		

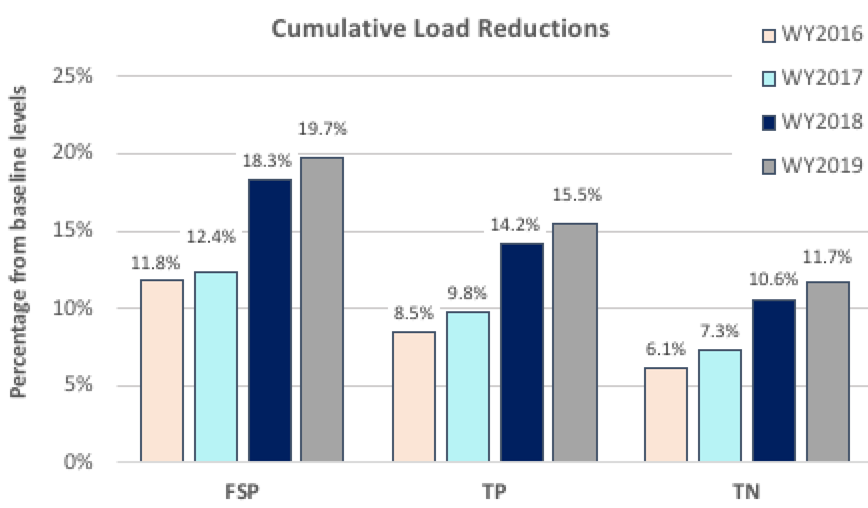

Figure A2.2. Cumulative load reductions achieved against baseline levels (adapted from LCCP 2019 and LCCP 2020).

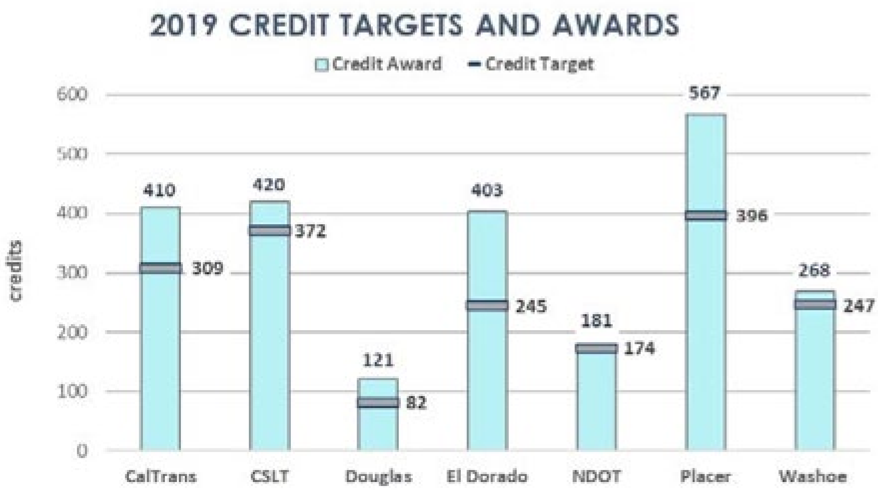

Figure A2.3. Clarity credits awarded through 2019 (from LCCP 2020).

It is possible to use average loading rates from urban sites (shown in Table 4.4) to evaluate Basin-wide loading against baseline levels, although it may be an over-extrapolation given the small total drainage area represented by RSWMP monitoring sites. Extrapolating to a total jurisdictional catchment area estimated at around 40,000 acres (per jurisdictional calculations), the average annual loading for FSP represents about 54% of the baseline from 2004. Accounting for an additional cumulative 18% modeled reduction (from PLRM, Table A2.2) would yield 73% of the baseline annual loading amount, which is fairly close considering the limited data and extrapolation. Similarly, using measured loadings for TP and TN (Table 4.4) then adding in the model-estimated reductions will yield 38% and 335% of baseline annual loadings, respectively. Although RSWMP drainages used in this analysis represent only 518 acres, less than 2% of urban jurisdictional catchments, they are representative of land uses and runoff characteristics for the Tahoe Basin (Table 4.2), and results are at least within a few hundred percent of values expected from the basin-wide average baseline annual loading rates. Interestingly, the TN loading estimated from measured values is substantially higher than baseline, while FSP and TP are both below baseline, suggesting that TN loading may be much higher than PLRM projections and has been increasing from baseline levels (Figure 4.6). Longer-term data with more sites in a stratified randomized design would be needed to improve these estimates, as originally intended in the program design for annual statistical assessment of Basin-wide urban loading rates to the lake each year (Heyvaert 2011).

Table A2.2. Cumulative average annual pollutant load reductions achieved (from LCCP 2020).

Water Year	FSP (lbs/yr)	TP (lbs/yr)	TN (lbs/yr)
2016	278,143	811	2314
2017	302,341	894	2598
2018	443,727	1332	3830
2019	476,992	1449	4203

Table A2.3. Monthly loads summed across RSWMP sites identified in Table 4.2 for the RSWMP statistical analyses represented in this document.

Year-month	Locations	TSS (kg)	FSP (kg)	TN (kg)	TP (kg)	Average precip (in)
2013-10	4	10.71	5.82	0.044	0.028	0.52
2013-11	4	9.67	5.77	0.047	0.025	0.46
2013-12	4	2.68	1.45	0.011	0.007	0.48
2014-01	4	176.60	100.71	0.811	0.484	1.91
2014-02	4	783.78	459.51	4.190	2.735	6.91
2014-03	4	220.30	156.07	1.188	0.810	1.78
2014-04	4	138.17	97.27	0.747	0.513	0.64
2014-05	4	120.76	87.58	0.647	0.426	1.45
2014-06	4	17.82	6.77	0.069	0.044	0.10
2014-07	4	225.38	100.01	1.270	0.593	1.56
2014-08	4	392.97	175.26	1.712	1.123	1.16
2014-09	4	778.29	340.36	3.189	2.207	1.29
2014-10	7	26.00	16.34	0.095	0.091	0.41
2014-11	7	176.83	120.70	0.996	0.591	1.59
2014-12	7	520.20	329.89	4.287	1.723	2.73
2015-01	7	5.93	3.89	0.037	0.018	0.17
2015-02	7	1,915.07	1,119.49	17.717	6.768	4.80
2015-03	7	88.99	76.18	1.012	0.342	0.31

Year-month	Locations	TSS (kg)	FSP (kg)	TN (kg)	TP (kg)	Average precip (in)
2015-04	7	338.33	241.93	4.785	1.299	1.68
2015-05	7	215.56	177.92	2.010	0.685	2.09
2015-06	7	106.33	51.89	2.320	0.377	0.80
2015-07	7	801.50	246.41	7.129	1.897	1.31
2015-08	7	23.84	9.77	0.393	0.062	0.18
2015-09	7	12.38	5.53	0.227	0.039	0.72
2015-10	7	614.46	519.06	4.496	2.253	1.69
2015-11	7	1,262.31	1,034.56	9.508	5.075	2.59
2015-12	7	1,567.98	1,307.12	14.327	6.617	5.53
2016-01	7	3,263.81	2,614.26	26.601	13.644	5.24
2016-02	7	283.12	227.06	2.014	1.144	0.84
2016-03	7	2,486.62	2,270.04	19.298	9.210	4.89
2016-04	7	1,346.92	1,253.38	8.872	4.595	2.44
2016-05	7	1,202.46	1,104.11	8.066	4.181	1.54
2016-06	7	206.56	41.85	2.752	0.787	0.05
2016-07	7	74.59	15.11	0.994	0.284	0.01
2016-08	7	663.43	134.71	8.958	2.538	0.24
2016-09	7	411.49	83.37	5.483	1.568	0.08
2016-10	7	2,017.59	1,225.69	23.082	7.884	6.41
2016-11	7	80.29	42.91	0.484	0.233	1.38
2016-12	7	2,496.87	1,523.99	31.639	10.303	6.30
2017-01	7	4,845.11	3,117.22	73.558	21.817	12.51
2017-02	7	10,900.07	7,259.23	174.630	49.730	12.00
2017-03	7	4,113.03	2,452.78	85.674	18.163	2.44
2017-04	7	3,811.48	2,365.71	83.997	17.218	2.55
2017-05	7	1,695.85	1,159.82	28.608	7.463	0.77
2017-06	7	1,070.48	635.84	29.447	5.351	0.20
2017-07	7	11.94	5.29	0.136	0.034	0.01
2017-08	7	488.10	252.40	10.562	2.071	0.46
2017-09	7	309.20	136.73	3.851	0.919	0.89
2017-10	7	47.05	20.96	0.926	0.154	0.41
2017-11	7	2,147.48	627.62	64.428	9.820	6.11
2017-12	7	19.35	7.04	0.465	0.076	0.32
2018-01	7	229.22	82.02	5.021	0.874	2.27
2018-02	7	157.73	49.76	4.002	0.672	0.39
2018-03	7	5,640.38	2,614.44	46.546	19.599	7.34
2018-04	7	2,055.82	922.09	18.696	7.128	1.70
2018-05	7	815.09	388.50	5.881	2.529	1.99
2018-06	7	0.80	0.36	0.009	0.002	0.03

Year-month	Locations	TSS (kg)	FSP (kg)	TN (kg)	TP (kg)	Average precip (in)
2018-07	7	156.18	53.62	3.792	0.700	0.87
2018-08	7	0.00	0.00	0.000	0.000	0.00
2018-09	7	0.02	0.01	0.000	0.000	0.00
2018-10	7	69.26	31.80	1.402	0.429	0.80
2018-11	7	254.76	122.67	5.450	1.354	2.86
2018-12	7	140.15	59.51	3.182	0.850	1.52
2019-01	7	508.92	232.66	13.165	2.642	4.22
2019-02	7	1,819.34	765.10	53.296	12.603	7.82
2019-03	7	2,010.28	1,232.91	28.458	8.103	2.94
2019-04	7	2,685.37	1,478.76	36.892	9.892	1.14
2019-05	7	686.15	437.22	8.869	2.890	1.66
2019-06	7	689.03	336.23	6.375	1.323	0.12
2019-07	7	0.44	0.25	0.004	0.002	0.03
2019-08	7	0.00	0.00	0.000	0.000	0.00
2019-09	7	136.76	64.77	1.361	0.269	0.63

Appendix 3 Supplemental information on Hypothesis 3

A3.1 Time Series of Secchi depth.

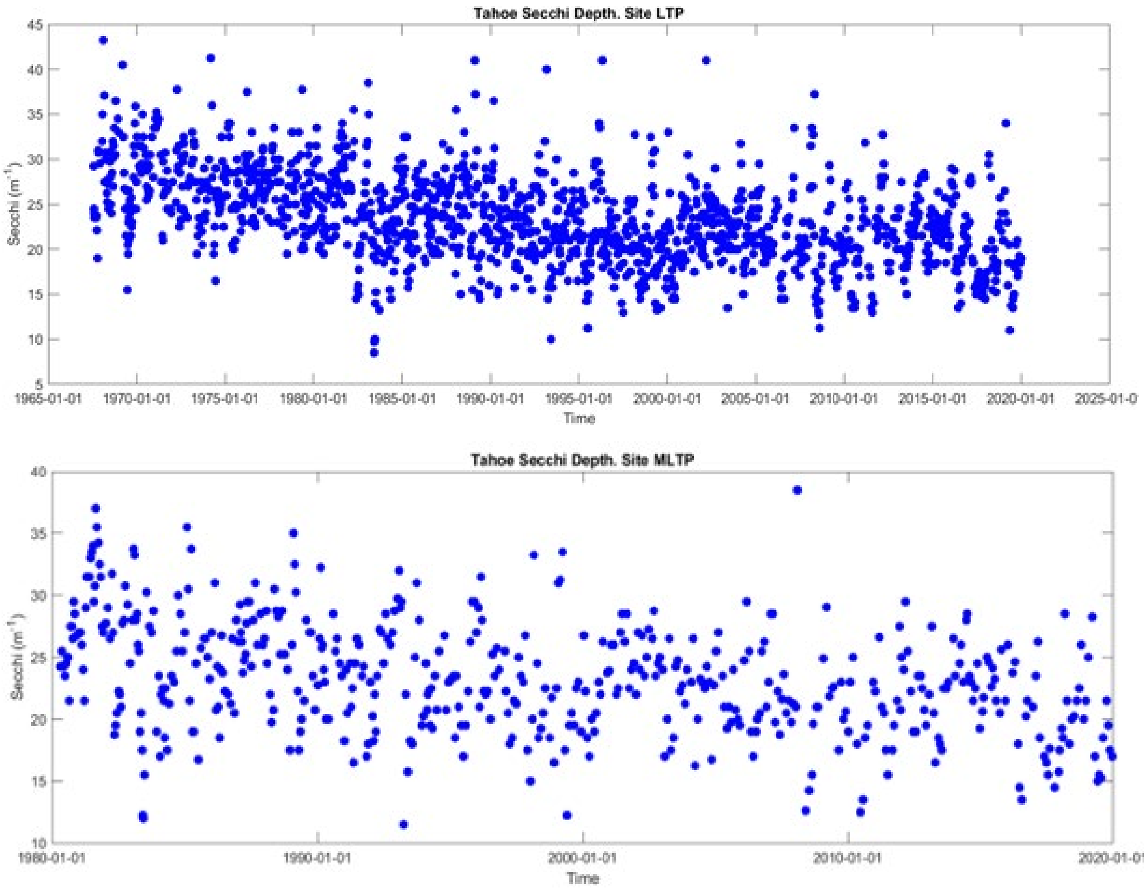

Figure A3.1**.** Time series of Secchi depth at LTP (upper) and MLTP (lower).

A3.2 Time Series of Lake temperatures.

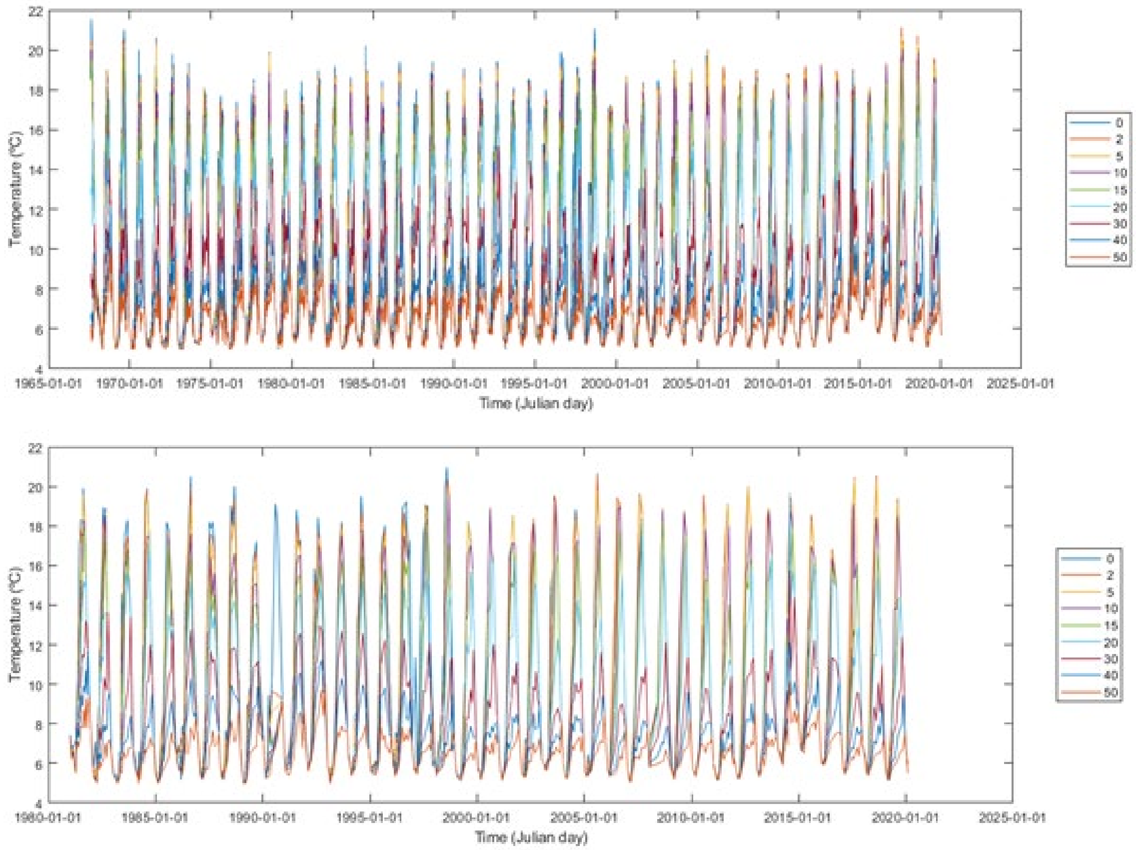

Figure A3.2. Time series of lake temperature at LTP and MLTP at 9 depths (legend shows depth in m).

A3.3 Time Series of particle size distribution of fine particles.

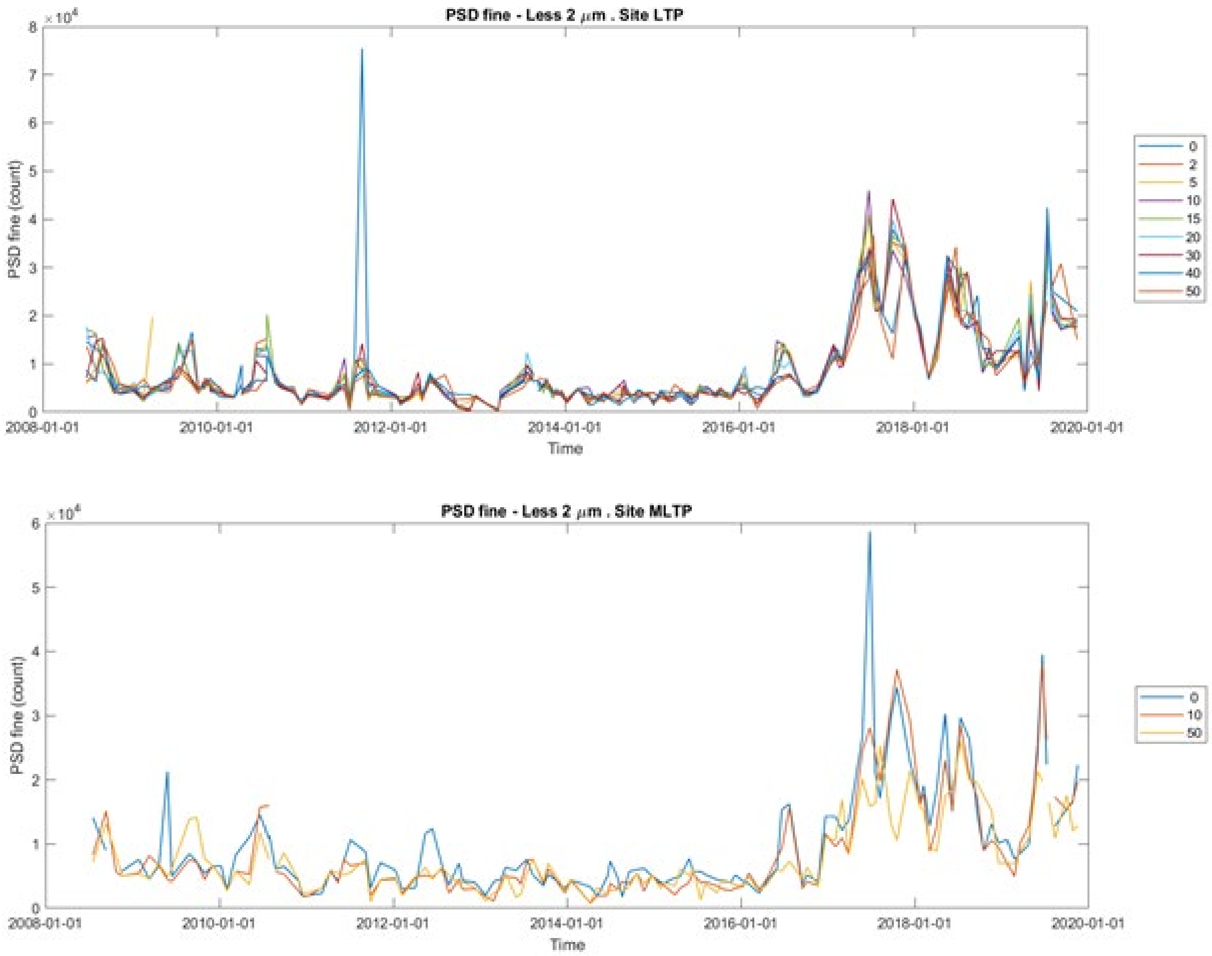

Figure A3.3. Time series of particle size distribution (PSD) of fine particles at LTP (upper) MLTP (lower) at 3 depths (legend shows depth in m).

A3.4 Time Series of Nitrate-N.

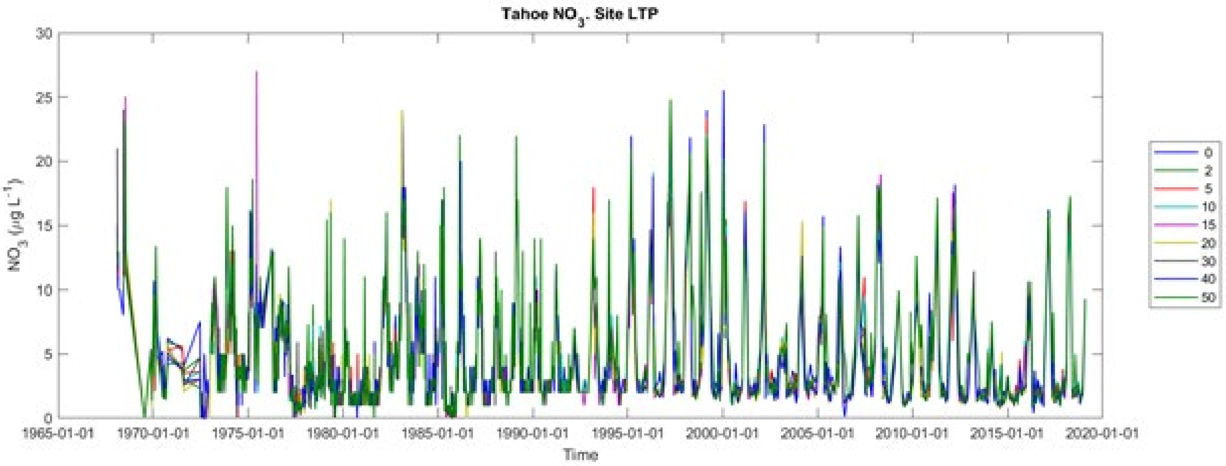

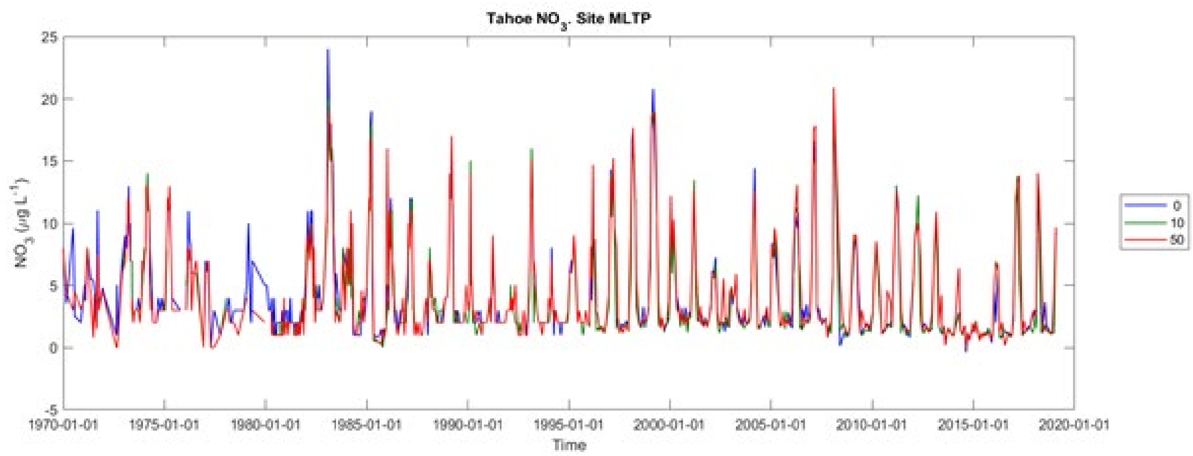

Figure A3.4. Time series of Nitrate-N (NO_3) at LTP (upper) and MLTP (lower) at 9 depths (legend shows depth in m).

A3.5 Time Series of Total Kjeldahl nitrogen and Total hydrolysable Phosphorous.

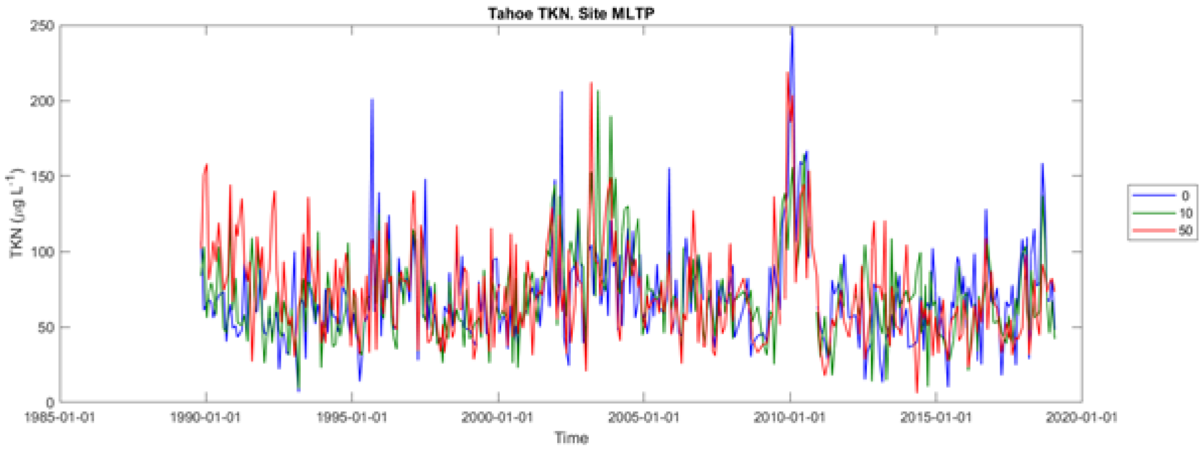

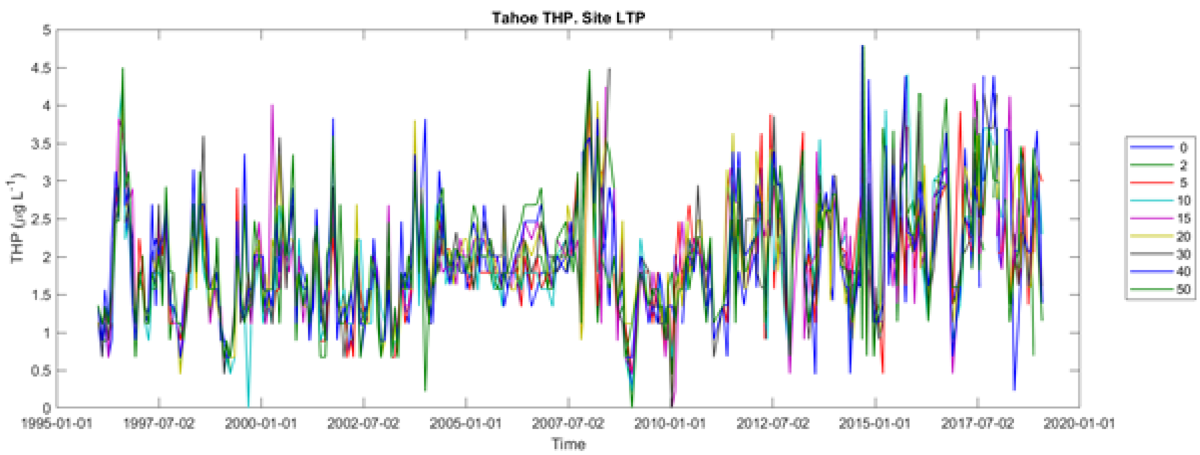

Figure A3.5. Time series of Total Kjeldahl nitrogen (TKN) at MLTP (upper), and Total hydrolyzable phosphorus (THP) at LPT (lower) (legend shows depth in m).

A3.6 Time Series of total hydrolysable phosphorous and total phosphorus.

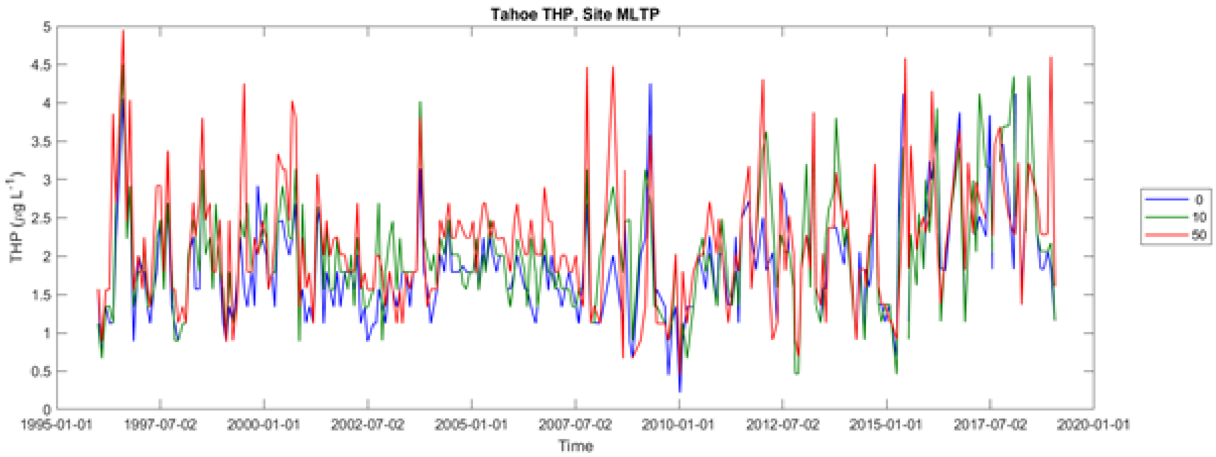

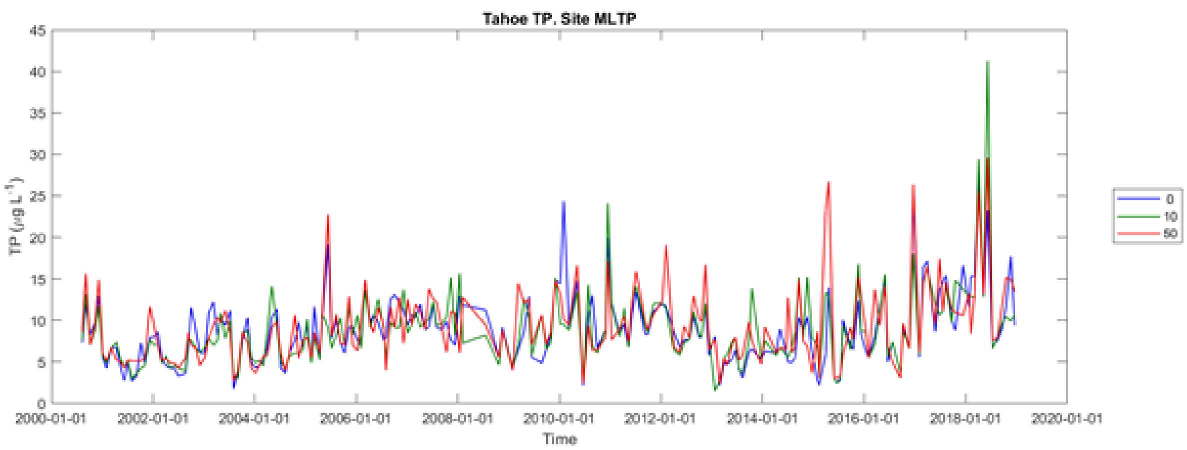

Figure A3.6. Time series of Total hydrolyzable phosphorus (THP) at MLTP (upper) and Total Phosphorus (TP) at MLTP (lower) at 3 depths (legend shows depth in m)

A3.7 Time series of Chlorophyll-a (Chl-a)

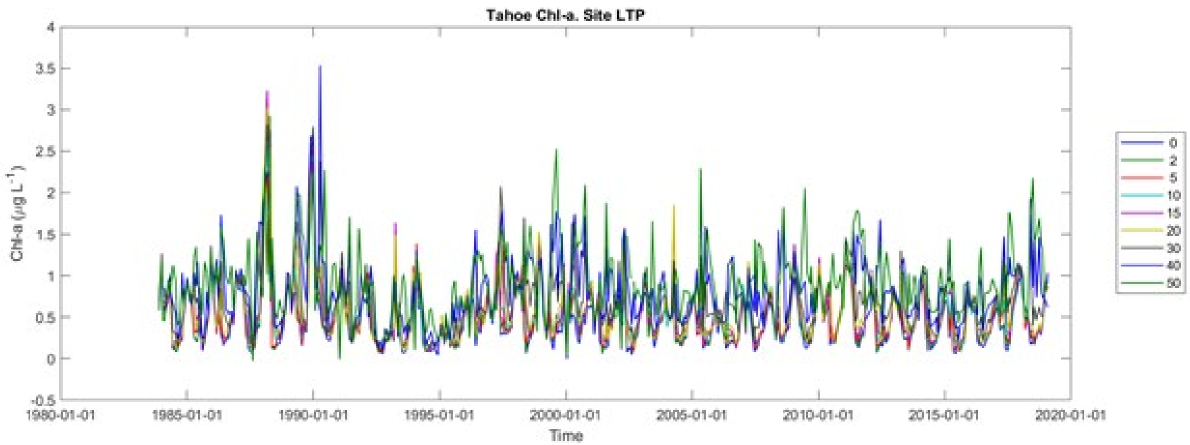

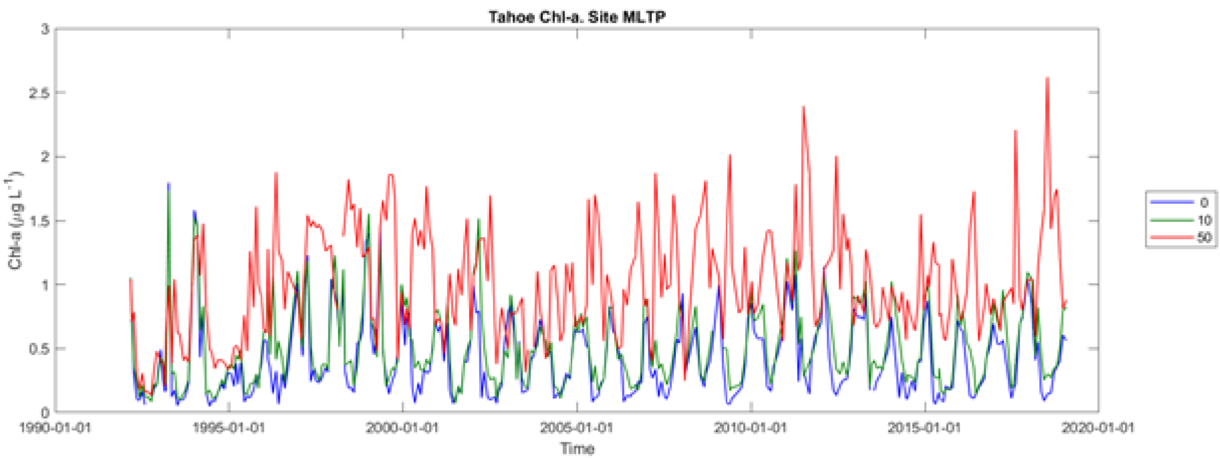

Figure A3.7. Time series of Chlorophyll-a (Chl-a) at LTP (upper) and MLTP (lower) at 9 depths (legend shows depth in m).

Appendix 4 Description of Variables used Correlation Analysis

Summer Variables	Description
Summer_Clarity	Summer median monthly clarity values
Summer_T	Summer Lake temperature observed at 10m LTP
Strat_days	Number of stratification days
Peak_Strat_Day	Day peak stratification occurred
Begin_Strat_day	Day stratification occurred
End_Strat_day	Day stratification ended
Summer_PeakBF	Summer peak buoyancy frequency (maximum value in vertical profile)
Summer_MaxBF	Summer maximum buoyancy frequency (top and bottom of profile)
Summer_GSI	Summer Stability Index
Summer_NO3N	Summer median nitrate-n concentrations at 10m LTP
Summer_TPH	Summer median total hydrolyzable phosphorus at 10m LTP
Summer_TP	Summer median total phosphorous at 10m LPT
Summer_Chla	Summer chlorophyll-a at 10m LPT
Summer_Particles	Summer Lake particles observed at 10m LPT
SWE_max	Maximum Snow Water Equivalent observed at SNOTEL Ward #3 site
Summer_Precip	Precipitation observed in Summer at SNOTEL Ward #3
UTR_Peakcfs	Upper Truckee River peak discharge in cfs
UTR_CM	Upper Truckee River discharge center of mass date
UTR_Vol_acreft	Upper Truckee River streamflow volume in acre-ft
BW_Peakcfs	Blackwood Creek peak discharge
BW_CM	Blackwood Creek center of mass day of year
BW_Vol	Blackwood Creek volume of streamflow
Summer_Cylcotella	Summer median Cyclotella observed at 10m LPT
Summer_BC_TN	Summer Blackwood Creek total phosphorous measured at LTIMP gage
Summer_UTR_TN	Summer Upper Truckee River total nitrogen measured at LTIMP gage
Summer_BC_TP	Summer Blackwood Creek total phosphorous measured at LTIMP gage
Summer_UTR_TP	Summer Upper Truckee River total phosphorous measured at LTIMP gage

Winter Variables	Description
Winter_Clarity	Median monthly winter clarity values
Winter_T	Winter lake temperature observed at 10m LTP
Mixing_Depth	Depth of maximum mixing at MLTP
Strat_days	Days of stratification
Peak_Strat_Day	Day peak stratification occurred
Begin_Strat_day	Day stratification occurred
End_Strat_day	Day stratification ended
Summer_PeakBF	Summer peak buoyancy frequency
Summer_MaxBF	Summer maximum buoyancy frequency
Winter_PeakBF	Winter peak buoyancy frequency (maximum value in vertical profile)
Winter_MaxBF	Winter maximum buoyancy frequency (top and bottom of profile)
Winter_GSI	Winter stability index
Winter_NO3N	Winter nitrate-n concentrations observed at LPT 10m
Winter_TPH	Winter total hydrolyzable phosphorus observed at LPT 10m
Winter_TP	Winter total phosphorus observed at LPT 10m
Winter_Chla	Winter chlorophyll-a observed at LPT 10m
Winter_Particles	Winter particles observed at LPT 10m
Winter_Cyclotella	Winter *Cyclotella* observed at LPT 10m
Winter_BC_TN	Winter Blackwood Creek total nitrogen measured at LTIMP gage
Winter_UTR_TN	Winter Upper Truckee River total nitrogen measured at LTIMP gage
Winter_BC_TP	Winter Blackwood Creek total phosphorus measured at LTIMP gage
Winter_UTR_TP	Winter Upper Truckee River total phosphorus observed at LTIMP gage
SWE_max	Maximum Snow Water Equivalent observed at SNOTEL Ward #3 site
Winter_Precip	Precipitation observed in Summer at SNOTEL Ward #3
UTR_Peakcfs	Upper Truckee River peak discharge in cfs
UTR_CM	Upper Truckee River discharge center of mass day of year
UTR_Vol_acreft	Upper Truckee River streamflow volume in acre-ft
BW_Peakcfs	Blackwood Creek peak discharge
BW_CM	Blackwood Creek center of mass date
BW_Vol	Blackwood Creek volume of streamflow
Summer_BC_TN	Summer Blackwood Creek total phosphorous measured at LTIMP gage
Summer_UTR_TN	Summer Upper Truckee River total nitrogen measured at LTIMP gage
Summer_BC_TP	Summer Blackwood Creek total phosphorous measured at LTIMP gage
Summer_UTR_TP	Summer Upper Truckee River total phosphorus measured at LTIMP gage